Utrecht University

2008 Master's Thesis

[*Hydrology and System Earth Modelling*]

Water Stress over the Year: Quantitative Analysis of Seasonality and Severity on a Global Scale

Supervisors (Utrecht University):
Prof. Dr. Ir. M.F.P. (Marc) Bierkens
Dr. L.P.H. (Rens) van Beek
Dr. Hans H. Dürr

Co-supervisors (University of Bern):
Prof. Dr. Rolf Weingartner
Dr. Daniel Viviroli

Name: Yoshihide Wada
Student Number: 3076709
E-mail Address: Y.Wada@students.uu.nl

Hydrology and System Earth Modelling
Department of Earth Sciences
Faculty of Geosciences
Utrecht University

Table of Contents

List of Figures

List of Tables

Abstract

Blue water (i.e. river discharge) and green water (i.e. soil water) are vital water resources to our society. Yet, assessments of water scarcity or water stress tend to focus on blue water only. This study assessed the amount of pressure put on both blue and green water resources by using the water scarcity index. Monthly water demand for the year 2000 was estimated as a bench mark year and contrasted against 44 years (duration: 1958-2001) of a long-term climate based on ERA-40 and CRU TS 2.1 meteorological data sets. The results indicate that 1.5 to 2.3 billion people (approximately one-third of the world's population) are currently experiencing moderate to high water stress on a global scale. The results vary significantly depending on a temporal resolution (i.e. yearly or monthly time scale).

Emerging high water stress regions where green water demand is exceeding green water availability are identified for the first time. In addition, this study reveals new dimension of water stress by using a finer temporal scale than previous studies (i.e. month). Our results indicate that the degrees of blue water stress are underestimated by existing annual assessments in large regions (e.g. Sub-Sahara, the eastern part of Brazil, the western part of Australia, Central Asia and India). The regions vulnerable to the spatiotemporal variability of blue water stress are identified. Also, the monthly time steps enable to assess the seasonality and the severity of global water stress. The severity is quantified by using statistics of persistence, recurrence, average intensity as well as the dynamic water stress developed by Porporato et al. (2001).

The results show that blue water stress estimated by this study generally corresponds well to the observation of past water shortage (i.e. extreme events) in the Netherlands and Japan. Even though estimated water demand of the year 2000 stays constant for 44 years, water stress (thus water shortage) was well reproduced by a long-term climate variability.

Keywords: *Macro-scale hydrological model; PCR-GLOBWB; Water availability; Water demand; Water scarcity; Water stress; Seasonality, Severity*

1. Introduction

1.1. Background and Problem Description

The existing imbalance of water availability and water demand causes water scarcity to be one of the most pressing environmental issues in the world today. Water scarcity may loom when- and wherever demand cannot be matched by available water. Water demand for the next decades is projected to increase due to the growing global population while available water is not likely to increase at the same rate. The concern for looming water scarcity and the call for appropriate management of freshwater resources have been continuously raised by various studies as well as international conferences such as the World Water Forum (World Water Council, 2006).

At present we only use 10% of maximum available blue water (renewable freshwater resources[1]) and 30% of maximum available green water (rainfall that is stored in the soil; Falkenmark et al., 1997) on a global scale (Oki and Kanae, 2006). However, water availability has a high variability in both time and space (Postel et al., 1996) so that it differs largely between in regions and over the year. In Asia, for example, 80% of runoff occurs between May and October (Shiklomanov, 1993). In tropical regions, a substantial share of annual runoff occurs during monsoon flooding (Jackson et al., 2001) so that the monthly mean discharge at Obidos station in the Amazon River differs by a factor of 2 between the highest (May-July; Marengo, 2005) and the lowest (November-January; Marengo, 2005) discharge months (Oki and Kanae, 2006). Flooding runoff water are not a practical supply for agricultural, industrial and domestic water use that need water to be delivered in controlled quantities at specific times (Jackson et al., 2001). River discharge is even more variable in smaller river basins (Oki and Kanae, 2006) and monthly river discharge is more variable than annual mean river discharge due to seasonality (i.e. the wet and dry season). Turning flooding water into an accessible supply generally requires dams and reservoirs to capture, store, and control the water (Jackson et al., 2001).

Available freshwater resources also vary significantly in space. Brazil, the Russian Federation, Canada, the United States of America (U.S.A.), the People's Republic of China (PRC) and India have more than 40% of total (i.e. global) annual river runoff

[1] Renewable freshwater resources is defined as freshwater flowing through the solar-powered hydrological cycle (Postel et al., 1996). Further references can be found in Postel et al. (1996) and Oki and Kanae (2006).

formed within their territories (Shiklomanov, 1998). River runoff is also unevenly distributed within the territories of these countries.

The spatiotemporal variability of water demand is characterized by changes in population size and land use. For example, growing urban population causes a high water demand at a particular geographic region. Many densely populated cities rely on water resources outside of their territories due to their high water demand or a lack of local freshwater resources. Irrigation water use requires a large amount of water in a specific season depending on the type of crops. One particular property of water demand is that it is often out-of-phase (or even in anti-phase: top of demand in periods with low water availability, i.e. the dry season) with water availability, which causes water stress to occur intensively during short periods, but also to be larger than based on annual average availability and demand.

While climate and geomorphology dominate the availability of freshwater resources, water demand is controlled by not only climate but also socio-economic factors such as population, food production and economic development. Water availability largely fluctuates over the year following dry and wet seasons and water demand fluctuates as well, often with its own dynamics. Due to the spatiotemporal variability of both water availability and water demand, different regions experience different degrees of water stress at different times.

The problems thus are to grasp the imbalance of water availability and water demand resulting excess and scarcity of water over the year and to assess the sustainability[2] of renewable freshwater resources over the seasons. Because current approaches to describe water stress work at a yearly temporal scale (see next sections), they are not able to grasp the timing, duration, intensity and magnitude of water stress over the year. Shorter temporal scales enable detailed assessments considering the effects of spatiotemporal variability in available freshwater resources (Oki and Kanae, 2006) as well as water demand. In conclusion, there is a great need to describe water availability and water demand (and thus water stress) at increased temporal (e.g. monthly) resolution.

Apart from increasing the temporal resolution of water stress assessment, our understanding can also be improved by better definition of both water availability and water demand. As mentioned before, dam and reservoir operations substantially alter river discharge (Hanasaki et al., 2006). Water which originates in upstream and flows into

[2] Sustainability has been defined as meeting the needs of the present without compromising the ability of future generations to meet their needs (Bruntland, 1987), considering limited renewable freshwater resources. Gleick (1998) defined the sustainable water use as water use that benefits to all current users are maintained, without reducing benefits to other users, including natural ecosystems over the long-term periods. Sustainable use of the freshwater resource can only be assured if the rate of use does not exceed the rate of renewal (Thyssen and EEA, 1999).

downstream has a large impact on water availability as well (Oki et al., 2001; Vörösmarty, et al., 2005a). Studies on water availability cannot be separated from the actual or projected demand for any given region on the globe (van Beek, 2007). Therefore, a better partitioning of water use into surface and groundwater resources is necessary to improve our assessment (van Beek, 2007a). Although the available global-scale information on water demand is limited (Oki et al., 2001), it is valuable to consider water demand in terms of purpose (agricultural, industrial and domestic sector) and determine a period (e.g. month) of demand, particularly for irrigation which has a large seasonal variability. These important components improve our water stress assessment.

1.2. Previous Work on the Problem

1.2.1. Historical Development

The study of water availability and water demand can be traced back to the 1970s. Among pioneering studies, Ledger (1972) estimated water availability and water demand in the Warwickshire Avon as a case study. Since then, together with the international hydrological decade (UNESCO, 1966), which promoted studies on global water balance (Heindl, 1979), the studies of water availability and water demand have been conducted mainly on a regional scale. Efforts to assess water availability, water demand and water stress on a global scale have increased over the past 10 years (Smakhtin et al., 2004). As an imbalance between water availability and water demand emerged in various regions of the world over past decades, the study of water stress has attracted more attention.

In the late 1980s, Falkenmark (1989) pioneered the concept of water stress based on available freshwater resources and water required per capita. Falkenmark (1989, 1990, 2004) also generalized the concept of using a threshold value of water stress (i.e. water scarcity index) to describe different degrees of water scarcity in various regions of the world. The index of water stress has evolved from simply domestic (households and municipalities) water use point of view into a more comprehensive analysis including agricultural (irrigation and livestock) and industrial water use. The water scarcity index is now widely used to indicate different degrees of water stress on both a regional and a global scale (Falkenmark, 1989; Alcamo et al., 2003b; Oki and Kanae, 2006; Vörösmarty, 2000). Oki and Kanae (2006) define the water scarcity index[3] as follows:

[3] Detailed descriptions of the water scarcity index can be found in Asheesh (2002) and Falkenmark and Rockström (2004).

$$Rws = (W - S)/Q, \tag{1.1}$$

where Rws is the water scarcity index (-), W is the annual water withdrawal by all the sectors, S is water generated by desalination and Q is the renewable freshwater resources.

A region is considered to experience high water stress when *Rws* is higher than 0.4 considering the sustainability of renewable water resources (Alcamo et al., 2003b; Falkenmark and Rockström, 2004; Oki and Kanae, 2006; Vörösmarty, 2000).

1.2.2. Macro-scale Hydrological Model (MHM)

While the concept of water stress has been generalized, macro-scale hydrological model (MHM) has been increasingly applied to provide assessments of water availability, water demand and water stress (e.g. Alcamo et al., 2003a, 2003b; Arnell, 2003; Döll et al., 2003; Oki et al., 2001; Takahashi et al., 2000; Vörösmarty et al., 2000; Widén-Nilsson et al., 2007). Below table 1.1 shows the different types of macro-scale hydrological models (MHMs) used by previous studies with some characteristics. Besides these MHMs, Yates (1997), Klepper and van Drecht (1998) and Nijssen et al. (2001a, 2001b) applied their MHMs to river basin to continental scales to compute runoff and river discharge.

Macroscale hydrological models (MHMs), which model the land surface hydrologic dynamics of continental scale river basins, have rapidly developed since the 1990s (Nijssen et al., 2001b). Some earlier studies (Yates, 1997, Klepper and van Drecht, 1998 and Nijssen et al., 2001) used a spatial resolution of 1°, 2° or even larger resolutions partly due to input data constraints. However, Yates (1997) assessed that the larger spatial resolution of 2° and 5° proved to be inadequate for consistently producing reasonable runoff estimates across the domains of both Western Europe and Africa. Nijssen et al. (2001b) also assessed that the coarse resolution (2°) of the precipitation data set failed to resolve strong spatial gradients in the precipitation. These experiences from earlier studies provided the motivation to develop MHMs with finer spatial resolution.

Table 1.1: Main Macro-scale Hydrological Models (MHMs) applied to compute global water balance[4].

	MHM	Spatial resolution	Temporal resolution	Duration	Climate input	Model output	Main feature
Vörösmarty et al. (1989, 1998, 2000)	Water Balance Model (WBM)	0.5°	Month	1961-1990	CGCM1[5] HadCM2[6]	River discharge	Coupled with 2 GCMs[7]
Alcamo et al. (1997, 2000, 2003a)	Water-Global Assessment and Prognosis (WaterGAP 1.0/2.0)	0.5°	Day	1950-2025 (Water use) 1961-1990 (Runoff and groundwater recharge)	CRU[8]	Runoff, Groundwater recharge and Water use (Agriculture, Industry and Domestic)	Global water use model and global hydrology model are linked to compute water stress indicators.
Arnell (1999b, 2003)	Macro-PDM	0.5°	Day (time step) Month (output)	1961-1990	CRU	Runoff and Streamflow (direct runoff)	Probability-distributed (statistical distribution) model (Moore, 1985)
Takahashi et al. (2000)	Bucket Model	0.5°	Month	1961-1990 2050-2059	LINK[9] ISLSCP[10]	Runoff and River discharge	Coupled with 3 GCMs
Oki et al. (2001)	Total Runoff Integrating Pathways (TRIP)	0.5°	10 days	1987-1988	ISLSCP	River Discharge	Coupled with 10 LSMs[11]
Döll et al. (2003)	WaterGAP Global Hydrology Model (WGHM)	0.5°	Day	1901-1995	CRU	Runoff, Groundwater recharge and River discharge	Tuning and regionalisation of calibration parameter
Widén-Nilsson et al. (2007)	Water and Snow Balance Modeling System (WASMOD-M)	0.5°	Month	1915-2000	CRU	Runoff	Simulation with regionalised parameter-value

[4] These descriptions are valid in studies of specified articles.

[5] CGCM1: Canadian Climate Center general circulation model; http://www.cccma.ec.gc.ca/eng_index.shtml

[6] HadCM2: Hadley Center circulation model; http://www.metoffice.gov.uk/research/hadleycentre/

[7] GCMs: General Circulation Models

[8] CRU: Climatic Research Unit; http://www.cru.uea.ac.uk/

[9] LINK project: British Atmospheric Data Centre (BADC); http://badc.nerc.ac.uk/data/link/

[10] ISLSCP: International Satellite Land Surface Climatology Project,;http://www.gewex.org/islscp.html

[11] LSMs: Land Surface Models

Along with the technological developments, global and regional assessments of water stress are visualized at finer spatial scales. At present, 0.5° is the highest resolution that is feasible for global hydrological models as the necessary climatic input is not available at a better resolution (Döll et al., 2003). As mentioned before, water availability is highly variable in space. Therefore, while most of the global climate models use grids of about 200 km by 300 km, i.e. around 2° grid scale, most of MHMs use smaller grids of about 50 km by 50 km, i.e. 0.5° grid scale, (e.g. Alcamo et al., 2003a; Arnell, 1999b; Döll et al., 2003; Meigh et al., 1999; Oki et al., 2001; Vörösmarty et al., 2000). Latest technological development of regional scale models and computations enables us to use even finer grids of about 1 km by 1 km, i.e. 0.01° grid scale, (Smakhtin et al., 2004). However, hydrological and climatic data are mainly available at grids of about 50 km by 50 km at present.

1.2.3. Assessment of Water Stress

Water stress occurs when the local water demand exceeds the local water availability. On a global scale, previous studies (Alcamo et al., 2003b; Alcamo and Henrichs, 2002; Arnell, 1999a, 2004; Islam et al., 2007; Oki et al., 2001; Vörösmarty et al., 2000) have provided assessments of water stress by comparing water availability and water demand at yearly time scales. These global assessments were used to identify the regions of present and future water scarcity (Smakhtin et al., 2004) and analyze the effects of the climate change. Regional scale studies on water stress have been conducted also at yearly time scales (Douglas et al., 2006; Klepper and van Drecht, 1998; Ledger, 1972; Meigh et al., 1999; Vörösmarty et al., 2005). Some of the recent regional scale studies intensively focus on the regions vulnerable to water stress such as Africa[12].

Many of the previous studies (Alcamo et al., 2003b; Alcamo and Henrichs, 2002; Arnell, 1999a; Islam et al., 2007; Oki et al., 2001; Vörösmarty et al., 2000) used the water scarcity index or similar indicators to assess water stress. These studies identified those areas where human water uses are threatened (high water stress) by inter-annual fluctuation in river discharge due to the climate change and high water demand caused by growing population. The different degrees of annual water scarcity were estimated by using MHMs.

[12] There are not sufficient infrastructure such as dams and reservoirs to store water so that Africa is more vulnerable to water scarcity, potentially causing high water stress.

1.3. Scientific Question and Research Objective

The main research question is how the seasonal variation of water stress for different parts of the world is characterised and how it differs from annual water stress. Because existing global and regional assessments use annual averages to describe water stress using the water scarcity index, we do not know the variation within the year. Meigh et al. (1999) noted that water shortages often first become apparent as occasional deficits at certain times of the year during periods of high demand or below average rainfall and may only affect a narrow region. This study aims to verify their argument on a global scale and highlight a possible problem region (i.e. high water stress) which is not well represented by existing assessments. In addition, if we can describe the development of water stress at a monthly time scale, we can also assess timing and duration of water stress over the year. This in turn enables us to quantify more precisely the severity of water stress. Institutions which are in charge of water supply are interested in assessing when water scarcity occurs over the year as it enables them to conduct precautionary measures before a potential water scarcity would occur.

The main research objective is thus to quantify the seasonal variation and the severity of water stress. Due to data deficiency, this study estimates water demand for the year 2000 as a bench mark year and contrasts it against 44 years (duration: 1958-2001) of a long-term climate variability (see section 1.5.1. for meteorological input). Water availability was computed over the overlap period between the ERA-40 and the CRU TS 2.1 meteorological data sets. ERA-40 daily variation of precipitation and evapotranspiration was then used to downscale the CRU TS 2.1 monthly data to daily values. The analysis of water stress was made based on the CRU TS 2.1 meteorological data set (see section 2.3. of chapter 2 for the choice of meteorological data). Average water stress with the water scarcity index between annual and monthly assessment is compared based on a long-term climate variability. The severity of water stress is quantified by using statistics of persistence, recurrence and average intensity. Apart from the water scarcity index, water stress is also assessed with dynamic water stress developed by Porporato et al. (2001), considering the frequency and the mean length of the water stress period. At last, the effect of the long-tern climate variability on past 44 years of water stress is assessed with the observation of past water shortage (i.e. extreme events) in the Netherlands and Japan.

These analyses are an initial step to identify any regions where the assessment of annual and monthly water stress is mismatched as well as quantify the seasonality and the severity of water stress at a finer temporal scale.

1.4. Methodology and Approach

This study makes use of the MHM of PCR-GLOBWB[13] (PCRaster GLOBal Water Balance) using the PCRaster modelling and GIS environment (http://pcraster.geog.uu.nl/index.html), developed by the Department of Physical Geography, Utrecht University. PCR-GLOBWB is a conceptual water balance model of the terrestrial part of the hydrological cycle linked to a simplified energy balance for surface water temperature and ice development. PCR-GLOBWB estimates monthly water availability derived from monthly runoff based on a daily time step. PCR-GLOBWB uses 0.5° by 0.5° (about 50 km by 50 km at the equator) longitude/latitude resolution (360 rows by 720 columns) on a global scale, the same as most of MHMs used by previous studies. Monthly water abstractions from surface freshwater and groundwater are estimated by the use of available data on agricultural, industrial and domestic water use with the same spatial resolution. We included upstream water use and implemented a reservoir operation scheme along with river networks to estimate the total river discharge. These components enable accurate estimates of available water. More detailed model description and implemented components are given in Chapter 2.

1.5. Data Requirements

1.5.1. Meteorological Input

The current version of PCR-GLOBWB requires meteorological input to be specified by an external source (e.g. observation or GCMs results, etc) and considers it as uniform over each grid cell (van Beek, 2007b). The model requires the following meteorological input: total precipitation, potential evapotranspiration, both in meter water slice, and temperature, in °C, as sums and averages over the duration of the model time step, e.g. per day (van Beek, 2007b). In this study, we used the meteorological data of the ERA-40 (duration: 1957-2002) and the CRU (duration: 1958-2001). The ERA-40 re-analysis data is provided by European Centre for Medium-Range Weather Forecasts (ECMWF; http://www.ecmwf.int/). The ERA-40 provides daily high-quality global analyses of atmosphere, land and ocean-wave conditions for the past four decades by using an up-to-date data assimilation system and exploiting, at any time, the maximum information from the available observational sources (for more details, see Kållberg et

[13] PCR-GLOBWB is developed by Dr. L.P.H. (Rens) van Beek of the Department of Physical Geography, Utrecht University. A detailed model description can be obtained by personal communication; r.vanbeek@geo.uu.nl.

al., 2005). The Global Climate Data set of the CRU (i.e. CRU TS 2.1) consists of long-term mean monthly climatology and timeseries for global land areas, excluding Antarctica at a 0.5° by 0.5° of longitude/latitude spatial resolution (New et al., 1999, 2000; Mitchell and Jones, 2005; http://www.cru.uea.ac.uk/cru/data/). New et al. (1999, 2000) used thin-plate splines to interpolate the climate surfaces as a function of latitude, longitude, and elevation, where no observation data is available. The CRU TS 2.1 monthly data was downscaled to daily values by using ERA-40 daily variation of precipitation and evapotranspiration.

The data link of the ERA-40 and the CRU is given in Appendix A.

1.5.2. Water Withdrawal and Socio-economic Data

For the water withdrawal and socio-economic data, we collected data from various sources. Data on water withdrawal, reservoir characteristics and population are initially based on those available from the World Water Assessment Programme (WWDR-II; http://wwdrii.sr.unh.edu/). To estimate global groundwater abstraction, we used data of IGRAC (International Groundwater Resources Assessment Centre; http://www.igrac.nl/). The data of the World Register of Dams 2003 provided by ICOLD (International Commission on Large Dams; http://www.icold-cigb.net/) was used to clarify dam usage or purpose. A global data set of monthly growing areas of 26 irrigated crops around the year 2000 (MIRCA2000; Portmann et al., 2008) was used to estimate monthly irrigation water demand. The Hydrology Group of Institute of Physical Geography, Johann Wolfgang Goethe University (Frankfurt) kindly provided this data set. Besides the water withdrawal data from the WWDR-II, we used data from EarthTrends (WRI: World Resources Institute; http://earthtrends.wri.org/) and AQUASTAT (FAO: Food and Agriculture Organization of the United Nations; http://www.fao.org/nr/water/aquastat/data/). These data are based on country statistics unlike the WWDR-II gridded data. We also used socio-economic data such as GDP (Gross Domestic Product) and GDP per capita from the World Bank (http://www.worldbank.org/). All data sources and detailed descriptions are given in chapter 3.

1.5.3. Data Availability

Data availability is a major problem in global water-balance modelling (Widén-Nilsson et al., 2007). Uncertainties and differences in model-input data, especially precipitation, are major sources of uncertainty in model output (Widén-Nilsson et al., 2007). Different

meteorological inputs (e.g. Global Soil Wetness Project (GSWP; http://www.iges.org/gswp/), International Satellite Land Surface Climatology Project (ISLSCP), CRU and ERA-40) result in different outputs (e.g. runoff and irrigation water demand). Decharme and Douville (2006b) assessed uncertainties in the GSWP precipitation forcing and their impacts on regional and global hydrological simulations. They pointed out that the reliability and accuracy of precipitation forcing remains limited (i.e. performed well in some regions but not others). Döll and Siebert (2002) and Hanasaki et al. (2006) estimated different irrigation water demand using the same method, however with different meteorological input, the CRU and the ISLSCP, respectively (see chapter 3).

Availability of water demand data is a major issue in global water stress assessments as well. This is considered as a main reason to hinder monthly water stress assessments on a global scale. Although finer spatial scales are being used due to recent technological developments, finer temporal scales (e.g. monthly) have not yet been realized. Water withdrawal data are mostly based on a yearly temporal scale. This particularly causes a difficulty to estimate monthly irrigation water demand due to different cultivation periods and crop growth. To overcome this difficulty, Döll and Siebert (2002) developed the criteria for the optimal starting date for growing crops; however, only irrigation water demand of rice and non-rice was computed. Later, Hanasaki et al. (2006) calculated irrigation water demand of rice and non-rice with the same method. Döll and Siebert (2002) stated that the simulated cropping patterns and growing seasons generally appear to reflect reality, but given the simplicity of the model, only the dominant features are represented, and some discrepancies certainly occur. The latest global data set of monthly growing areas of 26 irrigated crops around the year 2000 (MIRCA2000; Portmann et al., 2008) can lead to a major progress in estimating monthly irrigation water demand. This study made use of this data to improve the accuracy of irrigation water demand as well as to quantify more precisely the seasonal irrigation habits.

However, available global data on industrial and domestic water demand are still limited. It was eventually necessary to make assumptions to overcome these difficulties although this might, in turn, result in inaccuracies in the assessment. In this study, several assumptions were made resulting from data deficiency. Thus, population, livestock and industrial water demand, and reservoir volume are not changed over the year.

An overview of available data including meteorological, hydrological and water withdrawal data and detailed references are given in the Appendix A.

1.5.4. Validation

To reduce errors, it is important to evaluate the input (e.g. meteorological data) and validate the output (e.g. runoff, reservoir operation and water demand) comparing previous studies and observation data if available. Hanasaki et al. (2007a) tried to evaluate the meteorological forcing data using different data sources such as the GSWP, the ISLSCP, the CRU and the ERA-40 and validate the output, runoff, comparing observation data from GRDC (Global Runoff Data Centre; http://grdc.bafg.de/) and other studies (Baumgartner and Reichel, 1975; Nijssen et al., 2001b; Fekete et al., 2002; and Döll et al., 2003). They used the root mean square error (RMSE) to validate runoff. They tried to create the most accurate meteorological forcing data using different data sources. Tanaka et al. (2005) also evaluated meteorological forcing data of the GSWP, the ISLSCP, the CRU and the ERA-40. They ranked the accuracy of these data by using the RMSE.

In this study, we tried to include some validation processes for runoff, river discharge, reservoir operation and water demand. It was not possible to validate water demand estimation for livestock, industry and households and municipalities due to data constraints. For the reservoir operation, it was possible to validate simulation results (e.g. monthly releases from reservoirs) in a limited number of countries such as the U.S.A. and Thailand where reservoir operation data are publicly accessible.

2. Water Availability at a Monthly Time Scale

2.1. Introduction

At present, MHMs are widely used to estimate runoff and river discharge (i.e. blue water) on regional to global scales. In general, water availability often refers to blue water availability and blue water availability is defined as the total river discharge, which is precipitation minus evapotranspiration or the sum of surface runoff and groundwater recharge (Flörke and Alcamo, 2004). Blue water availability from surface sources or shallow groundwater wells depends on the seasonality and interannual variability of streamflow (Kundzewicz et al., 2007). In addition to blue water, there is also rainfall stored in the soil (i.e. green water; Falkenmark et al., 1997). Available green water depends on soil water holding capacity, soil properties, soil depth and soil saturation. Although green water is not available for industrial and domestic use, it is a very important resource for agricultural use to cultivate irrigated and rainfed crops. In this study, unlike previous studies of water stress assessment (see chapter 1) both blue water (the total river discharge) and green water (soil water or soil moisture storage) were included as water availability but the resulting scarcity was assessed separately.

Most MHMs are a hybrid of physically based as well as conceptual components (Nijssen et al., 2001b). They have a high level of process detail and spatiotemporal resolution. One practical problem in application of MHMs is a model parameterization; the energy exchange at the atmosphere-land surface interface is usually based on physical principles, while the runoff generation mechanisms tend to be more conceptual in nature (Nijssen et al., 2001b). Model outputs are largely affected by meteorological (climate) inputs as well. Although there are inherent uncertainties, MHMs are still useful tools to quantify global water availability.

In this study, we simulated runoff, river discharge and soil water storage on a global scale except Antarctica by using PCR-GLOBWB. We used a daily time step as temporal resolution to simulate transient behaviour of terrestrial hydrological processes. All drainage from the soil surface is passed to the open water surface; these surfaces are connected between cells and constitute a drainage network of rivers and wetlands, lakes or reservoirs through which water is routed to give discharge over time (van Beek, 2007b). Precipitation falling directly on the open water surface is added prior to routing whereas evaporation is withdrawn (van Beek, 2007b). In the end, we used mean monthly river discharge as blue water availability and mean monthly soil water storage as green water availability.

To test the model, we validated simulation results with previous studies by means of continental runoff (see section 2.3.). We also validated model results with available observation data of river discharge (e.g. Volga-Akhtuba[14]) after implementing reservoir operation scheme and tested on the temporal performance.

2.2. PCRaster GLOBal Water Balance Model (PCR-GLOBWB)

2.2.1. Model Concept

In this section of 2.2., the model descriptions of PCR-GLOBWB are given. These model descriptions including tables and figures are entirely based on the model descriptions written by van Beek (2007b). Further reference can be found in van Beek (2007b).

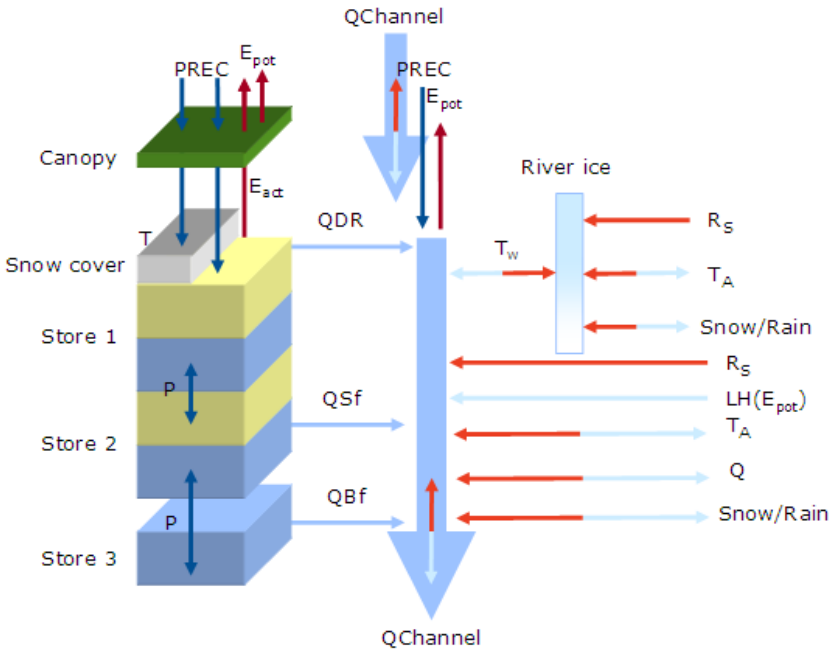

Figure 2.1: Model concept of PCR-GLOBWB.

PCR-GLOBWB is a hydrological model that simulates the terrestrial hydrology at macro-scales, e.g. continental to global, under various land use and climate conditions with an operational temporal resolution of one to several days. PCR-GLOBWB is written in the meta-language of the PCRaster GIS package (Wesseling et al., 1996). It is fully distributed and implemented on a regular grid; 0.5° grid cell sizes and daily time

[14] The observation data of river discharge in Volga-Akhtuba were obtained from Drs. Lara van den Bosch of the Department of Physical Geography, Utrecht University by personal communication.

steps were used for this study. Figure 2.1 shows the model concept of PCR-GLOBWB; on the left, the soil compartment, which is divided in the two upper soil stores and the third groundwater store and their corresponding drainage components: direct runoff (*QDR*), interflow (*QSf*) and base flow (*QBf*). In the centre, the resulting discharge along the channel (*QChannel*) with lateral in- and outflow and local gains and losses are depicted, on the right, the energy balance for the open water surface and the possible formation of ice are shown. In line with the general nature of the MHM the energy stored in open water is modelled in a simple manner as the balance between the heat exchange with the atmosphere and the net, advected energy. The water body exchanges energy with the atmosphere or with an ice cover if present. The water energy balance is evaluated together with that of a potential or actual ice cover. Ice will form or grow if the air temperature is below freezing point (TT = 0°C, see equation 2.5).

PCR-GLOBWB simulates the most direct pathways of water that reaches the Earth surface back to the ocean or atmosphere (see figure 2.1); within each cell precipitation in the form of rain or snow either falls on soil or in open water surface. Any precipitation that falls on the soil surface can be intercepted by vegetation and in part or in whole evaporated. Snow is accumulated when the temperature is sufficiently low, otherwise it melts and adds to the liquid precipitation that reaches the soil as rain or throughfall. A part of the liquid precipitation is transformed in direct or surface runoff, whereas the remainder infiltrates into the soil. The resulting soil moisture is subject to soil evaporation when the surface is bare and to transpiration when vegetated; the remainder contributes in the long-term to river discharge by means of slow drainage which is subdivided into subsurface storm flow from the soil and base flow from the groundwater reservoir.

2.2.2. Sub-grid Variability

PCR-GLOBWB returns the resulting states and fluxes of each of the above processes. Each cell represents a square area of size A_{Cell} [m^2] and sides $\sqrt{A_{Cell}}$ [m], with missing values where land is absent. The returned cell values represent averages over relatively large areas, with some sub-grid variability being taken into account. The most fundamental subdivision is that of each cell into the open water surface and the actual land surface, which is given by:

$$A_{Cell} = A_{Land} + A_{Water} = A_{Cell}\left(Frac_{Land} + Frac_{Water}\right), \tag{2.1}$$

where A_{Cell} is the area within a cell not occupied by oceans (total land surface, in [m^2]) and A_{Land}, A_{Water} and $Frac_{Land}$, $Frac_{Water}$ represent respectively the areas (m^2) and fractions [-] of land and open water surface within the cell.

The hydrological processes on the actual land surface or soil compartment are confined to a single cell. Within each cell, the parameterization is further subdivided on the basis of vegetation (see figure 2.2). A distinction is made between short and tall vegetation since tall vegetation more effectively draws water from deeper in the soil and generally incurs higher interception losses. Where a distinction is made between land cover types at the sub-grid level, state variables are stored as the cell average:

$$\bar{x} = (1-v)x_{short} + vx_{tall}\,, \tag{2.2}$$

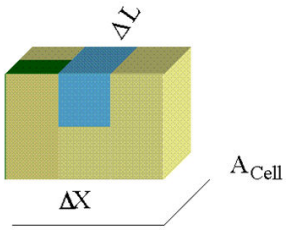

Figure 2.2: Sub-grid parameterization of each cell with cell area A_{Cell}, its width ΔX and length ΔL, subdivided into the open water surface (blue), short vegetation (beige) and tall vegetation (dark green).

Also, the production of direct runoff is dependent on the fraction of the saturated area given a distribution of the water holding capacity of the soil within the cell as described by the improved Arno Scheme (Hagemann and Gates, 2003).

2.2.3. Local Drain Direction (LDD)

Routing of water through the drainage network is prescribed by the local drain direction map or LDD which allows flow in 8 cardinal directions over 360° (see figure 2.3). Channel dimensions, gradient and roughness need to be specified. The model postulates a rectangular cross-section for which the width ΔX [m] is given by:

$$\Delta X = \frac{Frac_{Water} * A_{Cell}}{\Delta L}\,, \tag{2.3}$$

where ΔL is the channel length in m, which is calculated from the local drain direction and the cell area.

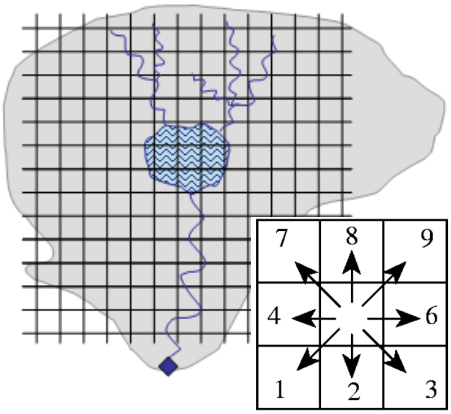

Figure 2.3: Representation of the open water network with lake surface interrupting flow within a catchment and outflow point (◆=5).

2.2.4. Land Surface

The land surface of PCR-GLOBWB coincides with that of the 5 minutes (i.e. 0.083° or roughly 9 km by 9 km at the equator) land mask of the FAO Digital Soil Map of the World (FAO, 1990) with Antarctica left out. Any 0.5° cell containing at least one 5 minutes land cell is represented as land surface with the corresponding surface area in m^2. The process descriptions are repeated for the two land cover types distinguished, i.e. *short* and *tall*, respectively on the basis of vegetation height.

2.2.5. Canopy: Interception and Evapotranspiration

For the two land cover types (*i*), fractional vegetation cover, c_v [-], partitions the potential evapotranspiration into the potential bare soil evaporation, $E_p i$, and canopy transpiration, $T_P i$. Also, it determines whether precipitation falls directly onto the surface or is intercepted by the canopy, for which no distinction between rain and snow is made:

$$P_{Net} i = (1 - c_v i) P_{Gross} + P_{Throughfall} i \,, \tag{2.4}$$

where P_{Net} is the net precipitation reaching the soil surface, P_{Gross} is the gross precipitation falling on the canopy and $P_{Throughfall}$ is the precipitation that is passed on to the soil surface when the interception storage is exceeded. The different precipitation components are the total amounts in [m] for the current time step. The index *i* denotes the type of vegetation cover under consideration, i.e., short or tall.

2.2.6. Snow Cover: Accumulation and Melt

Snow accumulation and melt are entirely temperature-dependent, conform the snow module of the HBV model (Bergström, 1995), with a threshold temperature, *TT* [°C], deciding whether precipitation accumulates as snow or the accumulated snow layer melts. By default, the threshold temperature is 0°C and the amount of snowfall can be corrected for undercatch and winter evaporation by means of a correction factor, *SFCF* [-]. Snow melt is calculated from a simple degree-day factor *CFMAX* [m °C^{-1}·day^{-1}] when the temperature exceeds the threshold temperature:

$$\Delta SC = CFMAX * (T - TT)\Delta t\,, \tag{2.5}$$

where ΔSC is the liquid water resulting from snow melt, T is the air temperature (°C) and Δt is the length of the time step (day).

2.2.7. Soil: Direct Runoff and Infiltration

Liquid water passed on from the snow cover to the soil surface infiltrates if sufficient storage capacity is available, else it drains over the surface as direct runoff. Following the concepts developed by Zhao (1977) and Todini (1996) the partitioning into infiltration and direct runoff is dependent on the degree of saturation and the distribution of available storage in the soil. In the original concept, the minimum storage capacity was zero, thus always yielding runoff when water falls onto the soil. Since this assumption may lead to an overestimation of runoff, the modification of Hagemann and Gates (2003) was implemented, which is known as the Improved Arno Scheme (IA).

According to the IA, the following relation holds reasonably well between the fractional area at saturation, x, and the ratio of the local soil moisture storage capacity w in [m] in relation to the minimum and maximum storage capacities w_{min} and w_{max} for the entire area:

$$x = 1 - \left(\frac{w_{max} - w}{w_{max} - w_{min}} \right)^{b}, \tag{2.6}$$

where b is a dimensionless shape factor (-) that defines the distribution of w between w_{min} and w_{max} over a large number of elements within the pervious area. This expression reduces to that of the Arno Scheme when w_{min}= 0.

Runoff, R, can only occur when liquid precipitation, P_n, falls on the surface and the stored moisture and the liquid precipitation combined exceed the minimum storage capacity, w_{min}. Moreover, any liquid precipitation is converted into direct runoff once pervious area is completely saturated. In terms of the area-averaged soil moisture storage W with W_{max} being the average storage capacity of the pervious area and W_{min} (= w_{min}) the minimum, runoff can now be calculated with the following equation:

$$R = P_n - \left(W_{max} - W\right) + \left(W_{max} - W_{min}\right)\left(\left(\frac{W_{max} - W}{W_{max} - W_{min}}\right)^{\frac{1}{b+1}} - \frac{P_n}{\left(b+1\right)\left(W_{max} - W_{min}\right)}\right)^{b+1} . \quad (2.7)$$

Equation 2.7 estimates the runoff when $w_{min} < P_n+w < w_{max}$ or in terms of the area-average storage capacities when:

$$P_n < \left(b+1\right)\left(W_{max} - W_{min}\right)\left(\frac{W_{max} - W}{W_{max} - W_{min}}\right)^{\frac{1}{b+1}}, \quad (2.8)$$

$$P_n + W - W_{min} > 0 . \quad (2.9)$$

Else, when $P_n+w \geq w_{max}$ or in terms of the area-average storage capacities when:

$$P_n \geq \left(b+1\right)\left(W_{max} - W_{min}\right)\left(\frac{W_{max} - W}{W_{max} - W_{min}}\right)^{\frac{1}{b+1}} . \quad (2.10)$$

The following relation holds:

$$R = P_n - \left(W_{max} - W\right). \quad (2.11)$$

Infiltration, $P_0 i$, is in this case the difference between the net liquid rainfall, $P_n i$, and the direct runoff, Ri, augmented with any initial storage to replenish the storage to W_{min}. When the infiltration rate exceeds the saturated hydraulic conductivity of the first layer, the infiltration excess is passed on to the direct runoff, if the total infiltration exceeds the storage capacity of the first layer, it is handed down to the second store.

2.2.8. Soil: Bare Soil Evaporation and Transpiration

Like precipitation, evaporation and transpiration are treated as uniform for each land cover type over the duration of a time step. Bare soil evaporation is drawn from the topsoil not covered by vegetation at the maximum rate of the potential evaporation:

$$E_a i = x \cdot E_p i + (1 - x) f \cdot E_p i \,, \tag{2.12}$$

where E_a is the actual evaporation, E_p is the potential evaporation, x and $1-x$ is the saturated and unsaturated part of the pervious area, respectively and the index i denotes the type of vegetation cover under consideration, i.e., short or tall, respectively.

Equation 2.12 stipulates that the bare soil evaporation is not limited for the saturated part of the pervious area, x, and occurs at a reduced rate, $f \cdot E_p$, for the unsaturated area, $1-x$, where f is a dimensionless reduction factor:

$$f = \frac{W_{max} + b(W_{max} - W_{min}) \left[1 - \frac{b+1}{b} \left(\frac{W_{max} - W}{W_{max} - W_{min}} \right)^{\frac{1}{b+1}} \right]}{W_{max} + b(W_{max} - W_{min}) \left[1 - \left(\frac{W_{max} - W}{W_{max} - W_{min}} \right)^{\frac{1}{b+1}} \right]} . \tag{2.13}$$

Vegetation extracts water from the soil by transpiration except when the soil is saturated and the lack of aeration prevents root water uptake. The area-averaged transpiration T_a is therefore entirely attributable to the unsaturated area $1-x$.

2.2.9. Soil: Percolation and Capillary Rise

Water moves through the soil proportional to the unsaturated hydraulic conductivity:

$$k(\theta_E)i,j = k_r(\theta_E)i,j \cdot k_s i,j\ , \tag{2.14}$$

where the indices i and j stand respectively for the land cover and soil layers, θ_E is the relative degree of saturation and $k_r(\theta_E)$ is the relative unsaturated hydraulic conductivity (both dimensionless and varying between 0-1), and k_s and $k(\theta_E)$ are respectively the saturated and unsaturated hydraulic conductivity [$m \cdot d^{-1}$]. The relative degree of saturation is calculated as the ratio between the actual storage in layer Si, j and its maximum storage capacity $S_C i, j$ [m].

In the model percolation, Pi, j, is driven by gravitational flow only and equal to:

$$Pi,j = k(\theta_E)i,j\Delta t. \tag{2.15}$$

If the relative degree of saturation of the top layer is smaller than that of the underlying second store, an upward capillary rise, CRi, j, will occur that is driven by the soil moisture deficit in the top layer and proportional to the unsaturated hydraulic conductivity of the second layer:

$$CRi,1 = (1-\theta_E i,1)k(\theta_E)i,2 \cdot \Delta t\ ,. \quad \text{if}\ \ \theta_E i,1 < \theta_E i,2\ , \tag{2.16}$$

or,

$$CRi,1 = 0\ , \quad \text{if}\ \ \theta_E i,1 \geq \theta_E i,2\ . \tag{2.17}$$

2.2.10. Soil: Interflow

From the two upper soil compartments water drains laterally over the height of the saturated wedge that may form over the contact with the third compartment (i.e. the groundwater reservoir) when the recharge in the upper soil is high, percolation to the groundwater is low and the gradient that drives lateral flow along the slope is high. This lateral drainage, known as subsurface storm flow or interflow, is modelled here using a simplified approach based on the work of Sloan and Moore (1984) and Ormsbee and Khan (1989) in which the soil is idealized as a uniform, sloping slab with an average soil depth and inclination.

$$L_s(t)v(t) - q(L_s,t) = L_s(t)v(t) - k_s h(L_s,t)\tan\beta_s = \frac{B_s(t+1) - B_s(t)}{\Delta t}, \qquad (2.18)$$

where $B_s(t)$ is the storage [m^3 per unit m in-plan depth] in the saturated wedge at time t [d], h is the groundwater height normal to the slope [m] and L_s is the slope length [m]. $v(t)$ is the percolation rate, i.e. net percolation minus net groundwater recharge [$m \cdot d^{-1}$], $q(L_s,t)$ is the discharge in [$m^3 \cdot d^{-1}$] per unit m in plan depth and k_s is the saturated hydraulic conductivity [$m \cdot d^{-1}$].

2.2.11. Soil: Base Flow

The third store of the soil compartment represents the deeper part of the soil that is exempt from any direct influence of vegetation and constitutes a groundwater reservoir fed by active recharge. This recharge consists of the net percolation (i.e. percolation from the second store minus capillary rise from the third into the second store). Drainage from this groundwater reservoir contributes as base flow to the total discharge. This is described by a linear store, with the drainage, Q_3 in [$m \cdot day^{-1}$], given by:

$$Q_3 = \alpha S_3 \Delta t, \qquad (2.19)$$

where α is the recession constant in [d^{-1}] and S_3 the storage in the third layer [m].

Additional subtractions of groundwater for consumptive water use can be specified.

2.2.12. Soil Water Balance

Combining the above fluxes per time step, the water balance comprises the following terms:

$$\Delta S_{i,j} = P_{i,j-1} + CR_{i,j+1} - \left(P_{i,j} + CR_{i,j} + E_{i,j} + Q_{i,j} + C\right), \qquad (2.20)$$

where ΔS is the change in storage for layer j and land cover type i with gains being included in the positive and losses in the negative term of the above; P is the percolation or infiltration, that is positive from the overlying store, negative towards the underlying store and CR is the

capillary rise, which is negative towards the overlying store, positive when coming from the underlying store. E is the actual evapotranspiration ($E = E_a + T_a$), E_a is the actual bare soil evaporation and T_a the actual canopy transpiration. Q is the lateral drainage and C is any sink due to water consumption, all negative. Units are all in [m] water slice per time step.

Reportable (output) names and descriptions of land cover dependent variables are given in table 2.1.

Table 2.1: Reportable names and descriptions of land cover dependent variables and cell-averaged ones from van Beek (2007b).

Land-cover dependent	Cell-averaged	Description	Unit
sc	snocov	Water-equibalent depth of snow cover	m: meter
scf	snowliq	Liquid water storage in snow cover	m
ints	intstor	Interception storage	m
	eact	Actual evapotranspiration	$m \cdot day^{-1}$
	qlx	Direct runoff, saturation and infiltration excess	$m \cdot day^{-1}$
	qls	Direct runoff attributable to snow melt	$m \cdot day^{-1}$
s1	stor1x	Storage in first store	$m \cdot day^{-1}$
q2	q2x	Interflow, drainage from scond store	$m \cdot day^{-1}$
s2	stor2x	Storage in second store	m
	r3x	Recharge to third store	$m \cdot day^{-1}$
	q3x	Base flow, drainage from third store	$m \cdot day^{-1}$
	stor3x	Storage in third store	m

2.2.13. Surface Water: River Discharge

River discharge is calculated by accumulating all specific runoff (i.e. precipitation minus actual evapotranspiration) along the LDD, taking evaporative loss over open water surface (i.e. lakes, wetlands and reservoirs) into account. The total runoff from the land surface is fed without delay to the river network prior to routing. Water of the contiguous areas of open water surface such as lakes, wetlands and reservoirs can evaporate freely at a rate set by the potential evaporation. Then, river discharge is calculated from the kinematic wave approximation of the Saint-Venant Equation (Chow et al., 1988). A numerical solution of the kinematic wave approximation is available as an internal function in PCRaster in which the new discharge Q_{t+1} at every point along the

channel is calculated from the discharge from the previous time step. The length of the channel and the time step are ΔL [m] and Δt [s], respectively. The lateral inflow in the channel, q, is calculated from the total drainage from the land surface and any direct inputs to the open water surface, Q_w [m·s^{-1}]. The calculated discharge at the outlet is added within the time step to the lateral inflow in the kinematic wave approximation:

$$q = \frac{Q_{tot}}{\Delta L} = \frac{A_{cell}}{\Delta L}\left(\left[1 - Frac_{Water}\right] \sum_i Q_i + Frac_{Water} \cdot Q_W \right), \tag{2.21}$$

where Q is the streamflow through the channel [m^3·s^{-1}], A is the channel cross-section [m^2], q is the inflow per length of channel [m^2·s^{-1}] and $\sum_i Q_i$ is the streamflow along the channel from the land surface [m·s^{-1}].

The change in river discharge is the balance of inflow and outflow if the lake interrupts the river network. The inflow is the incoming river discharge [m^3·s^{-1}], the outflow is calculated in analogy to the weir formula (Bos, 1989) as the discharge through a rectangular cross-section:

$$Q_{Out} = C \cdot \tfrac{2}{3}\sqrt{\tfrac{2}{3} g}\, b (h - h_0)^{3/2} \Delta t \approx 1.70\, C \cdot b (h - h_0)^{3/2} \Delta t\,, \tag{2.22}$$

where b is the breadth of the outlet [m], g is the gravitational acceleration [m·s^{-2}] and h and h_0 are respectively the actual lake level and the sill of the outlet [m]. Δt is the time step. C is a correction factor [m$^{4/3}$·s^{-1}] that corrects among others for the effects of back- and tail waters, viscosity, turbulence and deviations from the assumed uniform flow distribution, which was kept at unity in this study.

In addition, the change in river discharge due to the alteration by reservoirs (e.g. dams) is modeled separately from PCR-GLOBWB with a reservoir operation scheme (see section 2.4.).

2.2.14. Water Balance for the Open Water Surface

The water balance for the open water surface includes first an evaluation of the total volume of water per unit channel length that is added or subtracted from the surface water network, q [m^2]. This includes drainage from the soil compartment, direct pre-

cipitation and evaporation to the channel and any withdrawals for water consumption. By default, this amount is broken up in 6 4-hourly time steps for which the water balance and routing and any consequent changes in open water storage, be this in lakes, wetlands or river stretches, are evaluated jointly. 4-hourly time steps are used to maintain stability in the explicit numerical solution to the kinematic wave model. The reportable variables for the open water surface are listed in table 2.2.

Table 2.2: Reportable variables for the open water surface. Channel discharge and water height are also reported as a timeseries for catchment outlets or sample points of interest from van Beek (2007b).

Variable	Unit	Description
$Q_{Channel}$	[$m^3 \cdot s^{-1}$]	Channel discharge for river stretch or over lake surface
$Q_{Average}$	[$m^3 \cdot s^{-1}$]	Idem, averaged for year
WH	[m]	Water height for river stretch or lake surface
WI	[m]	Ice thickness over open water surface
TW	[°C]	Water temperature

2.3. Specific Runoff (runoff per unit drainage area)

Generally, runoff flows are less than 10% of the rainfall, whereas 50% or more of the rainfall is lost to the atmosphere as non-productive green water flows (direct evaporation; Falkenmark and Rockström, 2005). At present, we depend on data (i.e. observation) and model based climatology or meteorology to compute runoff on a global scale. However, the results of these estimates vary significantly as shown in table 2.3. This causes an inaccuracy of water stress assessment due to different degrees of water availability in a region.

There are two main obstacles to estimate runoff (Alsdorf et al., 2003; Brakenridge et al., 2005; Shiklomanov et al., 2002). One is that climate data collection or monitoring is inadequate within many land areas. It is well accepted that standard precipitation measurement techniques lead to a general underestimation of about 10-15% on a global scale (Bormann et al., 1999) including snow undercatch. The uncertainty of evapotranspiration caused by the spatial transfer of temperature, global radiation, air humidity and wind speed is low compared to the uncertainty caused by precipitation (Bormann et al., 1999). The other is that the data is not readily accessible. These problems are potential causes of uncertainty in estimation of runoff and its validation. Brakenridge et al. (2005) proposed the space-based measurement of river runoff that creates globally distributed

data. This might bring us a great improvement because of the large land areas where gauging station networks have been discontinued (Brakenridge et al., 2005).

We computed runoff by using PCR-GLOBWB with the meteorological data sets of both the ERA-40 (duration: 1957-2002) and the CRU (duration: 1958-2001). The results are given in table 2.3. For continental runoff computed by PCR-GLOBWB with the data of the ERA-40, runoff in each continent is generally much higher that other previous studies although runoff in Europe and North America agree relatively well with other previous studies. The overestimation of runoff in Asia, Africa, South America and Oceania generally attributes to the overestimation of precipitation mainly over the tropical regions. Troccoli and Kållberg (2004) analysed the ERA-40 reanalysis data and found excessive amounts of precipitation over tropical regions when compared to independent estimates of the Global Precipitation Climatology Project (GPCP; http://www.gewex.org/gpcpdata.htm, http://precip.gsfc.nasa.gov). This overestimation is caused by a fundamental problem in the variational analysis of humidity (i.e. humidity analysis deficiency) over tropical oceans in areas of high density observations, such as satellite radiances (Troccoli and Kållberg, 2004). Therefore, this overestimation is not apparent in pre-satellite observation years (Troccoli and Kållberg, 2004).

The precipitation of the period between 1973 and 1978 is especially overestimated not only due to the humidity scheme but also due to an error in the instruments of early NOAA satellites (Troccoli and Kållberg, 2004). This may explains that the runoff between 1961 and 1990 computed by PCR-GLOBWB is much higher than one between 1957 and 2002. The precipitation of the ERA-40 is consistently larger than the precipitation of the GPCP in the latitude of 0° to 15°N/S. For instance, in regions such as near Indonesia and west of Panama, precipitation exceeds 10 $mm \cdot day^{-1}$, which is about 7-10 $mm \cdot day^{-1}$ larger than the GPCP (Troccoli and Kållberg, 2004). Differences in precipitation between the ERA-40 and the GPCP are generally about 2-7 $mm \cdot day^{-1}$ in the tropical regions (Troccoli and Kållberg, 2004). Troccoli and Kållberg (2004) also reported that an overestimation of precipitation in 5 $mm \cdot day^{-1}$ occurs over Africa (between 10°S and 10°N). This explains the very high runoff in Africa between 1961 and 1990. Troccoli and Kållberg (2004) tried to find and applied the correction factor of precipitation over the entire ERA-40 period (1957-2002).

Table 2.3: Continental runoff based on data and model based estimates in $km^3 \cdot year^{-1}$.

Continents	Europe	Asia	Africa	North America	South America	Oceania	Global (except Antarctica)	Time Period
Data based estimates								
Baumgartner and Reichel (1975)	2564	12,467	3409	5840	11,039	2394	37,713	-
Korzun et al. (1978)	2970	14,100	4600	8180	12,200	2510	44,560	-
L'vovich (1979)	3110	13,190	4225	5960	10,380	1965	38,830	-
Shiklomanov (1997)	2900	13,508	4040	7770	12,030	2400	42,648	1921-1990
GRDC (2004)	3083	13,848	3690	6294	11,897	1722	40,533	1961-1990
Average	*2925*	*13,423*	*3993*	*6809*	*11,509*	*2198*	*40,857*	-
Model based estimates								
Fekete et al. (2000)	2772	13,091	4517	5892	11,715	1320	39,319	-
Vörösmarty et al. (2000)	2770	13,700	4520	5890	11,700	714	39,294	1961-1990
Nijssen et al. (2001b)	-	-	3615	6223	10,180	1712	36,006	1980-1993
Oki et al. (2001)	2191	9385	3616	3824	8789	1680	29,485	1987-1988
Döll et al. (2003)	2763	11,234	3592	5540	11,382	2239	36,687	1961-1990
Widén-Nilsson et al. (2007)	3669	13,611	3738	7009	9448	1129	38,605	1961-1990
Average	*2833*	*12,204*	*3933*	*5730*	*10,536*	*1466*	*36,566*	-
PCR-GLOBWB (ERA-40)	**2810**	**20,965**	**12,794**	**8343**	**16,749**	**4963**	**66,623**	**1961-1990**
PCR-GLOBWB (ERA-40)	**2724**	**18,864**	**6223**	**7256**	**15,010**	**6112**	**56,187**	**1957-2002**
PCR-GLOBWB (CRU)	**2472**	**12,513**	**8118**	**4651**	**13,992**	**2765**	**44,511**	**1961-1990**
PCR-GLOBWB (CRU)	**2476**	**11,365**	**7208**	**4508**	**13,487**	**2701**	**41,745**	**1958-2001**

For continental runoff computed by PCR-GLOBWB with the data of the CRU, runoff in each continent generally agrees well with other previous studies. However, there is a large overestimation of runoff in Africa. The continental runoff in Africa computed by this study is especially high and nearly doubled compared with other previous studies. This overestimation is likely caused by the insufficiency of the meteorological forcing data of evapotranspiration (i.e. evaporation from open water surface such as lakes, wetlands and floodplains) since we used same precipitation data as other studies (e.g. Döll et al., 2003; Vörösmarty et al., 2000; Widén-Nilsson et al., 2007) listed in table 2.3. These results of continental runoff computed by PCR-GLOBWB are without any correction factors or regionalisation parameters.

Since the simulated continental runoff based on the meteorological data of the ERA-40 is much higher than other studies. It is highly possible to cause overestimation in water availability (i.e. the total river discharge). Therefore, we used the simulated runoff based on the meteorological data of the CRU to estimate water availability (see figure 2.4 and 2.5). Figure 2.4 shows mean monthly specific runoff in million $m^3 \cdot month^{-1}$ in the four seasons over the years between 1958 and 2001 based on the meteorological data of the CRU. Figure 2.5 shows mean accumulated runoff along the LDD or river discharge in $m^3 \cdot second^{-1}$ in the four seasons over the years between 1958 and 2001.

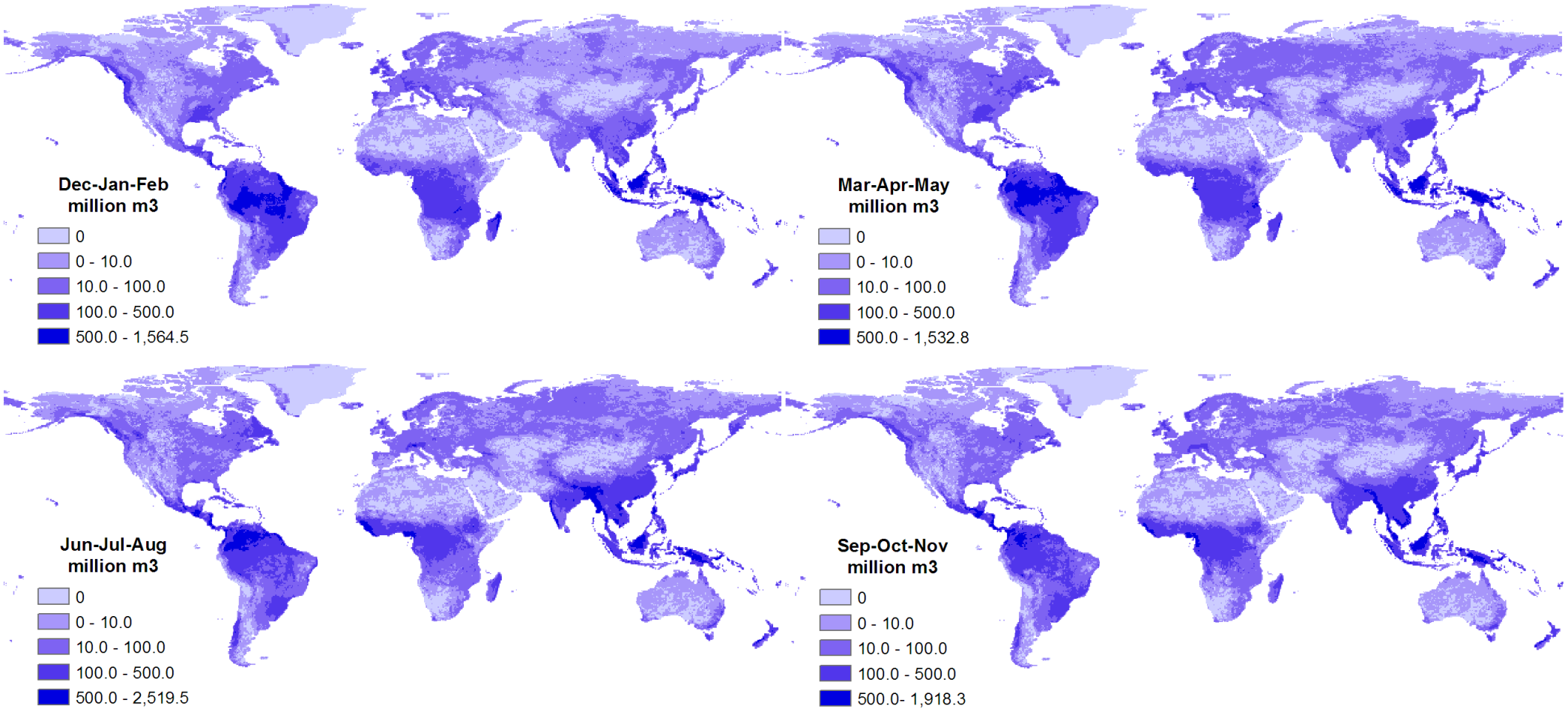

Figure 2.4: Mean specific runoff (million $m^3 \cdot month^{-1}$) in the four seasons over the years between 1958 and 2001.

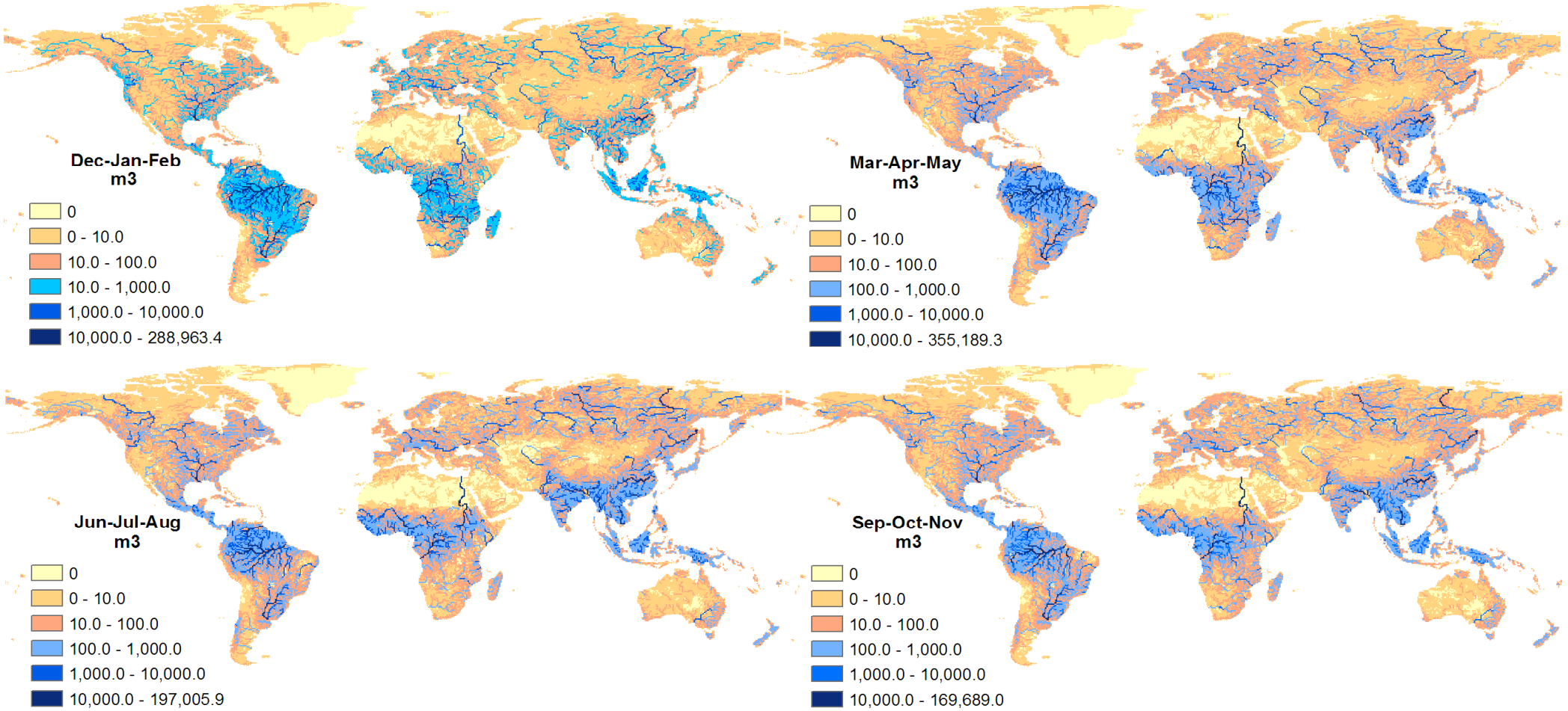

Figure 2.5: Mean river discharge ($m^3 \cdot second^{-1}$) in the four seasons over the years between 1958 and 2001.

2.4. Reservoir Operation

2.4.1. Reservoir Operation Scheme

Most of the world's major rivers are regulated (Nilsson et al., 2005; Vörösmarty et al., 2004) by artificial reservoirs (e.g. dams). The creation of reservoirs in most countries of the world is a result of the development of hydropower and flood control, and the expansion of irrigated areas (Avakyan and Ovchinnikova, 1971) to promote the development of water conservation and to improve water-supply systems (Avakyan, et al., 1979). In North America and many other regions, spring floodwaters from snowmelt are stored in reservoirs for later use (Jackson et al., 2001).

The World Register of Dams (WRD; ICOLD, 2003) reports nearly 50,000 large dams (defined as being 15 m or higher dam height) on a global scale. 35% of these large dams are designed for irrigation purposes only (Haddeland et al., 2006). Since the total storage capacity of reservoirs (7000 km^3) in the world comprises three times the annual average water storage in river channels (1200-2120 km^3) and one-sixth of the global annual river discharge (40,000 $km^3 \cdot year^{-1}$; Baumgartner and Reichel, 1975), the effect of reservoir operations on river discharge is not negligible. Hanasaki et al. (2006) indicated that river discharge was altered more than ± 20% after implementing a reservoir operation scheme. Therefore, reservoir operation significantly affects the amount of the water available to a region. Yet, global water balance models are rarely coupled with reservoir operation schemes at present.

Several previous studies (Coe, 2000; Dynesius and Nilsson, 1994; Haddeland et al., 2006; Hanasaki et al., 2006; Meigh et al., 1999; Nilsson et al., 2005; Vörösmarty et al., 1997) described about the effect of reservoir operations and some of them developed their own algorithm to include reservoir operations for simulating river discharges on both regional and global scales. Among them, Hanasaki et al. (2006) developed an algorithm to set operating rules for individual reservoirs of the 452 largest reservoirs on a global scale. At first, they defined monthly operating rules for reservoirs. Then, they categorized each month as either a recharge, where inflow exceeded the mean annual inflow, or a release month. Next, they coupled the categorized months with monthly river discharge and downstream water withdrawal (irrigation, industry and households and municipalities). Monthly water withdrawal of industry and domestic was set as constant because the data did not exist. Then, they also categorized reservoir purpose (usage) into two classes: irrigation and non-irrigation although initial database of the WRD (ICOLD, 1998) categorized into seven classes: hydropower, water supply, flood control, irrigation, navigation, recreation and other. Hanasaki et al. (2006) coupled res-

ervoir simulation with global river discharge simulation to quantify the impact of reservoir operations on the terrestrial water cycle. Hanasaki et al. (2006) indicated that reservoirs for irrigation water use influence largely the river discharges compared to the other categories. Irrigation water withdrawal exhibits large seasonal fluctuations and becomes zero during the non-cropping season (Hanasaki et al., 2006).

The algorithm of reservoir operations developed by Hanasaki et al. (2006) is a relatively simple structure for both non-irrigation (see equation 2.23) and irrigation purpose (see equation 2.24). In addition, they developed another algorithm to reproduce the reservoir release determined by the storage capacity (i.e. capacity-driven release; see equation 2.27 and 2.28). They tested capacity-driven release at the Canyon Ferry Reservoir (purpose: hydropower) and showed that the simulated release was close to the observed release (i.e. outflow). Hanasaki et al. (2006) also tested their algorithm of non-irrigation and irrigation purpose together with other algorithms of constant release (constant release of the mean monthly inflow), natural lake (equation 6 of Döll et al., 2003) and run-of-the-river (release is identical to inflow). Their results showed that the simulated release by their algorithm was closer to the observed release than that by other algorithms for both non-irrigation and irrigation purpose. This study categorized reservoirs into three classes: non-irrigation, irrigation and hydropower (i.e. capacity-driven). We applied capacity-driven release to hydropower. We used same algorithm of reservoir operation scheme developed by Hanasaki et al. (2006).

For a non-irrigation reservoir:

$$r'_{m,y} = i_{mean}, \tag{2.23}$$

where $r'_{m,y}$ is the provisional monthly release ($m^3 \cdot second^{-1}$) and i_{mean} is the mean annual inflow ($m^3 \cdot second^{-1}$).

For an irrigation reservoir:

$$r'_{m,y} = \begin{cases} \dfrac{i_{mean}}{2} \times \left(1 + \dfrac{\sum_{area} \left\{ k_{alc} \times \left(d_{irg,m,y} + d_{ind} + d_{dom} \right) \right\}}{d_{mean}} \right), \\ (d_{mean} \geq 0.5 \times i_{mean}), \\ i_{mean} + \sum_{area} \left\{ k_{alc} \times \left(d_{irg,m,y} + d_{ind} + d_{dom} \right) \right\} - d_{mean}, \\ (d_{mean} < 0.5 \times i_{mean}), \end{cases} \tag{2.24}$$

$$d_{mean} = \sum_{area} \left\{ k_{alc} \times \left(d_{irg,mean} + d_{ind} + d_{dom} \right) \right\}, \tag{2.25}$$

$$k_{alc} = \frac{1}{N_{up}}, \tag{2.26}$$

where $r'_{m,y}$ is the provisional monthly release ($m^3 \cdot second^{-1}$) and i_{mean} is the mean annual inflow ($m^3 \cdot second^{-1}$). $d_{irg,m,y}$ is the monthly irrigation water demand ($m^3 \cdot second^{-1}$), d_{ind} is the monthly industrial water demand ($m^3 \cdot second^{-1}$), d_{dom} is the monthly domestic water demand ($m^3 \cdot second^{-1}$) and d_{mean} is the mean annual total water demand of the reservoir ($m^3 \cdot second^{-1}$). $d_{irg,mean}$ is the monthly irrigation water demand ($m^3 \cdot second^{-1}$). The sub-scripts m, y and mean indicate month, year and mean annual, respectively. The term $\sum_{area}$ indicates integration over the basin downstream of each reservoir. Downstream was defined as including the reach down to the next reservoir, or, if there were no further reservoirs, down to the river mouth.

The term k_{alc} is a non-dimensional allocation coefficient for grid-squares that had more than one reservoir upstream. k_{alc} is determined by the number of upstream reservoirs or N_{up} (-). k_{alc} is proportional to the mean annual inflow from upstream reservoirs, and k_{alc} is 1 if the grid point has only one irrigation reservoir upstream.

For a hydropower reservoir:

$$r_{m,y} = k_{rls,y} \times r'_{m,y}, \qquad (c \geq 0.5), \tag{2.27}$$

$$\begin{aligned} r_{m,y} &= \left(\frac{c}{0.5} \right)^2 k_{rls,y} \times r'_{m,y} + \left\{ 1 - \left(\frac{c}{0.5} \right)^2 \right\} i_{m,y}, \\ r_{m,y} &= \left(\frac{c}{0.5} \right)^2 k_{rls,y} \times r'_{m,y} + \left\{ 1 - \left(\frac{c}{0.5} \right)^2 \right\} \left(i_{m,y} \times 2.0 \right), \end{aligned} \qquad (0 \leq c < 0.5), \tag{2.28}$$

$$k_{rls,y} = S_{first,y} / \lambda C, \tag{2.29}$$

where $r_{m,y}$ is the monthly release ($m^3 \cdot second^{-1}$), c is the ratio of storage capacity to mean total annual inflow ($c = C / I_{mean}$), $k_{rls,y}$ is the release coefficient, which reflects the storage capacity at the beginning of the operational year or $S_{first,y}$, $r'_{m,y}$ is the provisional monthly release ($m^3 \cdot second^{-1}$) for an irrigation reservoir and $i_{m,y}$ is the monthly inflow ($m^3 \cdot second^{-1}$).

For a hydropower reservoir, Hanasaki et al. (2006) conducted a sensitivity analysis of the monthly inflow, $i_{m,y}$. They multiplied $i_{m,y}$ by values ranging from 0.5 to 4.0. When $i_{m,y}$ is multiplied by 2.0 (see equation 2.28), constant release depending on the amount of inflow is generated (Hanasaki et al., 2006) that simulates the release closer to the observed release (i.e. outflow). The term λ is a non-dimensional constant. Hanasaki et al. (2006) developed λ by a sensitivity test with different λ values ranging from 0.65 to 0.95. A smaller λ value produces a larger $k_{rls,y}$, thus larger monthly release. They set λ = 0.85 for global application. We also set λ = 0.85 in this study.

The reservoir operation scheme derived by Hanasaki et al. (2006) is designed to reproduce mainly inter-annual fluctuations in reservoir release and monthly fluctuations estimated from irrigation water demand. This simplistic approach works well with currently available global data such as reservoirs, runoff, river discharge and water demand, and with river routing models (Hanasaki et al., 2006).

For the reservoir data, we used following three data sets, the WRD (ICOLD, 1998, 2003), UNEP (2007) and the WWDR-II. Initially, we obtained the data of 668 reservoirs from the WWDR-II. This data includes dam names, height, storage capacity and geographical locations (longitude/latitude, nearest city and country). For the data of dam purpose, at first we obtained the data from UNEP (2007), however, we found out that only about a half of 668 reservoirs of the WWDR-II matched with the data of UNEP (2007). Therefore, we additionally obtained this data from the World Register of Dams (WRD; ICOLD, 1998, 2003). We placed 668 reservoirs onto the 0.5° global drainage network map of PCR-GLOBWB. Due to the large spatial resolution, 2 or 3 reservoirs fell into the same cell. We took the largest dams based on storage capacity in case there was a coincidence between two or three reservoirs in one cell. In the end, 622 out of 668 reservoirs were placed on the global drainage network map. Figure 2.6 shows the locations of 622 reservoirs in the world.

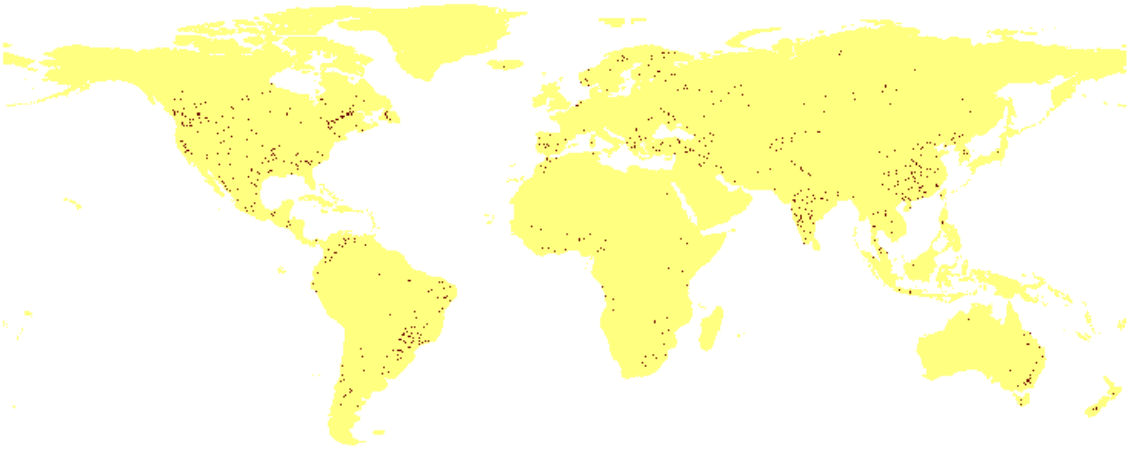

Figure 2.6: Geographical locations of 622 reservoirs in the world.

Reservoir operation data are often unavailable since they commonly involve competing economic interests and can also be in conflict with downstream water-supply needs (Brakenridge et al., 2005). However, some regional reservoir operation data can be obtained through national or local authorities or governments. Reservoir operation data are especially well-preserved and accessible in the U.S.A. in contrast to other countries. The major data of reservoir operations are yearly or monthly inflow and outflow, yearly or monthly storage, purposes of reservoir operations. These data can be used to develop and validate reservoir operation schemes coupled with river discharge and water withdrawal data (agriculture, industry and households and municipalities). However, validation of reservoir operations is rather limited due to unreadily accessible data on a global scale.

2.4.2. River Discharge under the Influence of Reservoirs

When we include the release from reservoirs that compensates for river water that is removed for irrigation and other purposes, this type of reservoir operation may produce more realistic global water resources assessments (Alcamo et al., 2003b; Oki et al., 2001; Vörösmarty et al., 2000). Yet, the applicability of reservoir operation scheme relies on whether its validation results are good enough. We obtained the reservoir operation data mainly from the U.S.A. (California Data Exchange Center, Department of Water Resources of California; http://thunder.water.ca.gov/reservoir.html) and Thailand (Energy Generation Agency of Thailand; http://tiwrm.hpcc.nectec.or.th/).

We compared the monthly inflow and outflow of reservoirs between the simulation results and the observation data as shown in figures from 2.7 to 2.13. Observed outflow (colour: navy blue) is comparable to simulate reservoir operation (colour: yel-

low). No reservoir (colour: light blue) indicates river discharge without the influence of the reservoir. Observed inflow (colour: pink) is the amount of water flows into the reservoirs. We also compared river discharge between global river discharge simulation (coupled with reservoir operation scheme) and available observation data of Volga-Akhtuba in the Volga River as shown in figure 2.14. Our results indicated that the reservoir operation scheme significantly altered the monthly outflow especially in the irrigation reservoirs, however, did not significantly alter the river discharge in the Volga River. This result may suggest that the effect of the current reservoir operation scheme might not be influential to a large catchment. We concluded that although the reservoir operation scheme does not fully represent actual reservoir operations, it reasonably reproduces actual monthly fluctuations (i.e. monthly outflow from reservoirs) and it is useful to couple with global water balance models to simulate river discharge, which improves accuracy of temporal trends. The reservoir operation scheme is particularly important to determine water availability at a monthly time scale, because the reservoir operation is largely influenced by seasonal irrigation water demand.

In the study of Hanasaki et al. (2006), the magnitudes of irrigation release were not well reproduced. This is probably because the estimated crop calendar did not match with the actual irrigation period. They simulated the crop calendar following the method of Döll and Siebert (2002). This method was a major advance to determine monthly irrigation water demand for rice and non-rice. However, this estimation method heavily relies on precipitation and temperature so that irrigation is assumed to be applied under the optimal climate conditions only. This in turn causes a contradiction. Döll and Siebert (2002) indicated the possibility that the existing water scarcity leads farmers to irrigate under less than the optimal climate conditions. To improve the estimation of actual water release for irrigation, more detailed information on irrigation practice was needed. To overcome this difficulty, we used the latest global data set of monthly irrigated areas and crop calendars for 26 crops (MIRCA2000; Portmann et al., 2008). Our simulated results showed that the reproduction of the magnitudes of irrigation release is close to observation (see figure 2.8 and figures 2.10 to 2.12).

Unlike the study of Hanasaki et al. (2006), we included rainfall gain and evaporative loss of reservoirs. These components are especially important for large reservoirs with large surface areas (Hanasaki et al., 2006). In addition, Döll et al. (2003) noted, in many cases, simulated water withdrawal exceeds simulated river discharge for some period in a year. During this period, groundwater or water from a surface reservoir may be used (Döll et al., 2003), and this water is not included in the study of Hanasaki et al. (2006) but included in this study. Finally, we simulated global river discharge coupled with the reservoir operation scheme between the year 1958 and 2001 with the present

situation of reservoirs. We did not precisely consider whether the reservoirs were present between the year 1958 and 2001 for the sake of long-term simulation. Therefore, reservoirs that were constructed until 2003 (ICOLD, 2003) are present in all years of our simulation. This likely causes a discrepancy for river discharge due to a hypothetical presence of reservoirs. The simulation period of Hanasaki et al. (2006) was 10 years (1987-1996) for non-irrigation reservoirs, 2 years (1987-1988) for irrigation reservoirs and 2 years (1987-1988) for a global river discharge simulation coupled with reservoir operations scheme. They excluded any reservoirs that were not present in their simulation periods.

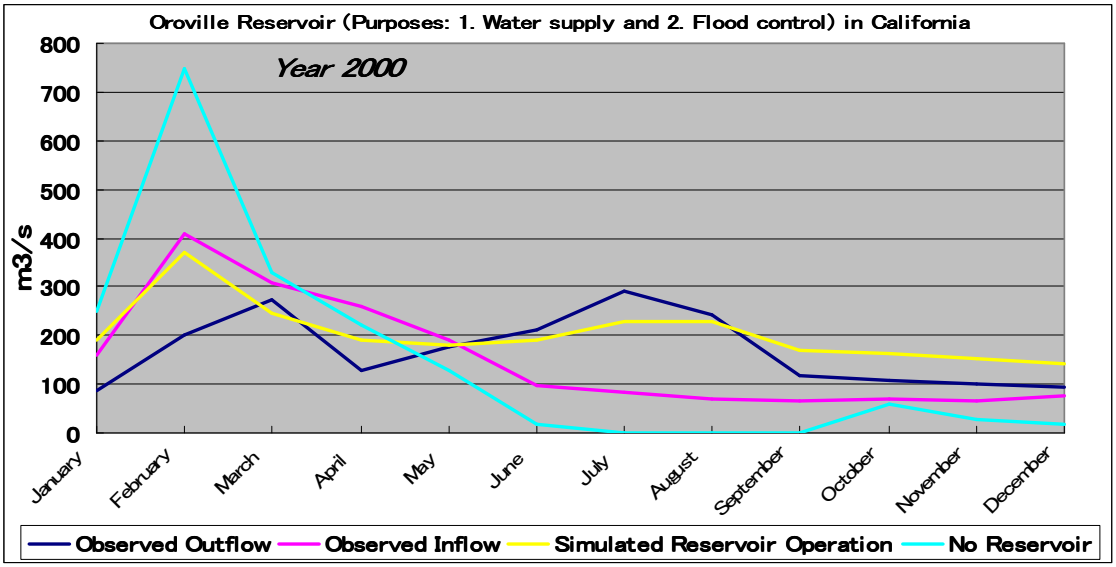

Figure 2.7: Simulated reservoir operation at the Oroville Reservoir in California, the U.S.A.

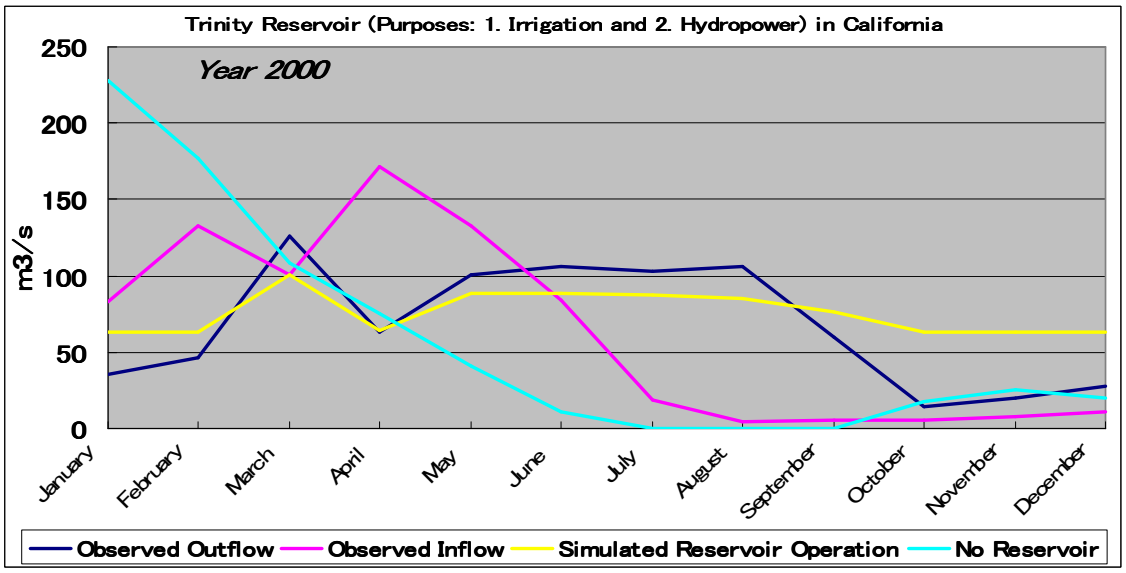

Figure 2.8: Simulated reservoir operation at the Trinity Reservoir in California, the U.S.A.

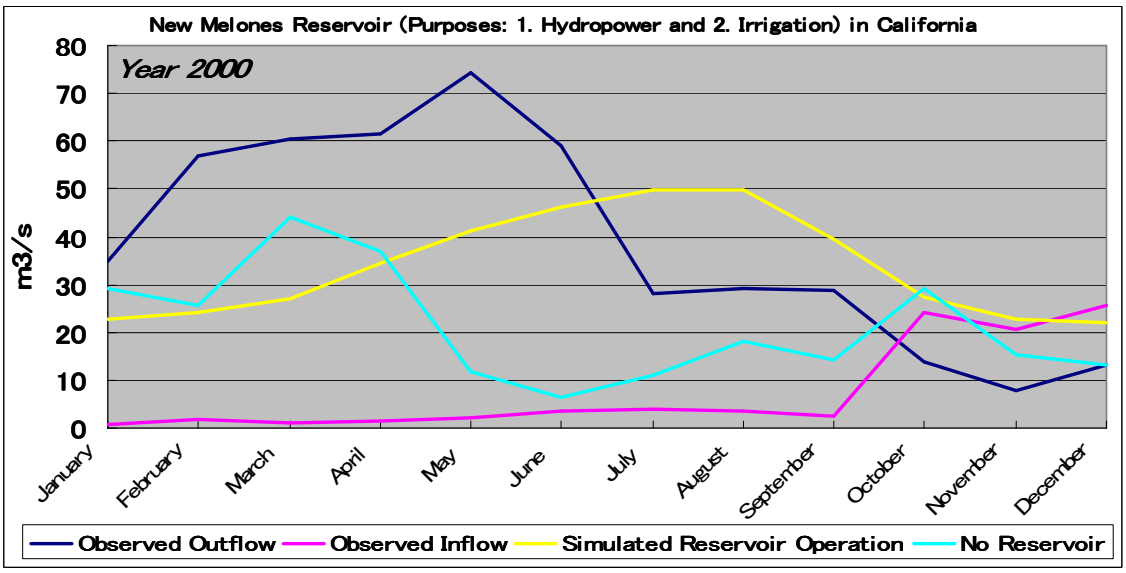

Figure 2.9: Simulated reservoir operation at the New Melones Reservoir in California, the U.S.A.

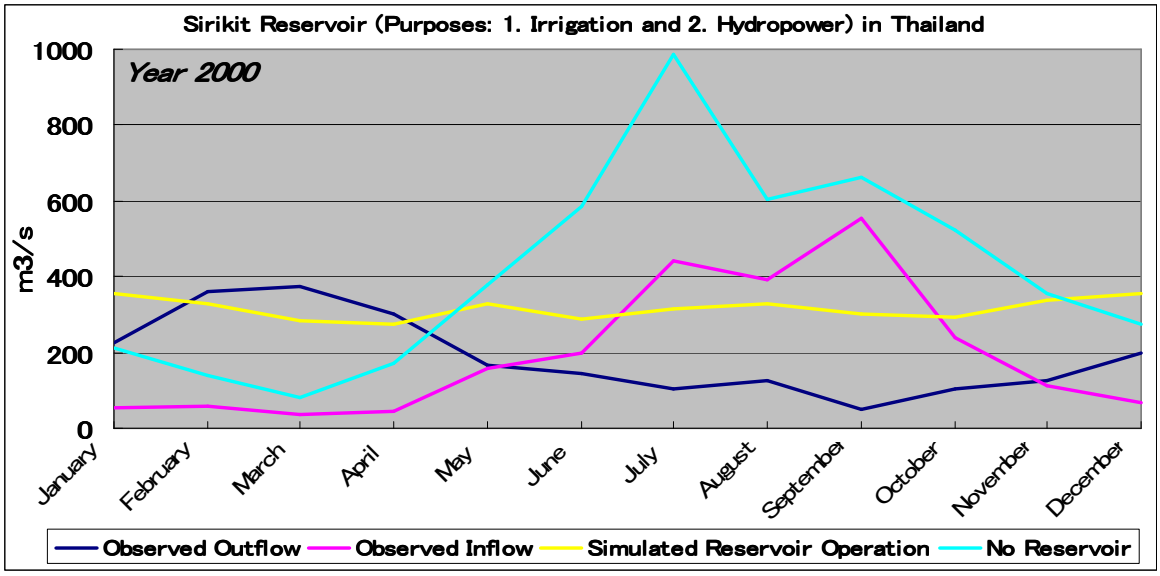

Figure 2.10: Simulated reservoir operation at the Sirikit Reservoir in Thailand.

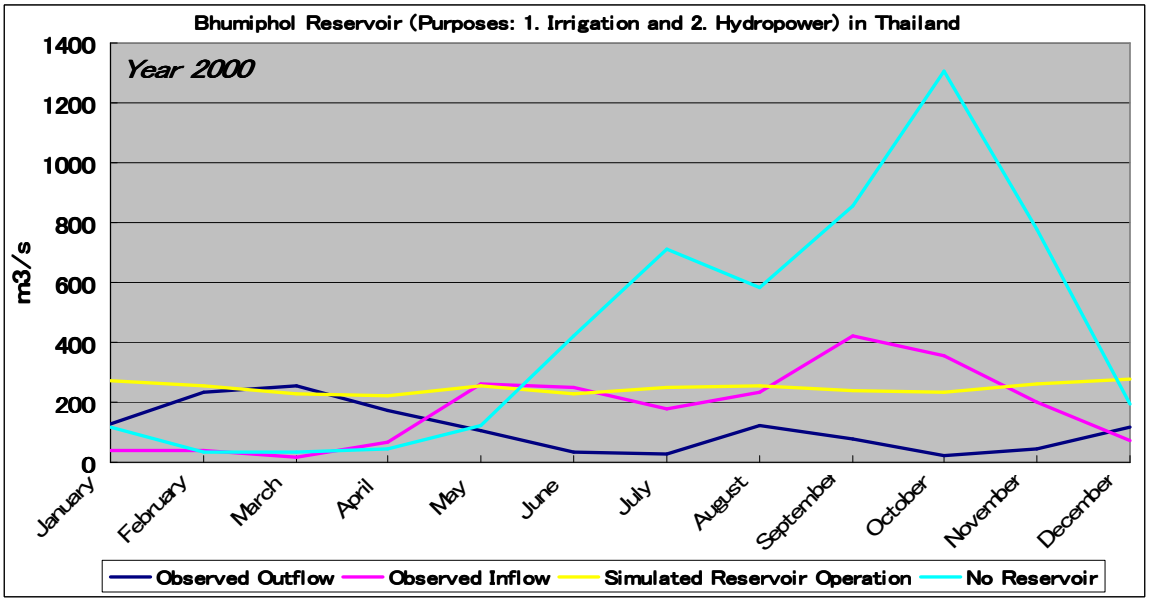

Figure 2.11: Simulated reservoir operation at the Bhumiphol Reservoir in Thailand.

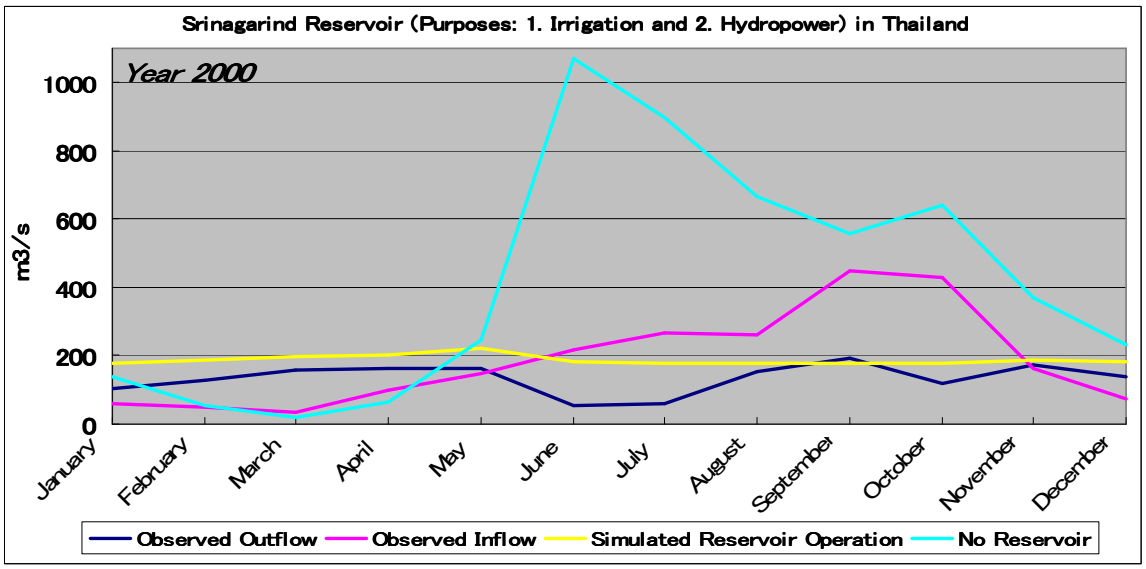

Figure 2.12: Simulated reservoir operation at the Srinagarind Reservoir in Thailand.

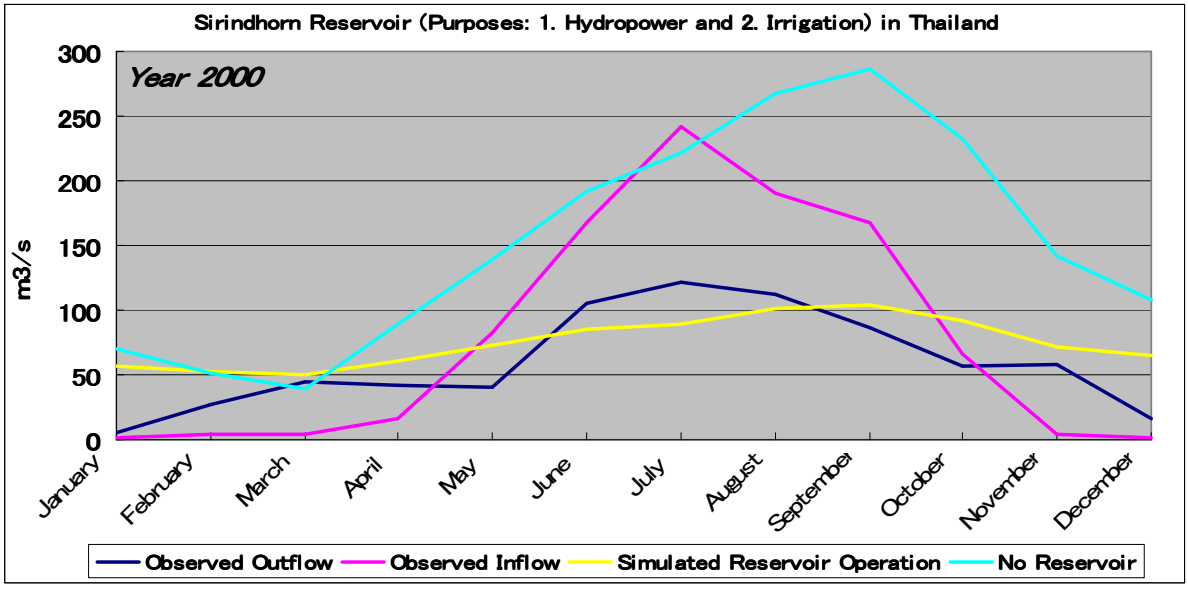

Figure 2.13: Simulated reservoir operation at the Sirindhorn Reservoir in Thailand.

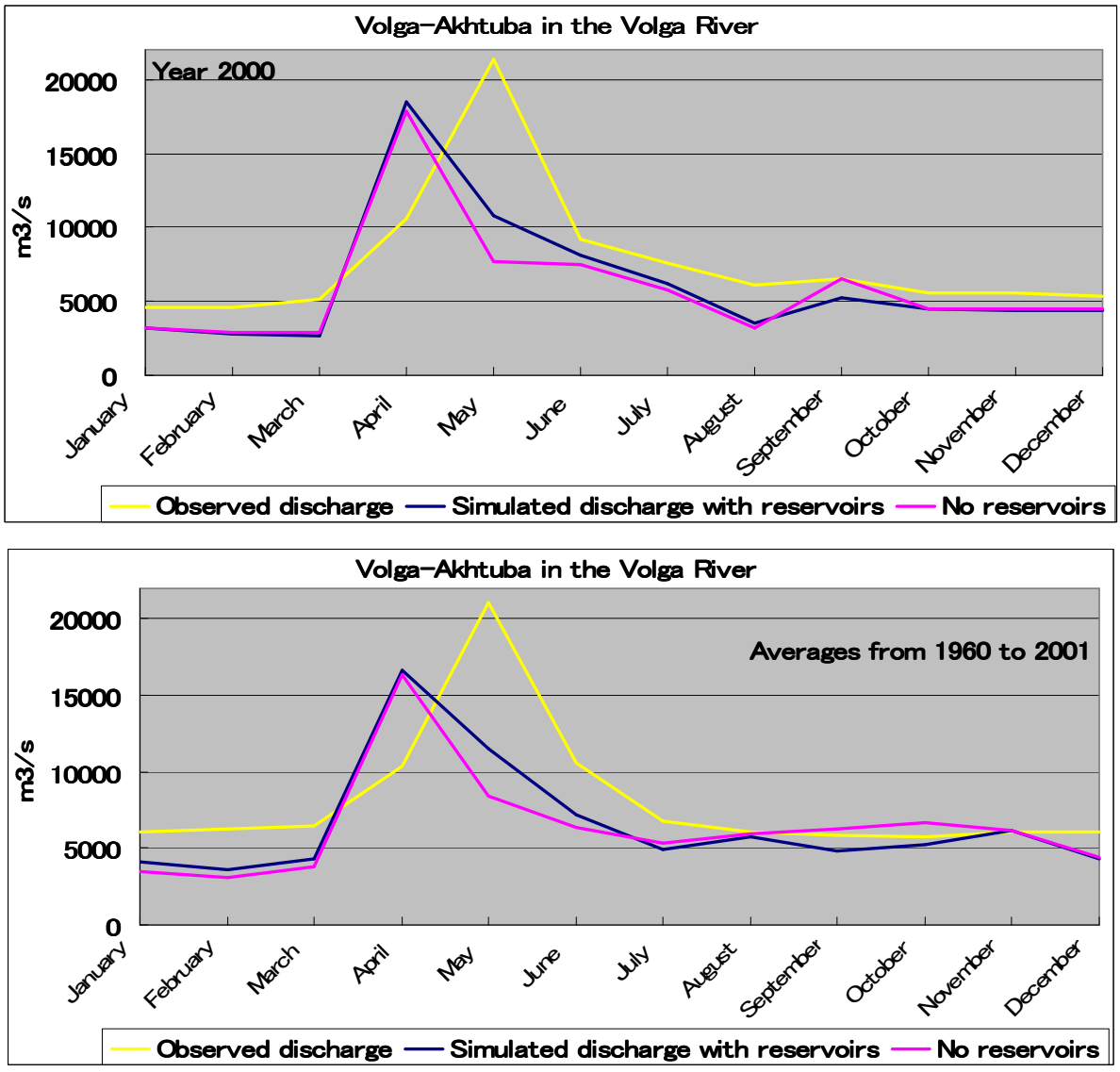

Figure 2.14: River discharge under the influence of reservoirs at the Volga-Akhtuba in the Volga River for the year 2000 (upper) and the averages from 1960 to 2001 (bottom).

2.5. Exogenous Runoff from Upstream

Exogenous runoff, i.e. water from outside of the region (grid box) to the within the region, is a important component for water stress assessment. Exogenous runoff flows along the LDD while being accumulated to downstream. Importantly, upstream water use along the LDD determines the volumes of water for downstream use or blue water availability downstream (Falkenmark and Rockström, 2005).

Oki et al. (2001) analysed the effect of availability of upstream water on water stress by means of α value (i.e. coefficient):

$$Q = R + \alpha \sum D_{up} \ , \tag{2.30}$$

where Q is the river discharge within the grid box ($km^3 \cdot year^{-1}$), R the is locally generated runoff ($km^3 \cdot year^{-1}$) and D_{up} is the river discharge from grid boxes upstream ($km^3 \cdot year^{-1}$).

The term α is the ratio of water from outside of the region (grid box) that contributes to water resources within the grid box (Oki et al., 2001). When α = 1.0, all the water generated upstream can be used downstream, and when α = 0.0, only the runoff generated within the region (grid box) can be used (Oki et al., 2001). Oki et al. (2001) noted that the number of people affected by water stress (water withdrawal to availability ratio) clearly depends on this α value. Oki et al. (2001) used the sensitivity analysis to compare the results based on different α values (0.0-1.0). The results indicated the number of people under water stress is affected by more than ±20% due to different α values.

Later, Islam et al. (2007) also applied this method developed by Oki et al. (2001) in their water stress assessment. Most of other previous studies (Alcamo and Henrichs, 2002; Arnell, 1999a, 2004; Vörösmarty et al., 2000) assessed water stress based on water availability under the optimal condition. They assumed that all water generated upstream is usable in the downstream reach (i.e. this is comparable to α = 1.0 of Oki et al., 2001). However, in reality, a significant portion of this exogenous runoff is not available at the downstream grids because of upstream withdrawal (Islam et al., 2007) and flooding runoff (i.e. reservoirs do not have enough capacity to store all of the water). Islam et al. (2007) suggested that in the changing world with increasing population and industrial activities, it is already evident that the upstream water withdrawal rates are increasing gradually, thus decreasing the value of α = 1.0 over time.

In this study, we combined the method of Oki et al. (2001) with the PCRaster command operations to consider the effect of exogenous runoff together with the upstream water withdrawal at each grid box. We used the PCRaster command operations *"accuthresholdflux"* and *"accuthresholdstate"* (PCRaster Research and Development Team, 2005). These operations describe accumulation of material (e.g. runoff and river discharge) in a drainage network with transport limited by a threshold: transport will only occur if a certain threshold of losses has been reached (PCRaster Research and Development Team, 2005). For each cell, *"accuthresholdflux"* assigns the amount of material that is transported out of the cell and *"accuthresholdstate"* assigns the amount that is stored in the cell (PCRaster Research and Development Team, 2005). We applied the following formula to compute river discharge:

$$\begin{aligned} Q &= R + \alpha \sum D_{up} - \sum WD_{up} \\ Q &= R + \sum \left(\alpha D_{up} - WD_{up} \right) \end{aligned} , \tag{2.31}$$

where Q is the river discharge within the grid box ($km^3 \cdot year^{-1}$), R is the locally generated runoff ($km^3 \cdot year^{-1}$), D_{up} is the river discharge from grid boxes upstream ($km^3 \cdot year^{-1}$) and WD_{up} ($km^3 \cdot year^{-1}$) is the water demand from grid boxes upstream.

The term α determines rather the efficiency for the amount of upstream river discharge we can use (i.e. capture) at each grid box however it does not include a reduction due to upstream water use. These PCRaster command operations enables to compute river discharge minus water demand (i.e. threshold) at each grid box and exceeded river discharge is used for downstream.

Except locally generated runoff, upstream river discharge is actually an uncertain amount of water for a particular grid (Islam et al., 2007). We tested α = 0.5 and 1.0 considering upstream water withdrawal at each grid box (PCRaster command operations) to estimate water availability and resulting water stress on a global scale.

It is more desirable if we could process both water availability and water demand simultaneously at each grid box. In this study, we computed water availability and water demand separately to assess water stress.

2.6. Soil Water Storage

The rainfall water stored in the soil or soil water storage is often called green water or green water availability (in contrast to blue water or blue water availability). Green wa-

ter is productively used for plant transpiration and an important water resource particularly in rainfed agriculture (Gerten et al., 2005). About 60% of all food globally is produced under non-irrigated rainfed conditions, that is, with green water (Cosgrove and Rijsberman, 2000). Gerten et al. (2005) estimated global transpiration of 41,370 $km^3 \cdot year^{-1}$ (39% of total precipitation over land); total evapotranspiration reaches 63,906 $km^3 \cdot year^{-1}$ by using the LPJ (Lund-Potsdam-Jena) model. These results support the importance of green water availability and rainfed agriculture on a global scale.

We computed soil water or soil moisture storage by using PCR-GLOBWB with the meteorological data of the CRU (duration: 1958-2001) as described in section 2.2. of chapter 2. To determine the availability of soil water or green water to plants and rainfed crops, it is necessary to take into account the wilting point of the soil. At wilting point, crops and plants are not able to extract soil water and they can no longer recover its turgidity. The wilting point depends on a type of crops and plans, soil property and soil depth. We computed green water availability in the soil as follows:

$$W_{availability\_green} = SW - SW_{wp}, \tag{2.32}$$

$$SW_t = SW_{t-1} + P_t - \left(Ea_t + D_t + R_t\right), \tag{2.33}$$

where $W_{availability\_green}$ is the green water availability (m), SW is the soil water storage (m), SW_{wp} is the soil water storage at the wilting point (m), t is the time step, P is the precipitation (m), Ea is the actual evapotranspiration (m), D is the drainage to groundwater system (m) and R is the surface runoff (m).

$$SW_{wp} = D_{soil} \cdot \theta_E \cdot \left(\theta_s - \theta_r\right), \tag{2.34}$$

$$\theta_E = \frac{\theta_w - \theta_r}{\theta_s - \theta_r}, \tag{2.35}$$

where SW_{wp} is the soil water storage at the wilting point (m), D_{soil} is the depth of soil (m), θ_E is the effective degree of saturation (-), θ_s is the saturated water content (m), θ_r is the residual water content (m) and θ_w is the water content at the wilting point (m).

Figure 2.15 shows mean soil water storage (m) in the four seasons over the years between 1958 and 2001. Figure 2.16: shows average green water availability (m) in the four seasons over the years between 1958 and 2001.

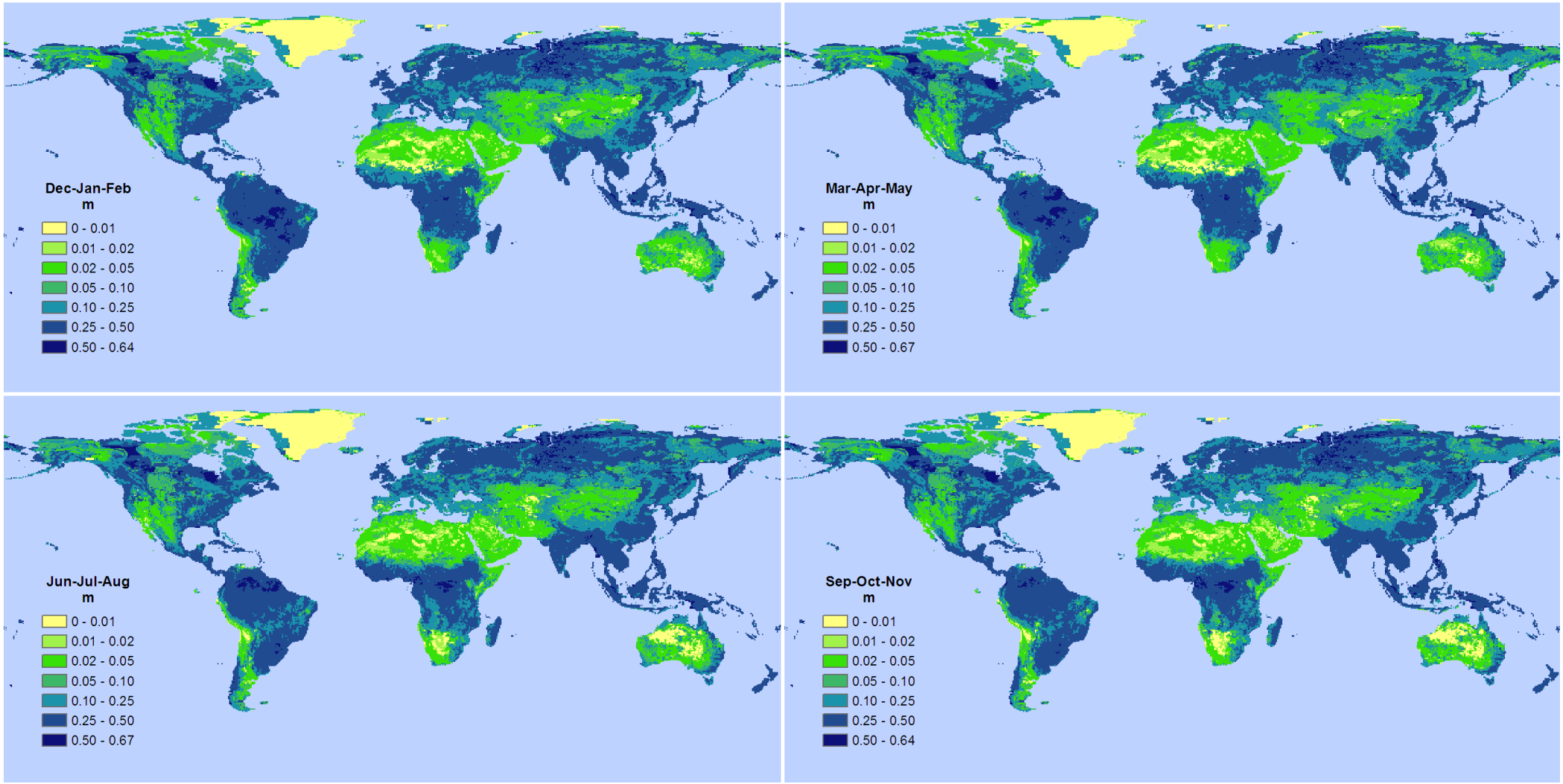

Figure 2.15: Mean soil water storage (m) in the four seasons over the years between 1958 and 2001.

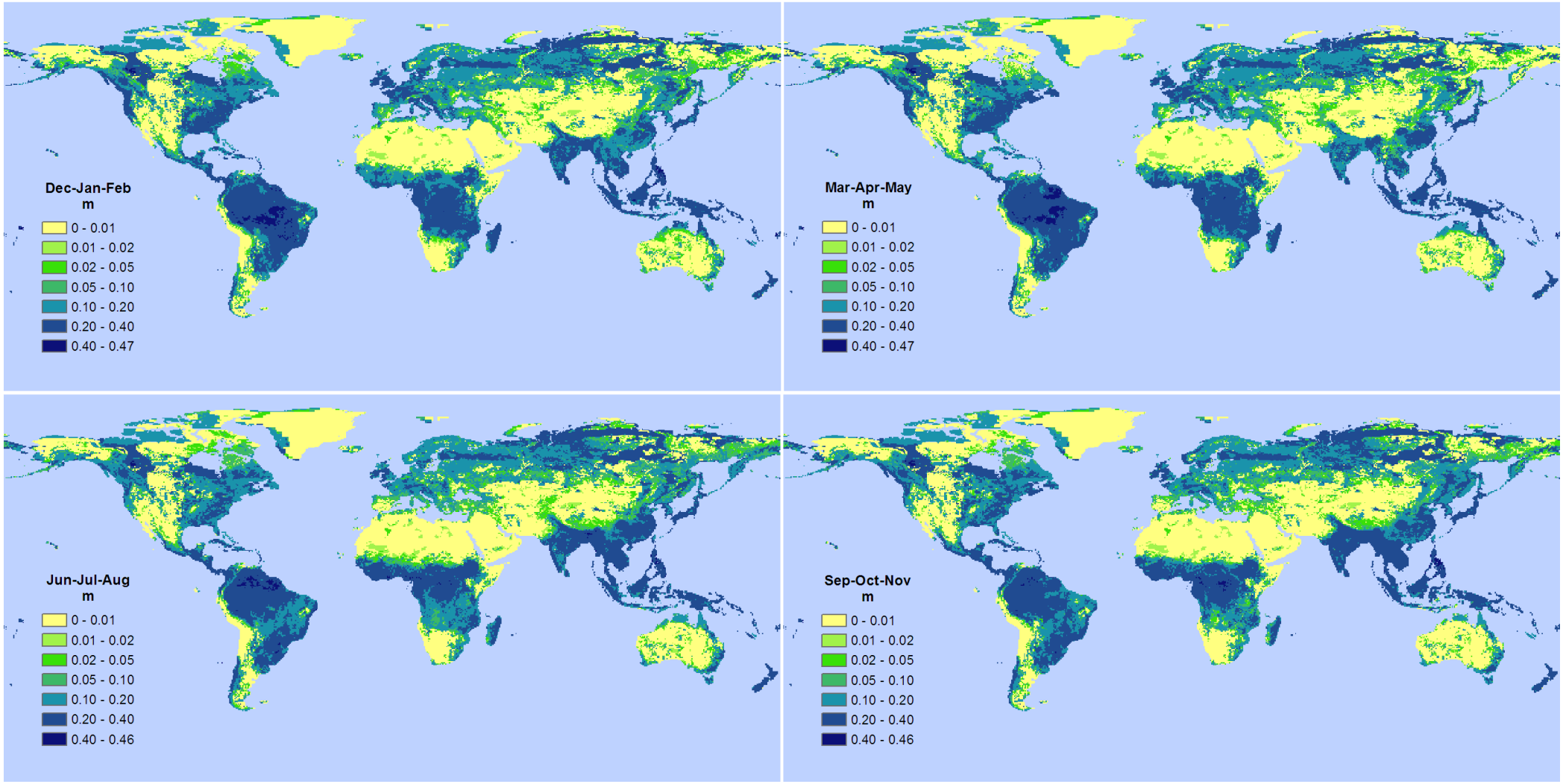

Figure 2.16: Average green water availability (m) in the four seasons over the years between 1958 and 2001.

3. Water Demand at a Monthly Time Scale and Particular Water Resources

3.1. Introduction

Water demand is generally classified into three sectors, agricultural (livestock and irrigation), industrial and domestic (households and municipalities) water demand. Water demand often refers to the demand for blue water, as water availability just described earlier in chapter 2. In addition, however, water demand for rainfed agriculture which relies its water resource entirely on soil water or green water is present. Green water demand is not often included in total water demand (Falkenmark and Rockström, 2005) and total water demand refers to blue water demand unless it is described otherwise. We estimated the green water demand of rainfed agriculture by using the rainfed agricultural area and a crop factor for rainfed crops derived by this study with laborious works.

Water use from particular resources (i.e. desalinated water use and groundwater abstraction) is also described in this chapter. Desalinated water use and groundwater abstraction are part of total water demand but their sources are sea water and groundwater, respectively. The amount of desalinated water use and groundwater abstraction is eventually added to blue water availability. Blue water is generated by only river discharge.

In most countries of the world, water demand has increased over the last decades due to demographic and economic growth, changes in lifestyle, and expanded water supply systems (Kundzewicz et al., 2007). Table 3.1 shows the statistics of population and water use by sectors (%) based on continents and GDP per capita classes in the year 2000/2001. Domestic and industrial water use is about 13% and 18% of total water use, respectively. Agricultural water use is nearly 69% of total water use and by far the largest among three sectors on a global scale. Most of the agricultural water is used for irrigation purpose and livestock water use takes up only a small amount.

On a continental scale, water use shows different trends. Nearly 85% of total water use is for agriculture in Africa, Asia and South America. Agricultural water use is close to the global average in Oceania. However, agricultural water use is less than a half of total water use in Europe and North America. In Europe, industrial water use is nearly 50% and the largest among three sectors. This result suggests the correlation between water use and economic development. Water use based on GDP per capita classes supports above statement. It can be clearly seen that the large amount of water use is

shifted to industrial and domestic purpose from agriculture through economic development. 86% and 69% of total water use is for agriculture in low and middle income countries. In high income countries, agricultural water use is almost the same amount as industrial water use, which is about 40%.

In this study, we computed monthly water demand by using PCRaster modelling and GIS environment. The monthly water demand of three sectors was estimated at a spatial resolution of 0.5° on a global scale. Initially, we used gridded data on water withdrawal based on those available from the WWDR-II. In addition, we also used country statistics data from EarthTrends (WRI) and AQUASTAT (FAO), and gridded data of global livestock density from FAO (2007). We took sub-grid variability into account in case only country statistics data were available when downscaling to 0.5° PCRaster map (e.g. desalinated water use and groundwater abstraction). Sub-grid variability was determined by using the gridded country map of 1 minutes resolution (i.e. 0.016° or roughly 2 km by 2 km) from ESRI data (ESRI: Environmental System Research Institute; http://www.esri.com/data/index.html).

One of the biggest challenge was to estimate water demand at a monthly time scale since all available data are at a yearly time scale. Due to the data deficiency, we focused to estimate monthly irrigation water demand, which has the largest share of total water demand. For livestock and industrial water demand, we eventually set them as constant over the year due to data constraints. For domestic water demand, we developed a formula to reproduce monthly fluctuation over the year based on observation data of country statistics.

Table 3.1: Population in the year 2000 and 2005 and water use by sectors (%) based on continents and GDP per capita classes in the year 2000/2001[15].

	Population in 2000 (millions)	Population in 2005 (millions)	Total Freshwater Withdrawal ($km^3 \cdot year^{-1}$)	Per Capita Withdrawal ($m^3 \cdot capita^{-1} \cdot year^{-1}$)	Agricultural Use (%)	Industrial Use (%)	Domestic Use (%)
Continents							
Africa	818.7	904.6	213.2	260.4	**83.1**	**4.3**	**12.6**
Asia	3679.8	3,900.8	2,294.8	623.6	**84.9**	**7.2**	**7.9**
Europe	729.2	728.0	392.2	537.8	**29.3**	**48.5**	**22.2**
North America	476.1	510.9	622.5	1307.5	**44.1**	**33.9**	**22.0**
South America	341.2	375.0	164.6	482.4	**84.8**	**6.4**	**8.8**
Oceania	28.7	31.4	26.3	916.4	**64.9**	**10.4**	**24.7**
GDP per capita classes[16]							
Low Income Countries[17]	2203.2	2,404.4	1,288.2	584.7	**86.0**	**7.7**	**6.3**
Middle Income Countries[18]	2961.7	3,095.0	1,549.4	523.2	**69.0**	**16.1**	**14.9**
High Income Countries[19]	908.8	951.3	875.7	963.6	**39.6**	**39.4**	**21.0**
Globe	6073.7	6450.7	3713.7	611.4	**68.6**	**18.1**	**13.3**

[15] These data are based on FAO AQUASTAT, Gleick et al. (2006) and Pacific Institute, The World's Water website; http://www.worldwater.org/data.html. If there is no data in the year 2000, data in the year 2001 was used.
[16] GDP per capita is based on the year 2000/2001 (year 2000 US dollar; The World Bank, World Development Indicators 2000-2004).
[17] GDP per capita of low income countries is less than 755 US dollar (year 2000 US dollar; country classification by the World Bank in the year 2000/2001) and the average GDP per capita of these countries is 358.9 US dollar.
[18] GDP per capita of middle income countries is between 756-9265 US dollar (year 2000 US dollar; country classification by the World Bank in the year 2000/2001) and the average GDP per capita of these countries is 2,842.5 US dollar.
[19] GDP per capita of high income countries is more than 9266 US dollar (year 2000 US dollar; country classification by the World Bank in the year 2000/2001) and the average GDP per capita of these countries is 21,879.6 US dollar.

3.2. Livestock Water Demand

Agricultural water demand is often defined as the sum of water demand for livestock and irrigation. Water demand of rainfed agriculture is not included in this sector (see section 3.4.). Although the amount of water used by livestock is very small (less than 1-2 % of total water use) in most countries compared to irrigation, industrial and domestic water use, the livestock water use may play a considerable role if irrigation water use is low (Flörke and Alcamo, 2004).

Livestock water demand was computed from the grid-based distribution of six major types of livestock and their water consumption rate. We followed the method of Alcamo et al. (2003a) to estimate annual livestock water demand at a spatial resolution of 0.5°on a global scale. It is assumed that the water withdrawals for livestock are equal to their consumptive water use (Alcamo et al., 2003a; Flörke and Alcamo, 2004). We obtained the gridded data of global livestock density from FAO (Gridded Livestock of the World 2007; http://www.fao.org/ag/AGAinfo/resources/en/glw/GLW_dens.html) developed by both FAO and ERGO (Environmental Research Group Oxford; http://ergodd.zoo.ox.ac.uk/). The data are provided at a spatial resolution of 3 minutes (i.e. 0.05° or roughly 5 km by 5km at the equator) for cattle, buffalo, sheep, goats, pigs and poultry/chickens. The data are both observed (based on census) and predicted six major types of livestock density in the year 2000 and 2005. More detailed descriptions of the data as well as the methodology are given in FAO (2007). We simply multiplied the number of livestock of each grid cell by the amount of their specific daily water consumption to estimate livestock water demand. We obtained the daily value of livestock water consumption rate from the study of Alcamo et al. (1997; see table 3.2).

Table 3.2: Daily water consumption rate of six major types of livestock (Alcamo et al., 1997).

Livestock	*Water consumption rate* *(liter·day^{-1})*
Cattle	25.0
Buffaloes	25.0
Goats	2.25
Sheep	2.25
Pigs	4.0
Poultry/Chickens	0.028

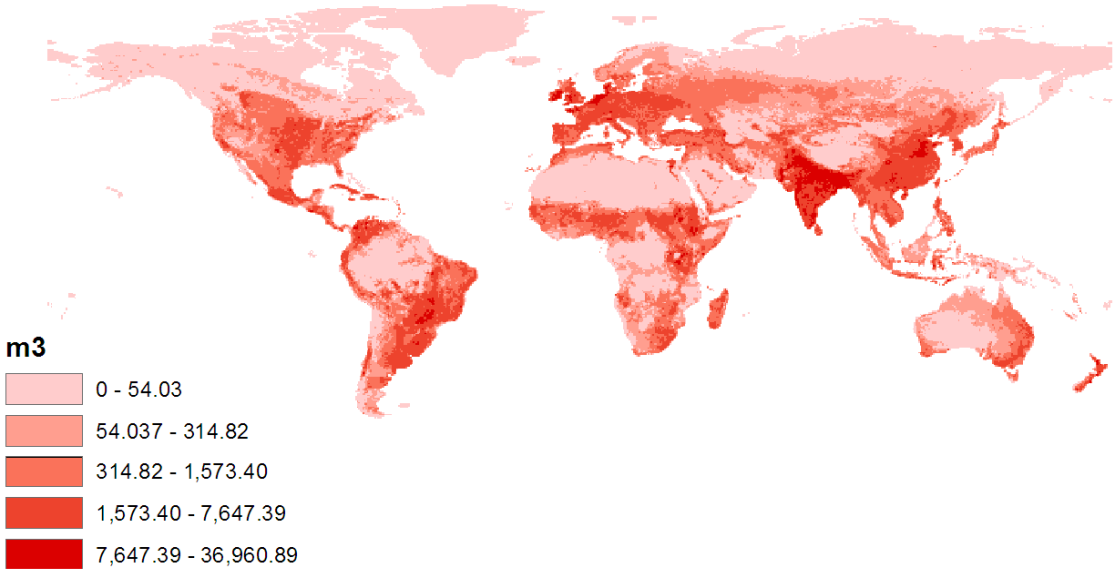

Figure 3.1: Monthly livestock water demand ($m^3 \cdot month^{-1}$) for the year 2000.

After we obtained annual livestock water demand, we disaggregated annual value to monthly values based on the assumption that livestock water demand is constant over the year. Figure 3.1 shows the monthly livestock water demand ($m^3 \cdot month^{-1}$) for the year 2000. Each grid cell has same value from January to December.

3.3. Irrigation Water Demand

3.3.1. Introduction

Irrigation water demand is particularly important because it comprises nearly 70 to 80 % of total water demand on a global scale (Raskin et al., 1997; Shiklomanov, 2000; see table 3.1). The most important drivers of irrigation water demand are the extent of irrigated areas (Kundzewicz et al., 2007) and food production. Leff et al. (2004) and Ramankutty et al. (2008) estimated a global cropland of about 15 million km^2 (an area roughly the size of South America) on a global scale. Monfreda et al. (2008) estimated a global crop-harvested area of about 13 million km^2. About 279 million ha (2.79 million km^2) of the global cropland were equipped for irrigation around the year 2000 (Siebert et al., 2006). Importantly, irrigation water demand has a large seasonal variability due to the growing season of different types of crops. In addition, irrigation water demand is region specific depending upon types of cropping practices and climatic conditions. Thus, it is sensitive to meteorological conditions (Hanasaki et al., 2006).

Among previous studies, Döll and Siebert (2002) estimated global irrigation water demand at 0.5° spatial resolution by using CROPWAT method (Smith, 1992) based on global gridded hydrometeorological data provided by New et al. (2000). First, they estimated the global daily crop calendar. They assigned a score to the suitability for cropping of current hydrometeorological conditions (precipitation and temperature) and find the maximum accumulated score, i.e., the best cropping times for points on a grid. The cropping period was assumed to be five months for every crop (some crops have two growing seasons over the year). They distinguished only paddy and non-paddy cropping situations, because paddy fields are inundated and extra water is consumed. Hanasaki et al. (2006) also estimated global irrigation water demand following Döll and Siebert (2002). They used the ISLSCP global meteorological data set. The global net annual irrigation water demand and total (i.e. gross) annual irrigation water demand were calculated by Döll and Siebert (2002) to be 1092 and 2549 $km^3 \cdot year^{-1}$ for 1961 to 1990 under average climatic conditions. Hanasaki et al. (2006) calculated these values to be 1127 and 2254 $km^3 \cdot year^{-1}$, respectively. Flörke and Alcamo (2004) also applied the same method as Döll and Siebert (2002) to estimate irrigation water demand in Europe.

The global net irrigation water demand refers to the part of the irrigation water that is evapotranspirated by plants and total irrigation water demand refers to the total volume of water that is withdrawn from its source (Alcamo et al., 2003a; Döll and Siebert, 2002; Flörke and Alcamo, 2004). In general, about half of the water diverted for irrigation of crops is consumed through evapotranspiration (Jackson et al., 2001). The ratio of net to total irrigation demand is called irrigation water use efficiency (Flörke and Alcamo, 2004).

The global net annual irrigation water demand and total annual irrigation water demand estimated by both Döll and Siebert (2002) and Hanasaki et al. (2006) are based on the simulated cropping patterns and growing seasons for rice (paddy) and non-rice (non-paddy). Their criteria for the optimal starting date depending climate conditions for growing crops of rice and non-rice may cause inaccuracies. In this study, the latest global data set of monthly growing areas of 26 irrigated crops around the year 2000 (MIRCA2000; Portmann et al., 2008) was used to obtain more accurate estimates of irrigation water demand. This latest data set includes monthly cropping patterns and monthly cropping calendars for major 26 crops on a global scale at a spatial resolution of 5 and 30 minutes (i.e. 0.083° or 9 km by 9 km and 0.5° or 50 km by 50 km at the equator, respectively). Both are cell-specific values and each crop has up to 9 sub-crops. Sub-crops represent multi-cropping systems, varieties of the same crop growing in different seasons in different areas of the grid cell or different specific crops included in

crop groups (MIRCA2000; Portmann et al., 2008). For an example for multi-cropping systems, rice is grown more than once a year on the same field in many regions of the world (MIRCA2000; Portmann et al., 2008).

Siebert and Döll (2008) computed the global net annual irrigation water demand and total annual irrigation water demand for 26 crops by using this data set. They partitioned crop water use between blue (irrigation) water and green (precipitation) water based on daily soil water balance for the first time. They used meteorological input derived from the CRU data set and computed crop water use around the year 2000 (average between the year 1998 and the year 2002) at a spatial resolution of 5 minutes.

3.3.2. Monthly Irrigation Water Demand

We estimated total and net irrigation water demand by using the global data set of monthly growing areas of 26 irrigated crops around the year 2000 (MIRCA2000; Portmann et al., 2008) at a spatial resolution of 30 minutes (i.e. 0.5°). Both are estimated at a monthly and yearly time scale. We followed the method of Siebert and Döll (2008) to estimate the total irrigation water demand but used a different method to estimate the net irrigation water demand from Siebert and Döll (2008).

We applied same length of crop development stages as fraction of the whole growing period for initial (*L_ini)*, crop development (*L_dev*), mid season (*L_mid*) and late season (*L_late*) as well as crop coefficients for initial period (*kc_ini*), mid season (*kc_mid*) and at the end of season (*kc_end*) as described in table 2 of Siebert and Döll (2008; see table 3.3) to estimate the total irrigation water demand. This study computed the total irrigation water demand as follows:

$$D_{irrig,total} = ET_c = k_c ET_o , \tag{3.1}$$

where $D_{irrig,total}$ is the total irrigation water demand (m·day^{-1}), ET_c is the potential crop evapotranspiration (m·day^{-1}), k_c is a crop coefficient (-) and ET_o is the reference evapotranspiration (m·day^{-1}).

Table 3.3: Length of crop development stages as fraction of the whole growing period for initial (*L_ini)*, crop development (*L_dev*), mid season (*L_mid*) and late season (*L_late*), crop coefficients for initial period (*kc_ini*), mid season (*kc_mid*) and at the end of season (*kc_end*), rooting depth (*rd*) on irrigated and rainfed land and standard crop depletion fraction (*pstd)* from table 2 of Siebert and Döll (2008).

Crop	Length of crop development stage (-)				Crop coefficients (-)			Rooting depth *rd* (m)		p_{std} (-)
	L_ini	*L_dev*	*L_mid*	*L_late*	k_c_ini	k_c_mid	k_c_end	Irrigated	Rainfed	
Wheat (1)	0.15	0.25	0.40	0.20	0.40	1.15	0.30	1.25	1.60	0.55
Maize (2)	0.17	0.28	0.33	0.22	0.30	1.20	0.40	1.00	1.60	0.55
Rice (3)	0.17	0.18	0.44	0.21	1.05	1.20	0.75	0.50	1.00	0.00
Barley (4)	0.15	0.25	0.40	0.20	0.30	1.15	0.25	1.00	1.50	0.55
Rye (5)	0.10	0.60	0.20	0.10	0.40	1.15	0.30	1.25	1.60	0.55
Millet (6)	0.14	0.22	0.40	0.24	0.30	1.00	0.30	1.00	1.80	0.55
Sorghum (7)	0.15	0.28	0.33	0.24	0.30	1.10	0.55	1.00	1.80	0.55
Soybeans (8)	0.15	0.20	0.45	0.20	0.40	1.15	0.50	0.60	1.30	0.50
Sunflower (9)	0.19	0.27	0.35	0.19	0.35	1.10	0.25	0.80	1.50	0.45
Potatoes (10)	0.20	0.25	0.35	0.20	0.35	1.15	0.50	0.40	0.60	0.35
Cassava (11)	0.10	0.20	0.43	0.27	0.30	0.95	0.40	0.60	0.90	0.35
Sugar cane (12)	0.00	0.00	1.00	0.00	n.a.	0.90	n.a.	1.20	1.80	0.65
Sugar beets (13)	0.20	0.25	0.35	0.20	0.35	1.20	0.80	0.70	1.20	0.55
Oil palm (14)	0.00	0.00	1.00	0.00	n.a.	1.00	n.a.	0.70	1.10	0.65
Rapeseed / canola (15)	0.30	0.25	0.30	0.15	0.35	1.10	0.35	1.00	1.50	0.60
Groundnuts / Peanuts (16)	0.22	0.28	0.30	0.20	0.40	1.15	0.60	0.50	1.00	0.50
Pulses (17)	0.18	0.27	0.35	0.20	0.45	1.10	0.60	0.55	0.85	0.45
Citrus (18)	0.00	0.00	1.00	0.00	n.a.	0.80	n.a.	1.00	1.30	0.50
Date palm (19)	0.00	0.00	1.00	0.00	n.a.	0.95	n.a.	1.50	2.20	0.50
Grapes / vine (20)	0.30	0.14	0.20	0.36	0.30	0.80	0.30	1.00	1.80	0.40
Cotton (21)	0.17	0.33	0.25	0.25	0.35	1.18	0.60	1.00	1.50	0.65
Cocoa (22)	0.00	0.00	1.00	0.00	n.a.	1.05	n.a.	0.70	1.00	0.30
Coffee (23)	0.00	0.00	1.00	0.00	n.a.	1.00	n.a.	0.90	1.50	0.40
Others (perennial) (24)	0.00	0.00	1.00	0.00	n.a.	0.80	n.a.	0.80	1.20	0.50
Managed grassland/pasture (25)	0.00	0.00	1.00	0.00	n.a.	1.00	n.a.	1.00	1.50	0.55
Others (annual) (26)	0.15	0.25	0.40	0.20	0.40	1.05	0.50	1.00	1.50	0.55

Reference evapotranspiration (ET_o) was calculated with the meteorological data of the CRU (duration: 1901-2002) by the FAO Penman-Monteith equation (Dingman, 1994; equation 7-51, p 282).

$$ET_o = \left(\frac{s(T_a)(K+L) + \gamma \rho_a c_a C_{at} \left[e_{sat}(T_a) \right] (1 - W_a)}{\rho_w \lambda_v \left\{ s(T_a) + \gamma \left[1 + C_{at} / C_{can} \right] \right\}} \right) \cdot 86400 , \tag{3.2}$$

where ET_o is reference evapotranspiration (m·day^{-1}), s is the slope of the relation between saturation vapor pressure (Pa) and temperature (°C) (Pa/°C), T_a is the air temperature (°C), K is the net shortwave radiation (W·m^{-2}), L is the net long-wave radiation (W·m^{-2}), γ is the psychrometric constant (Pa/°C), ρ_a is the mass density of air (kg·m^{-3}; 1.2047), c_a is the specific heat capacity of air at constant Pressure, 1013 hPa (J·kg^{-1}·K^{-1}; 1004), C_{at} is the atmospheric conductance (m·second^{-1}), e_{sat} is the saturation vapor pressure (Pa), W_a is the relative humidity (-), ρ_w is the mass density of water (kg·m^{-3}; 1.000), λ_v is the latent heat of vaporization of water (J·kg^{-1}), C_{can} is the canopy resistance (m·second^{-1}).

Previous studies of Döll and Siebert (2002) and Hanasaki et al. (2006) estimated the global net annual irrigation water demand by using the formula of effective precipitation as described below.

$$D_{irrig,net} = ET_c - P_{eff} , \tag{3.3}$$

$$P_{eff} = \begin{cases} P(1 - 0.048P), & P < 8.3 \\ 4.17 + 0.1P, & P \geq 8.3 \end{cases}, \tag{3.4}$$

where $D_{irrig,net}$ is the net irrigation water demand (mm·day^{-1}), P_{eff} is the effective precipitation (mm·day^{-1}) and P is the precipitation (mm·day^{-1}). Effective precipitation is the fraction of the total precipitation as rainfall and snowmelt that is available to the crop and does not run off (Döll and Siebert, 2002). The formula of effective precipitation was obtained from the U.S. Department of Agriculture Soil Conservation Method (Smith, 1992).

However, the formula of effective precipitation (see equation 3.4) is a simple approximation and this certainly causes inaccuracies (Döll and Siebert, 2002). This study used a different approach to estimate the net irrigation water demand based on soil water balance (green water availability and demand) rather than effective precipitation.

Our approach is similar with the study of Allen et al. (1998) and Siebert and Döll (2008) and is described after the introduction of the study of Siebert and Döll (2008) that used the following method:

$$D_{irrig,net} = ET_c - ET_a , \tag{3.5}$$

$$ET_a = k_s ET_c , \tag{3.6}$$

where $D_{irrig,net}$ is the net irrigation water demand (m·day^{-1}), ET_c is the potential crop evapotranspiration (m·day^{-1}), ET_a is the actual crop evapotranspiration (m·day^{-1}) and k_s is a transpiration reduction factor (-).

$$k_s = \begin{cases} \dfrac{S_t}{(1-p)S_{\max}} & if \quad S_t < (1-p)S_{\max} \\ 1 & otherwise \end{cases} , \tag{3.7}$$

$$p = p_{std} + 0.04\{5 - (ET_c \cdot 1000)\} , \tag{3.8}$$

where k_s is a transpiration reduction factor (-), S_t is the actual soil water storage (updated each month; m) and $S_{\max}$ is the total available soil water capacity (m). p is the fraction of $S_{\max}$ that a crop can extract from the root zone without suffering water stress and p_{std} is a crop specific depletion fraction valid for an evapotranspiration level of about 0.005 m·day^{-1} (-) and ET_c is the potential crop evapotranspiration (m·day^{-1}).

$$S_{t+1} = S_t + Prec_{t+1} + I_{t+1} - R_{t+1} - ET_a , \tag{3.9}$$

$$I_{t+1} = S_{\max} - S_t , \tag{3.10}$$

$$R_{t+1} = (Prec_{t+1} + I_{t+1}) \left(\frac{S_t}{S_{\max}} \right)^{\gamma_r} , \tag{3.11}$$

where *Prec* is the amount of water added to the soil by precipitation (m), *I* is the amount of water added to the soil by irrigation (m) and *R* is the amount of runoff (m). For irrigated crops, irrigation water was added to the soil if $S_t < (1-p)S_{\max}$ before computing ET_a, so that the water stress coefficient k_s was always 1 and thus ET_a was always ET_c. Lower values for the parameter γ_r increase runoff and higher values decrease runoff. Since irri-

gated land is usually flat and in many cases covered with irrigation basins, surface runoff will be lower than on average and the parameter γ was set to 3 (Siebert and Döll, 2008).

Siebert and Döll (2008) computed $S_{\max}$ by multiplying the total available water capacity in 1 m soil (mm; Batjes, 2005, 2006) with the rooting depth *rd* (m). The rooting depth *rd* is crop specific and varies between irrigated and rainfed crops with lower rooting depth under irrigated conditions (Allen et al., 1998; Siebert and Döll, 2008) as shown table 3.3. The fraction of the total available soil water that a crop can extract from the root zone without suffering water stress (*p*) depends on crop type and maximum crop evapotranspiration (Allen et al., 1998; Siebert and Döll, 2008). p_{std} derived from Allen et al. (1998) is given in table 3.3. Importantly, Siebert and Döll (2008) noted that a crop might suffer water stress even at a relatively high soil moisture level if the evaporative power of the atmosphere is high.

The approach of this study also quantified the actual crop evapotranspiration by using PCR-GLOBWB but by a different method to calculate a transpiration reduction, i.e. actual to potential transpiration rate. Actual crop evapotranspiration refers to the amount of water used by crops from soil water, i.e. green water, including actual bare soil evaporation. Therefore, the actual crop evapotranspiration refers to green water availability while the potential crop evapotranspiration described earlier refers to the total (i.e. gross) irrigation water demand. Thus, the difference between the actual crop evapotranspiration and the potential crop evapotranspiration gives an irrigation demand from blue water (i.e. river discharge or groundwater). This is also called the net irrigation water demand or the potential net irrigation water demand.

In this study, PCR-GLOBWB makes a distinction between bare soil evaporation (see section 2.2.8. of chapter 2) and transpiration by vegetation, which is drawn from both soil layers in proportion to the relative root volume after deduction of any evaporation of intercepted rainfall. The maximum soil depth of layer one is 30 cm and that of layer two is 120 cm. The maximum soil depth of both layers is thus 150 cm in the model. PCR-GLOBWB then calculated bare soil evaporation and transpiration from two soil layers with the meteorological data of the CRU. We distinguished the potential and actual net irrigation water demand based on the calculation of the potential and actual bare soil evaporation and transpiration as follows:

$$D_{pot,net,irrig} = ET_c - ET_a , \tag{3.12}$$

$$D_{act,net,irrig} = \left(ET_c - ES_o\right) - \left(ET_a - ES_a\right) = T_o - T_a , \tag{3.13}$$

$$T_o = ET_c - ES_o = \left(k_c - k_{cmin}\right) ET_o \,, \tag{3.14}$$

$$T_a = ET_a - ES_a = f_t \cdot T_o \,, \tag{3.15}$$

$$ES_a = x \cdot min\left(k_{s1}, ES_o\right) + \left(1 - x\right) \cdot min\left(k\left(\theta_E\right)_1, ES_o\right), \tag{3.16}$$

where $D_{pot,net,irrig}$ is the potential net irrigation water demand based on actual crop evapotranspiration (m·day^{-1}), $D_{act,net,irrig}$ is the actual net irrigation water demand based on actual crop transpiration (m·day^{-1}), ET_c is the potential crop evapotranspiration (m·day^{-1}), ET_a is the actual crop evapotranspiration (m·day^{-1}), T_o is the potential transpiration (m·day^{-1}) and T_a is the actual transpiration (m·day^{-1}). f_t is an actual to potential transpiration reduction ratio (-; this is comparable to a transpiration reduction factor of Siebert and Döll, 2008). ES_o is the potential bare soil evaporation (m·day^{-1}) and ES_a is the actual bare soil evaporation (m·day^{-1}), thus $ES_o - ES_a$ gives the irrigation losses (m·day^{-1}). k_c and k_{cmin} are a crop factor and a minimum crop factor for bare soil, respectively (-). x and $1-x$ is the saturated and the unsaturated part of the cell, respectively and k_{s1} and $k\left(\theta_E\right)_1$ is the saturated and the unsaturated hydraulic conductivity of the upper layer, respectively.

The uptake of transpiration by plants depends on the total available moisture in the soil layers. Importantly, the lack of aeration prevents the uptake of moisture by root under saturated conditions. Thus, the average degree of saturation over the unsaturated fraction of the cell is given by θ_E. The fraction of actual to potential transpiration rate is now calculated by:

$$f_t = \frac{1}{1 + \left(\theta_E / \theta_{E50}\right)^{-3B}} \,, \tag{3.17}$$

$$\theta_E = {w(x)}\Big/{w} = \frac{W_{max} + b\left(W_{max} - W_{min}\right)\left[1 - \frac{b+1}{b}\left(\frac{W_{max} - W}{W_{max} - W_{min}}\right)^{\frac{1}{b+1}}\right]}{W_{max} + b\left(W_{max} - W_{min}\right)\left[1 - \left(\frac{W_{max} - W}{W_{max} - W_{min}}\right)^{\frac{1}{b+1}}\right]} \,, \tag{3.18}$$

where θ_{E50} is the effective degree of saturation at which the potential transpiration is halved and B is the coefficient of the soil water retention curve. w is the sub-grid distributed maximum moisture storage and $w(x)$ is the actual moisture storage corresponding to the

fraction x of saturation. W, W_{min}, W_{max} are the cell-averaged, minimum and maximum storage capacities, respectively (m) and b is the shape factor describing the distribution of w.

In the equation 3.17, the root fraction, r_{frac}, is only considered in obtaining the parameters B and θ_{E50} of the scaling function, for which the soil water retention characteristics of layers i were weighted by both the root fraction and the maximum storage capacity per layer, $W_{max,i}$. The actual transpiration rate is partitioned over the two soil layers on the basis of the relative storage by local soil water availability, $W_i / \sum W_i$.

$$\sum_i W_{max,i} \cdot r_{frac} \,. \tag{3.19}$$

The results of this study compared with the study of Siebert and Döll (2008) are shown in table 3.4. The total irrigation water demand and the net irrigation water demand estimated by this study is 2023.4 $km^3 \cdot year^{-1}$ and 1069.5 $km^3 \cdot year^{-1}$ around the year 2000 (average between the year 1998 and the year 2002; same time period as the study of Siebert and Döll, 2008). As shown in table 3.4, the results of this study show general agreement with the study of Siebert and Döll (2008). However, the total irrigation water demand of rice and soybeans is lower than the study of Siebert and Döll (2008). The deviation should come from the difference of the reference evapotranspiration, i.e. ET_o between this study and the study of Siebert and Döll (2008). The actual crop evapotranspiration estimated by this study and the study of Siebert and Döll (2008) show differences in terms of crops such as millet, potatoes, pulses and others (annual). These differences are likely caused by the different approaches to calculate a transpiration reduction, i.e. actual to potential transpiration rate.

In conclusion, we used the net irrigation water demand, i.e. the potential net irrigation water demand, and the actual crop evapotranspiration for our water stress assessment. The amount of water actually used by crops is the net irrigation water demand. This is because only part of the water withdrawn for irrigation is actually used by crops and other part of the water withdrawn for irrigation runs off or returns to the groundwater system. Figure 3.2 shows the average annual net irrigation water demand (million $m^3 \cdot year^{-1}$) over the years between 1958 and 2001. Figure 3.3 shows the average net irrigation water demand (million $m^3 \cdot month^{-1}$) in the four seasons over the years between 1958 and 2001. Figure 3.4 shows the average relative contribution of net irrigation water demand (-) in the four seasons over the years between 1958 and 2001.

Table 3.4: Net irrigation or blue water demand (Net/Blue), actual crop evapotranspiration (Green) and total irrigation water demand (Total) by irrigated crops in $km^3 \cdot year^{-1}$ around the year 2000.

	Siebert and Döll (2008)			This study		
Type of Crop	Net/Blue	Green	Total	Net/Blue	Green	Total
Wheat	207.9	115.4	323.3	205.9	122.3	328.2
Maize	84.2	98.1	182.3	82.3	93.8	176.1
Rice	307.8	337.1	644.9	280.9	334.4	615.3
Barley	10.9	8.5	19.4	9.6	8.8	18.4
Rye	1.0	1.2	2.2	1.3	1.1	2.4
Millet	4.0	4.3	8.3	2.1	5.4	7.5
Sorghum	10.8	10.0	20.8	10.9	9.2	20.1
Soybeans	17.3	25.0	42.3	10.9	25.3	36.2
Sunflower	4.1	3.5	7.6	3.6	3.9	7.5
Potatoes	13.3	8.5	21.8	12.4	10.8	23.2
Cassava	0.0	0.0	0.0	0.02	0.04	0.06
Sugar cane	68.6	70.9	139.5	56.2	79.2	135.3
Sugar beets	9.1	3.0	12.1	9.2	3.8	13.0
Oil palm	0.0	0.1	0.1	0.01	0.10	0.11
Rapeseed/canola	7.9	3.0	10.9	5.1	4.5	9.6
Groundnuts/peanuts	7.5	13.1	20.6	6.5	13.6	20.0
Pulses	22.4	7.7	30.1	17.6	12.4	30.0
Citrus	22.6	17.8	40.4	22.0	19.7	41.7
Date palm	10.3	1.3	11.6	11.8	1.4	13.2
Grapes/vine	7.0	5.0	12.0	5.2	7.1	12.2
Cotton	82.9	46.8	129.7	80.2	50.8	131.0
Cocoa	0.0	0.1	0.1	0.02	0.04	0.06
Coffee	1.1	1.4	2.5	0.7	1.5	2.1
Others (perennial)	84.2	55.9	140.1	83.5	65.4	148.9
Managed grassland/pasture	90.1	47.0	137.1	102.5	38.1	140.5
Others (annual)	62.2	34.2	96.4	49.3	41.3	90.6
Total	**1137.2**	**918.9**	**2056.1**	**1069.48**	**953.89**	**2023.37**

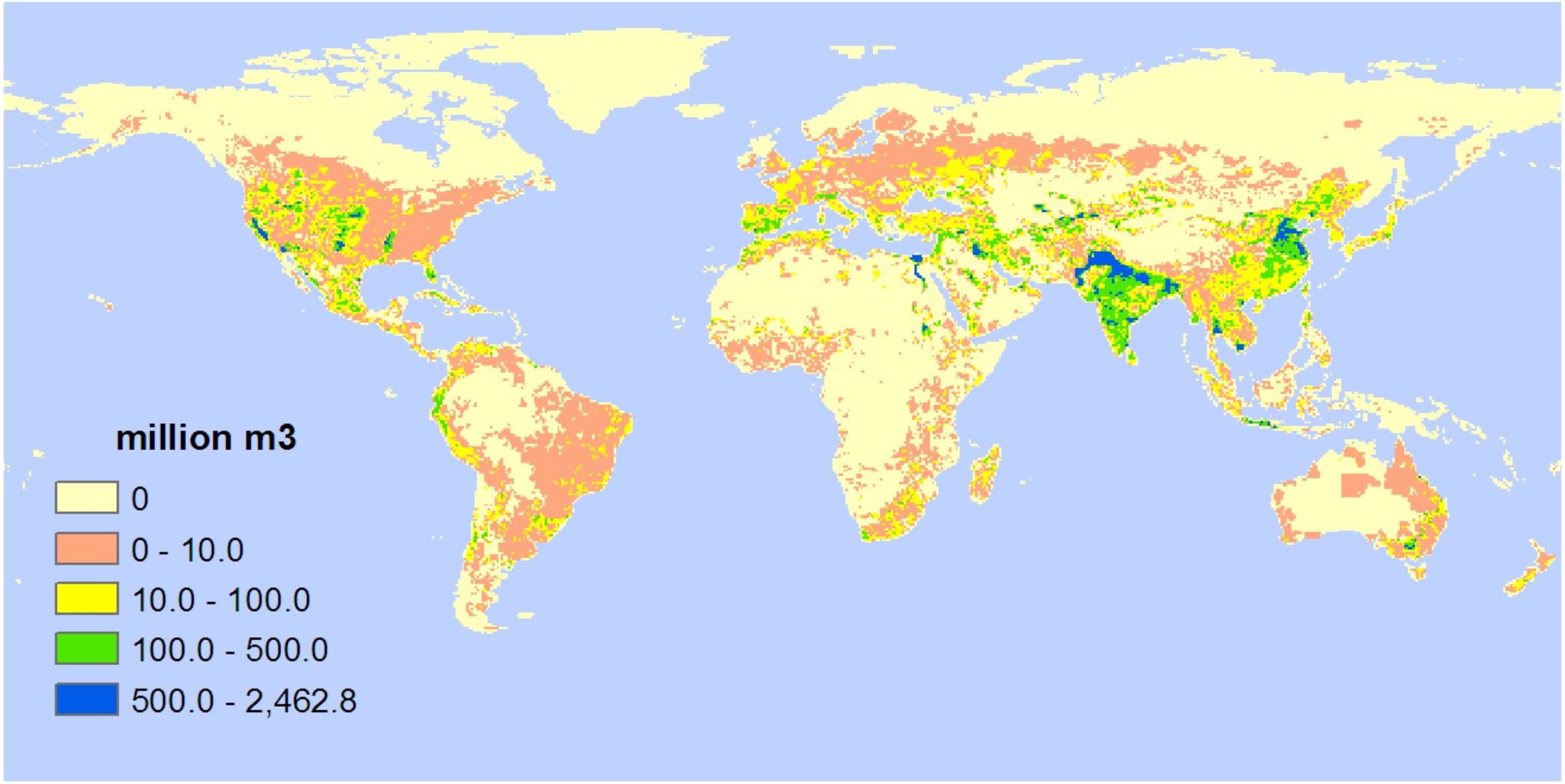

Figure 3.2: Average annual net irrigation water demand (million $m^3 \cdot year^{-1}$) over the years between 1958 and 2001.

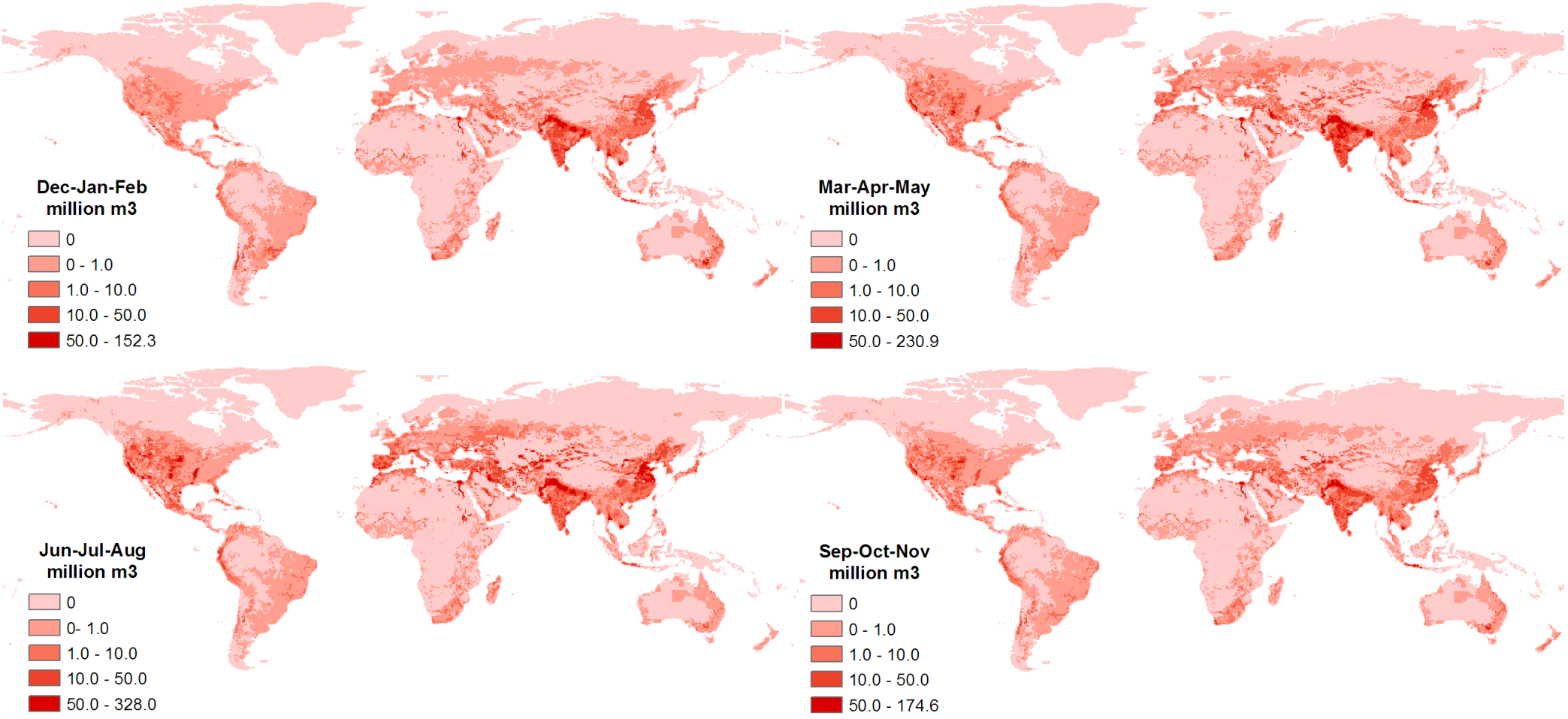

Figure 3.3: Average net irrigation water demand (million $m^3 \cdot month^{-1}$) in the four seasons over the years between 1958 and 2001.

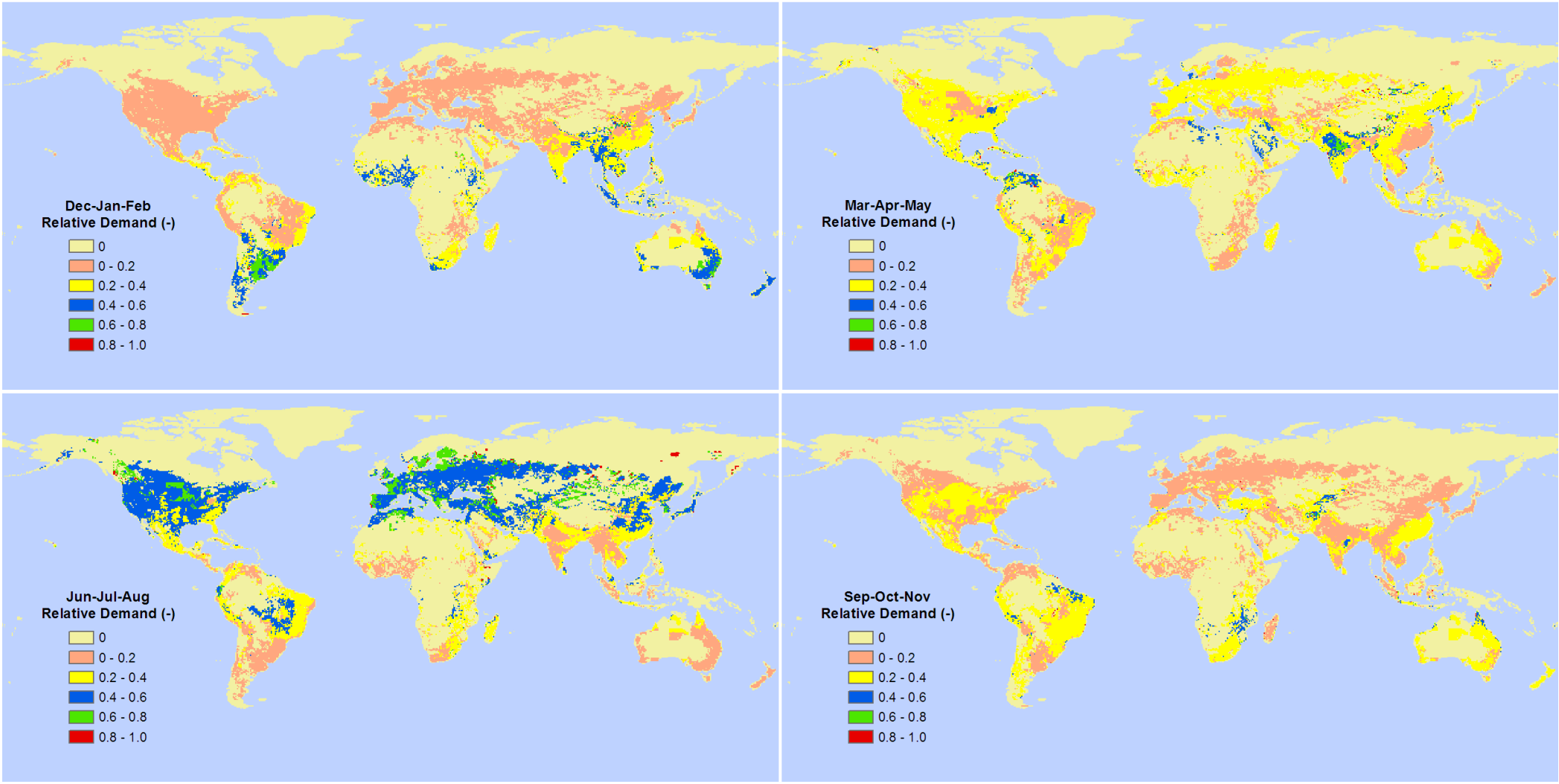

Figure 3.4: Average relative contribution of net irrigation water demand (-) in the four seasons over the years between 1958 and 2001.

3.4. Rainfed Crop Water Demand

3.4.1. Introduction

Besides green water demand for irrigation, there is even much larger demand for green water by rainfed agriculture. Green water is vital to our society as much as blue water; however, availability and demand of green water have not been well estimated except by Falkenmark and Rockström (2005). Falkenmark and Rockström (2005) estimated that today's food production involves a consumptive water use of about 6800 $km^3 \cdot year^{-1}$ out of which only 1800 $km^3 \cdot year^{-1}$ are supplied from blue water resources. In addition, most global crop production (e.g. 60 to 70% of global food production) is rainfed or by green water even in poor water scarcity prone regions (Falkenmark and Rockström, 2005) where most of the developing countries are located. Most of Sub-Saharan Africa stands out as dominantly rainfed (over 95% of the agricultural land is rainfed; Falkenmark and Rockström, 2005). Importantly, rainfed crop water demand is nearly three times as much as total irrigation water demand.

3.4.2. Monthly Rainfed Crop Water Demand

Monthly water demand of rainfed agriculture was estimated at a spatial resolution of 30 minutes (i.e. 0.5°). We used a similar method to estimate rainfed agricultural demand as irrigation demand in the previous section. Global ecosystem types derived by Hagemann et al. (1999) were used to classify rainfed crops from any other vegetation types. We upscaled this data to a spatial resolution of 30 minutes from 0.5 minutes (i.e. 0.0083° or around 1 km by 1 km). We derived a crop factor for rainfed crops following the method of Allen et al. (1998). We computed the rainfed crop water demand as follows:

$$D_{rainfed} = ET_{rainfed} = k_{cb,full/mid} ET_o , \tag{3.20}$$

where $D_{rainfed}$ is the rainfed crop water demand ($m \cdot day^{-1}$), $ET_{rainfed}$ is the potential rainfed crop evapotranspiration ($m \cdot day^{-1}$), $k_{cb,full/mid}$ is a crop coefficient (-) and ET_o is the reference evapotranspiration ($m \cdot day^{-1}$).

$$k_{cb,full} = k_{cb,h} + \left[0.04\left(u_2 - 2\right) - 0.004\left(RH_{\min} - 45\right)\right]\left(\frac{h}{3}\right)^{0.3}, \quad (3.21)$$

$$k_{cb,h} = \begin{cases} 1.0 + 0.1h & if \quad h \le 2m \\ 1.2 & otherwise \end{cases}, \quad (3.22)$$

where $k_{cb,full}$ is a basal crop coefficient (-), $k_{cb,h}$ is a basal crop coefficient (-) for full cover vegetation (Leaf Area Index or LAI >3) under sub-humid and calm wind conditions ($RH_{\min}$ = 45% and u_2 = 2 m·second^{-1}), u_2 is the mean value for wind speed at 2 m height during the mid-season (m·second^{-1}), $RH_{\min}$ is the mean value for minimum daily relative humidity during the mid-season (%) and h is the mean maximum crop height (m).

$$k_{cb,mid} = k_{c,\min} + \left(k_{cb,ful} - k_{c,\min}\right)\left(1 - \exp\left[-0.7LAI\right]\right), \quad (3.23)$$

where $k_{cb,mid}$ is a basal crop coefficient (-) when plant diversity and/or leaf area are lower than for full cover conditions, $k_{c,\min}$ is the minimum k_c for bare soil ($k_{c,\min} \approx 0.15 - 0.20$), $k_{cb,full}$ is a basal crop coefficient (-) for full cover vegetation (Leaf Area Index or LAI >3) and LAI is the actual leaf area index, defined as the area of leaves per area of underlying ground surface averaged over a large area (LAI is changing over the season; m^2·m^{-2}).

This study estimated rainfed crop water demand of around 6,000 km^3·year^{-1} for the year 2000 on a global scale. Our estimate is 20% higher than that of Falkenmark and Rockström (2005). They estimated rainfed crop water demand of 5000 km^3·year^{-1}. The difference between two studies might be caused by a different area of rainfed agriculture. Figure 3.5 shows the average annual water demand of rainfed agriculture (million m^3·year^{-1}) over the years between 1958 and 2001. Figure 3.6 shows the average rainfed agricultural water demand (million m^3·month^{-1}) in the four seasons over the years between 1958 and 2001. Figure 3.7 shows the average relative contribution of rainfed agricultural water demand (-) in the four seasons over the years between 1958 and 2001.

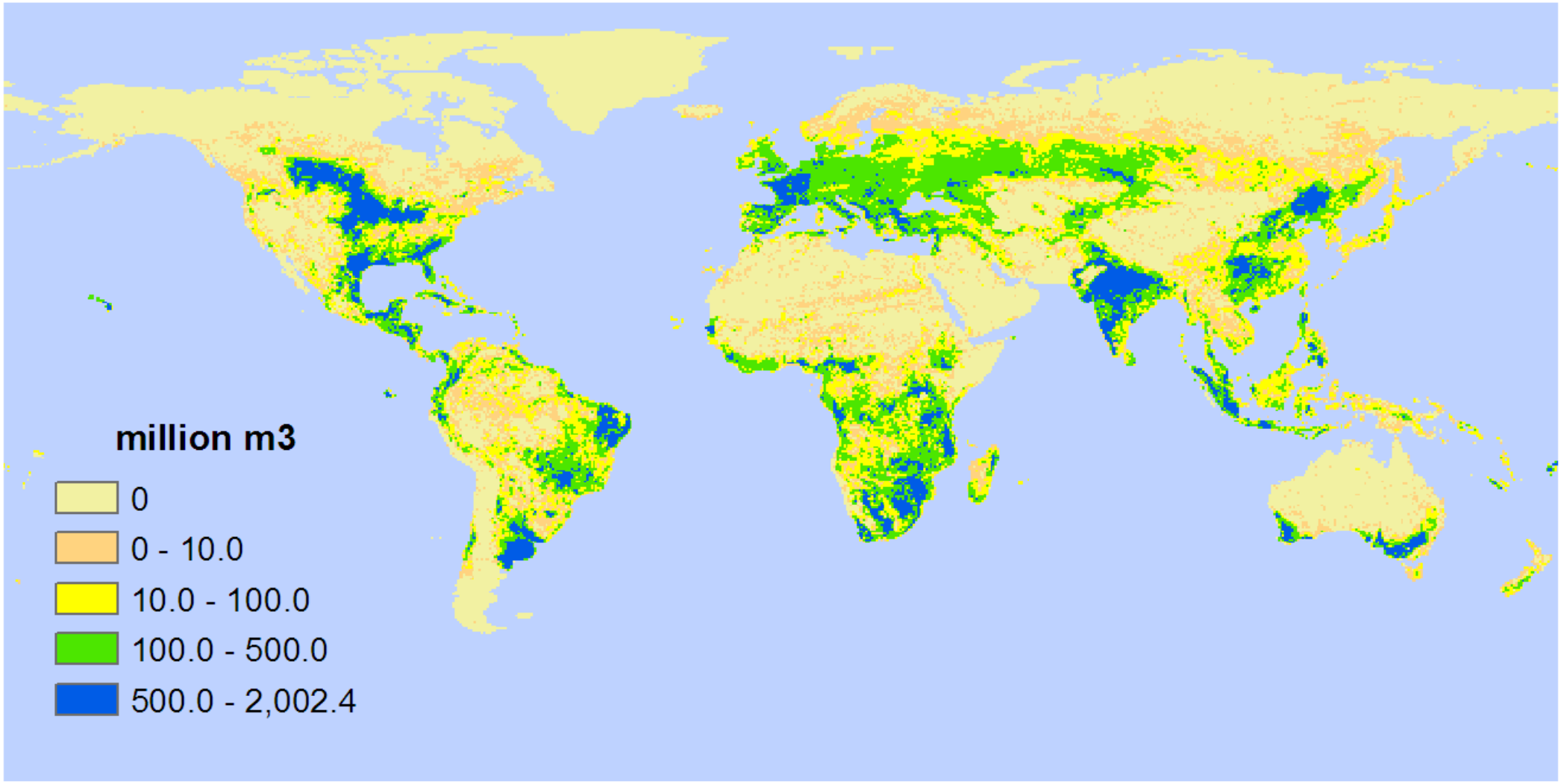

Figure 3.5: Average annual water demand of rainfed agriculture (million $m^3 \cdot year^{-1}$) over the years between 1958 and 2001.

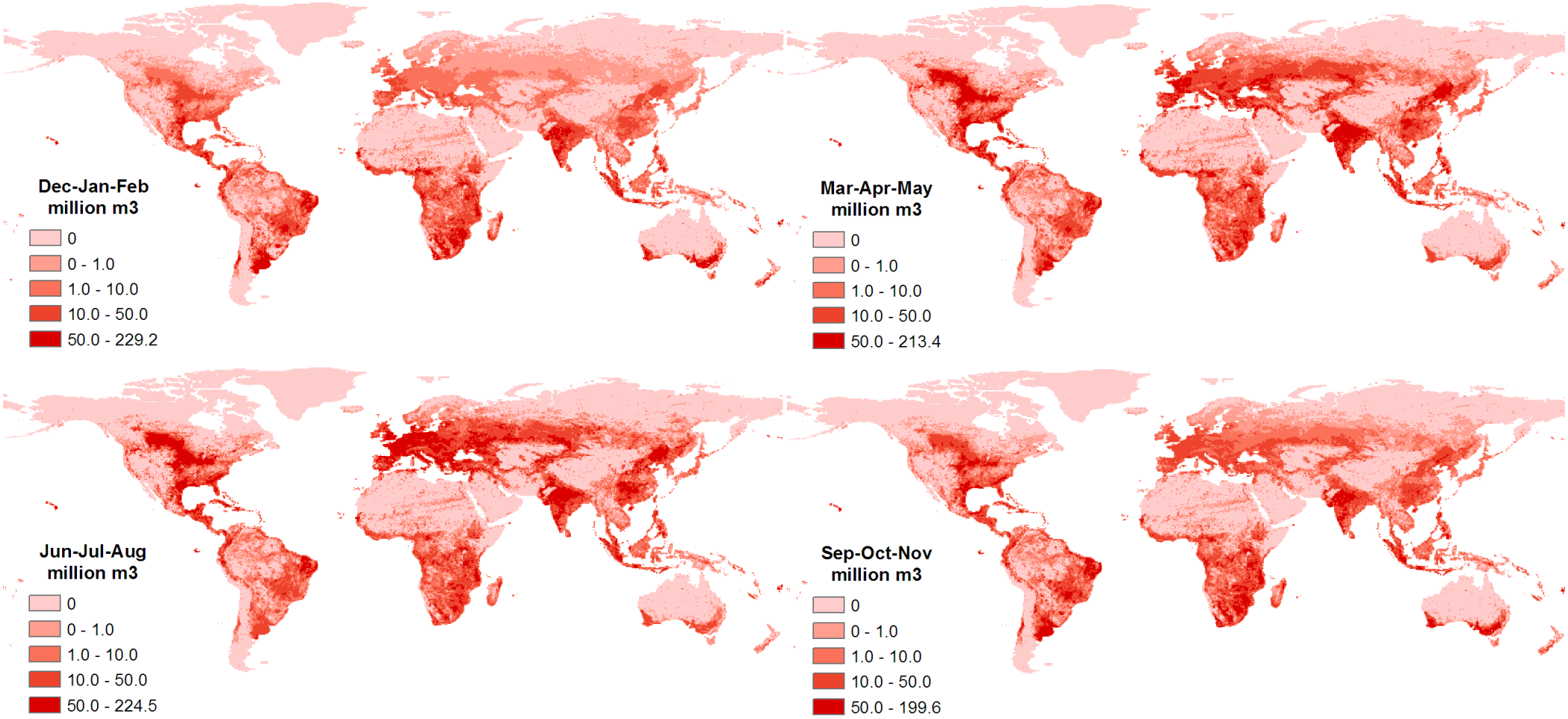

Figure 3.6: Average rainfed agricultural water demand (million $m^3 \cdot month^{-1}$) in the four seasons over the years between 1958 and 2001.

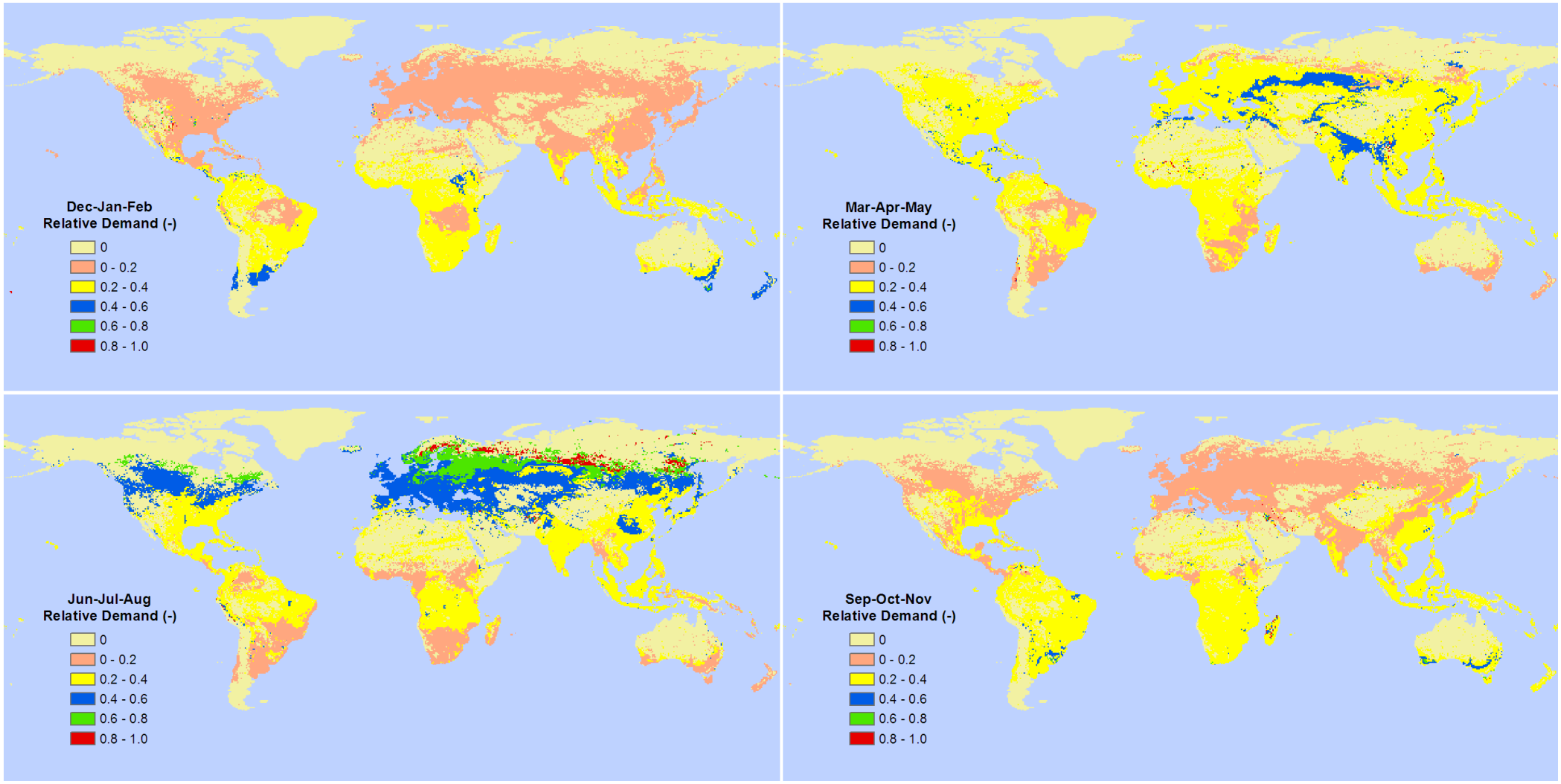

Figure 3.7: Average relative contribution of rainfed agricultural water demand (-) in the four seasons over the years between 1958 and 2001.

3.5. Industrial Water Demand

3.5.1. Introduction

Industrial water demand amounts to about 20% (The World Bank, 2006a; see table 3.1) of total water demand on a global scale. It is less than a half of agricultural water demand however it often comprises more than a half of the total water demand in developed (i.e. industrialized) countries. According to *the World's Water 2006-2007* (Gleick et al., 2006), the ratio of industrial water demand to total water demand in Finland, the United Kingdom, France, Canada, Germany and the Russian Federation is 84%, 75%, 74%, 69%, 68% and 64%, respectively. There is a regional spatial variability where industrial water demand is especially high in Europe. It is also known that industrial water demand has increased along with GDP (Oki and Kanae, 2006).

The most important drivers of industrial water demand are economic and technological development and a type of industry (Kundzewicz et al., 2007). A large amount of industrial water is used for cooling of thermal and nuclear power generation (Shiklomanov, 2000).

3.5.2. Water Recycling in Industry

Economic growth and industrial development depends on the provision of adequate quantities of water resources (Lens et al., 2002). However, there are already many regions of the world where demand is outgrowing water availability and this situation is getting more severe due to the continuous growth of population and urban development (Lens et al., 2002). Therefore, most of the industrial water is recycled, re-used or recovered, especially in developed countries (e.g. Japan). Oki et al. (2001) suggested that the recycling ratio of water for industry is 86%. Later, Oki and Kanae (2006) stated that recycling technology has reduced the net intake of industrial water for factories and nearly 80% of water used in the industrial sectors in Japan is currently recycled (MLIT, 2007). This suggests that the amounts of water recycled for industry are rather significant and need to be taken into account.

Recycling technology of industrial water has been widely developed and applied to the industry of many countries to improve water use efficiency. The recycling ratio is considered as high as Japan in other developed countries. Among the developing countries, the recycling ratio is about 60 to 65% in the People's Republic of China (PRC) in the year of 2004 (MWR, 2007). This indicates that the recycling ratio increases with economic growth and industrial development.

The water recycling in industry has been recognized as an important factor to estimate industrial water demand (Oki et al., 2001; Oki and Kanae, 2006). However, it has been considered as difficult to include the water recycling in industry due to a lack of data. Thus, past estimates of industrial water demand (Alcamo et al., 2003b; IWMI, 2000; Oki et al., 2001; Shiklomanov, 2000; Vörösmarty et al., 2000) tends to overestimate industrial water demand on a global scale. Oki et al. (2001) roughly estimated the water recycling for agriculture (25%), industry (86%) and municipal (60%) use as the first order approximation.

To include water recycling in industry, it is necessary to obtain data of the water recycling ratios for almost all countries in the world. It would be even more accurate if there are data of recycling ratio depending on the types of industry on each country. However, due to a lack of data, this study interpolated the recycling ratio for other countries based on the historical data of recycling ratio of Japan. We obtained the available data of the recycling ratio in industry between 1965 and 2007 from the Ministry of Land, Infrastructure and Transport (MLIT; http://www.mlit.go.jp/) in Japan.

To interpolate the recycling ratio, we simplified world countries into three groups depending on their economic development stage defined by the World Bank (2006a): groups of developing, emerging and developed countries. The definition of country classification by using GDP per capita is given in the World Bank (2006b). These groups are comparable to the GDP/water use in GDP per capita classes in figure 3.8. The group of developing countries is equivalent to the low-income countries. The group of emerging countries is equivalent to the lower and upper middle-income countries. At last, the group of developed countries is equivalent to the high-income countries. There is a clear difference among these three groups in terms of GDP/water use.

Table 3.5 shows three development stages and their mean recycling ratio of Japan. For developed countries, we simply used the recycling ratio of Japan as a representative value. This value agrees well with the recycling ratio of the U.S.A. which is around 80 % (U.S. EPA: United States Environmental Protection Agency; http://www.epa.gov/ebtpages/water.html). For emerging and developing countries, we interpolated the ratio by using the historical data of Japan. From the year 1965 to 2007, we classified Japan into developing, emerging and developed stages based on GDP per capita (Year 2000 US dollar). Each year of GDP per capita during the periods was indexed for the year 2000 considering deflation (i.e. GDP deflator; The World Bank, 2006a, 2007). The recycling ratio interpolated for emerging countries is 65%. The PRC is classified into emerging countries and its recycling ratios between the statistical and the interpolated values agree well. The recycling ratio interpolated for developing countries is 40%.

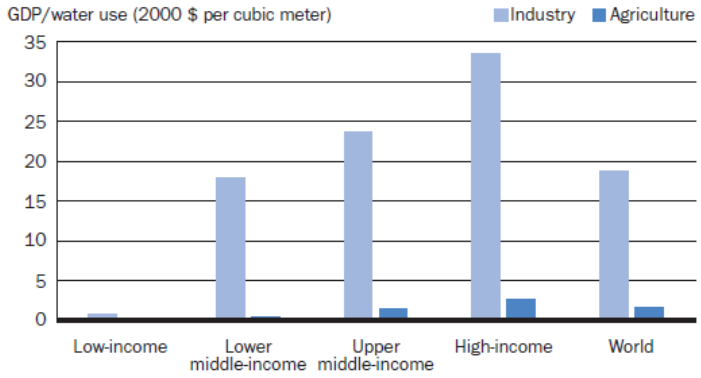

Figure 3.8: GDP/water use in GDP per capita classes in the year 2000 (The World Bank, 2007).

Table 3.5: Interpolated recycling ratio of developing, emerging and developed countries.

Year	Development stages (Japan)	Country classification (The World Bank, 2006b)	GDP per capita (Year 2000 US dollar)	Mean ratio (%)	**Interpolated ratio (%)**
1965-1969	Developing	Low income	≦755	42.1	**40**
1970-1979	Emerging	Middle income (lower and upper)	756-9265	64.3	**65**
1980-2007	Developed	High income	≧9266	76.7	**80**
1965-2007	*Total*	-	-	*69.3*	*70*

3.5.3. Monthly Industrial Water Demand

We estimated monthly industrial water demand at a spatial resolution of 0.5° on a global scale. We originally used water withdrawal data of 0.5° spatial resolution from the WWDR-II. We modified this data considering water recycling in industry. We distributed the recycling ratios of three groups to each country in the world. Then, we reduced the amount of industrial water demand by multiplying the original data with the recycling ratios. If there were no economic (i.e. GDP per capita) data, we put one for the recycling ratio so that we used the value of the original data.

Due to a lack of global monthly data of industrial water demand, we assumed that industrial water demand is constant over the year as the study of Hanasaki et al. (2006). We simply split the yearly data into 12 months. The validation was not possible because many countries use aggregated daily values for yearly values (thus, no monthly data).

We do not expect that there is a significant monthly fluctuation for industrial water demand. Thus, we concluded that this assumption is reasonable with present available data.

Figure 3.9 shows the monthly industrial water demand (million $m^3 \cdot month^{-1}$) for the year 2000. Each grid cell has same value from January to December.

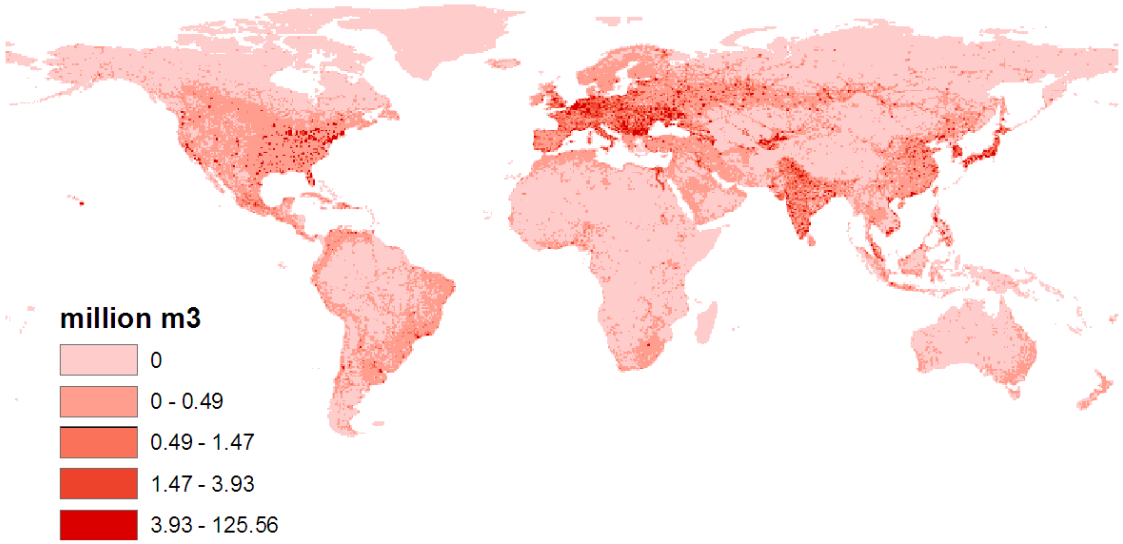

Figure 3.9: Monthly industrial water demand (million $m^3 \cdot month^{-1}$) for the year 2000.

3.6. Domestic Water Demand

3.6.1. Introduction

Domestic water demand consists of water use by households and municipalities. On a global scale, domestic water demand constitutes about 13% of total water use (see table 3.1). The most important drivers of domestic water demand are population and economic development (Kundzewicz et al., 2007). Domestic water demand typically ranges from 500 to 800 $liter \cdot capita^{-1} \cdot day^{-1}$ (about 300 $m^3 \cdot capita^{-1} \cdot year^{-1}$) in developed countries and from 60 to 150 $liter \cdot capita^{-1} \cdot day^{-1}$ (about 20 $m^3 \cdot capita^{-1} \cdot year^{-1}$) in developing countries (UNESCO, 2000). In some regions in Africa where the access to safe water is not guaranteed, domestic water demand ranges only from 20 to 60 $liter \cdot capita^{-1} \cdot day^{-1}$ (about 10 $m^3 \cdot capita^{-1} \cdot year^{-1}$; UNESCO, 2000).

3.6.2. Return Flow

A greater part of water that is withdrawn for households and municipalities is returned (purified or not) as wastewater mainly to river networks (Shiklomanov, 2000). The amount of water that returned to river networks depends on the development of drainage (sewerage) systems. In this study, we used the formula below to estimate the amount of water that is actually used. We did not find any specific values related with return flow or the recycling (reuse) of domestic water demand so that we simply applied same recycling ratio as the industry. We considered that return flow only occurs in urban area where drainage systems are well developed. Although we did not consider the effect of any repetitive uses of domestic water demand through river networks, our approach may be an initial step to consider how much the amount of domestic water is actually returned to river networks.

$$D_{dom,return} = D_{dom,month} \cdot \left(1 - \left(U_{fraction} \cdot R_{recycling,ind}\right)\right), \tag{3.24}$$

where $D_{dom,return}$ is the amount of water that is actually used considering return flow to river networks (million $m^3 \cdot month^{-1}$), $D_{dom,month}$ is monthly domestic water withdrawal (million $m^3 \cdot month^{-1}$), $U_{fraction}$ is the fraction of urban population over total population (-) and $R_{recycling,ind}$ is the recycling ratio developed for water recycling in industry (-).

3.6.3. Monthly Domestic Water Demand

Domestic water demand is a complex function of socio-economic characteristics, climatic factors and public water policies and strategies (Babel et al., 2007). At present, no global data set of monthly domestic water demand exists. All available data set is at a yearly time scale. This causes a difficulty to estimate monthly domestic water demand on a global scale. Babel et al. (2007) and CPM (2000) used a stochastic approach to estimate water demand of small regions. The most commonly used variables are population size, household size, the number of households, income or factors representing the standards of living, price of water, educational level and climatic factors such as temperature and rainfall (Babel et al., 2007). We found that these approaches are not feasible at present on a global scale due to data constraints.

In this study, we initially assumed monthly domestic water demand as constant over the year by disaggregating the yearly data. We estimated monthly domestic water demand at a spatial resolution of 0.5° by using water withdrawal data of the WWDR-II.

However, we found some country statistics related to domestic water demand in several studies. Figure 3.10 shows seasonal fluctuations of domestic water demand over the year in Japan, Australia, Iran, Nigeria and Spain in different years. These data are important indicators of how seasonal fluctuations occur over the year.

In general, there is a high demand around summer for households and municipalities (June to September in the Northern Hemisphere and December to March in the Southern Hemisphere). Therefore, we assumed that domestic water demand is a function of temperature although we recognized that domestic water demand is influenced by various variables as studied by Babel et al. (2007) and CPM (2000). We developed the formula to estimate monthly domestic water demand as a function of temperature:

$$D_{dom,month} = \frac{D_{dom,annual}}{12} \cdot \left(\left(\frac{T - \overline{T_{avg}}}{T_{\max} - T_{\min}} \cdot R_{dom,month} \right) + 1 \right), \tag{3.25}$$

$$D_{dom,month} = \frac{D_{dom,annual}}{12} \cdot \left(\left(\frac{T - \overline{T_{avg}}}{T_{\max} - T_{\min}} \cdot 0.10 \right) + 1 \right), \tag{3.26}$$

where $D_{dom,month}$ is monthly domestic water demand (million $m^3 \cdot month^{-1}$) and $D_{dom,annual}$ is annual domestic water demand based on the WWDR-II (million $m^3 \cdot year^{-1}$). T, $\overline{T_{avg}}$, $T_{\max}$ and $T_{\min}$ are temperature, average temperature, maximum temperature and minimum temperature, all monthly average, respectively (°C), based on CRU climatology (duration: 1961-1990). $R_{dom,month}$ is the percentage of how much domestic water demand in summer is higher than in otehr seasons (-).

In this formula, monthly domestic water demand fluctuates as temperature changes with the magnitude as specified by $R_{dom,month}$. Higher values of $R_{dom,month}$ give larger fluctuations of monthly domestic water demand. In this study, we used a value of 0.10 for $R_{dom,month}$. This gives about 10 % higher water demand in summer than water demand in other seasons. In Nigeria, temperature is more or less constant over the year so that there is almost no monthly fluctuations of domestic water demand. In this study we used a relatively low value of 0.10 to assure the small fluctuations occurred in Japan and Spain. It might be possible to apply different values of $R_{dom,month}$ in different regions of the world if we have additional data of monthly domestic water demand in other countries.

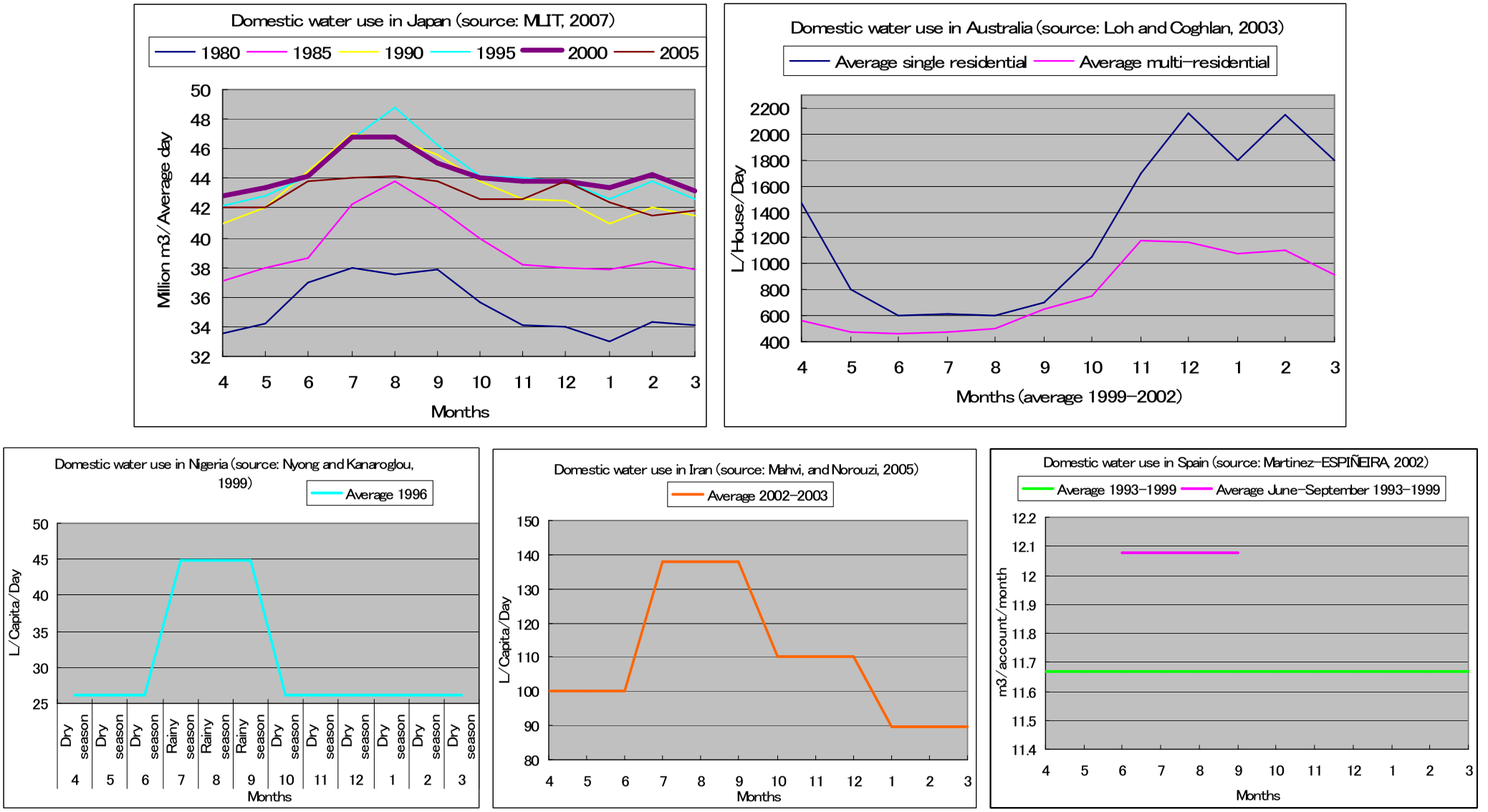

Figure 3.10: Seasonal trends of domestic water use in limited countries.

Figure 3.11 shows the average domestic water demand (million $m^3 \cdot month^{-1}$) in the four seasons for the year 2000. There is a higher water demand from June to August in the Northern Hemisphere and December to February in the Southern Hemisphere.

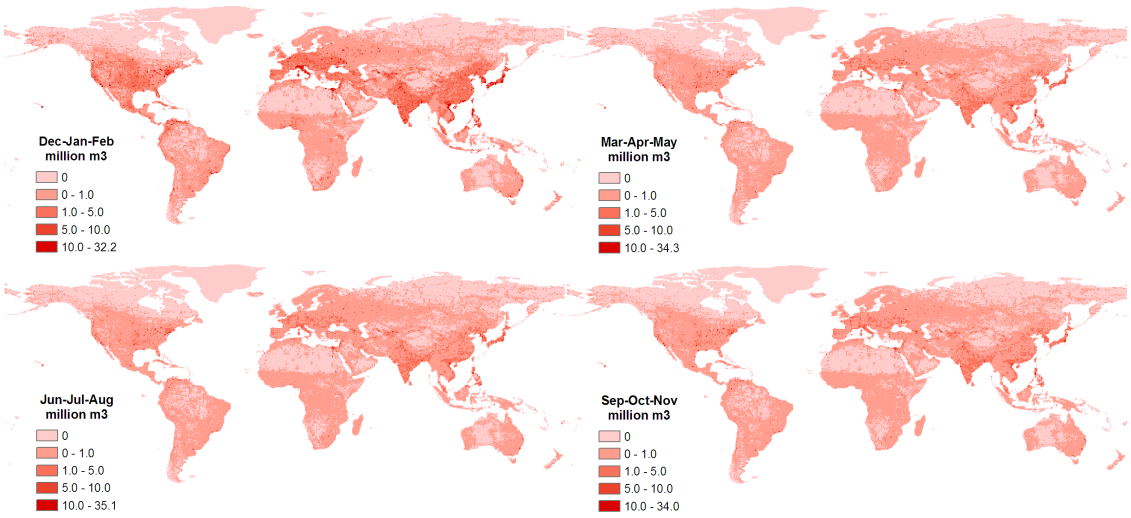

Figure 3.11: Average domestic water demand (million $m^3 \cdot month^{-1}$) in the four seasons for the year 2000.

3.7. Desalinated Water Use

Desalinated water is used in some countries and regions (i.e. Middle East) as an alternative where freshwater resources are scarce. Although there are unresolved concerns about the environmental impacts of the safe disposal of highly concentrated brines and high energy consumption (Kundzewicz et al., 2007), the amount of desalinated water use is increasing each year. According to AQUASTAT, the total amount of desalinated water use is around 3,000 million $m^3 \cdot year^{-1}$ in the year 2000. Saudi Arabia used the largest amount of desalinated water in the world, i.e. around 700 million $m^3 \cdot year^{-1}$ in the year 2000. Desalinated water is mainly used for industry and households and municipalities.

We obtained the data of desalinated water use from EarthTrends, AQUASTAT and Global Water Resource Data Archive (Oki and Kanae Laboratory, the University of Tokyo; http://hydro.iis.u-tokyo.ac.jp/GW/). The data of EarthTrends and AQUASTAT is based on country statistics. The data of Global Water Resource Data Archive is provided by 0.5° spatial resolution for the year 1995. The original data of country statistics was downscaled to 0.5° spatial resolution weighted by population density (Oki and Kanae Laboratory).

Among the three data sets, the latest data are listed in AQUASTAT so that we used the data based on AQUASTAT. Although we used the data for the year 2000, if there is no data for the year 2000, we used the values for the year 1995 or 1990 (indexed by per capita use). Population data of the WWDR-II was then used to downscale the country statistics to 0.5° grid cells while taking sub-grid variability of country borders into account. We calculated population density up to 40 km from the coast. It is reasonable to assume that people who live along the coast use desalinated water.

In this study, we assumed monthly desalinated water use as constant over the year. Figure 3.12 shows the monthly desalinated water use in million $m^3 \cdot month^{-1}$ and in $m^3 \cdot capita^{-1} \cdot month^{-1}$ for the year 2000. Each grid cell has same value from January to December.

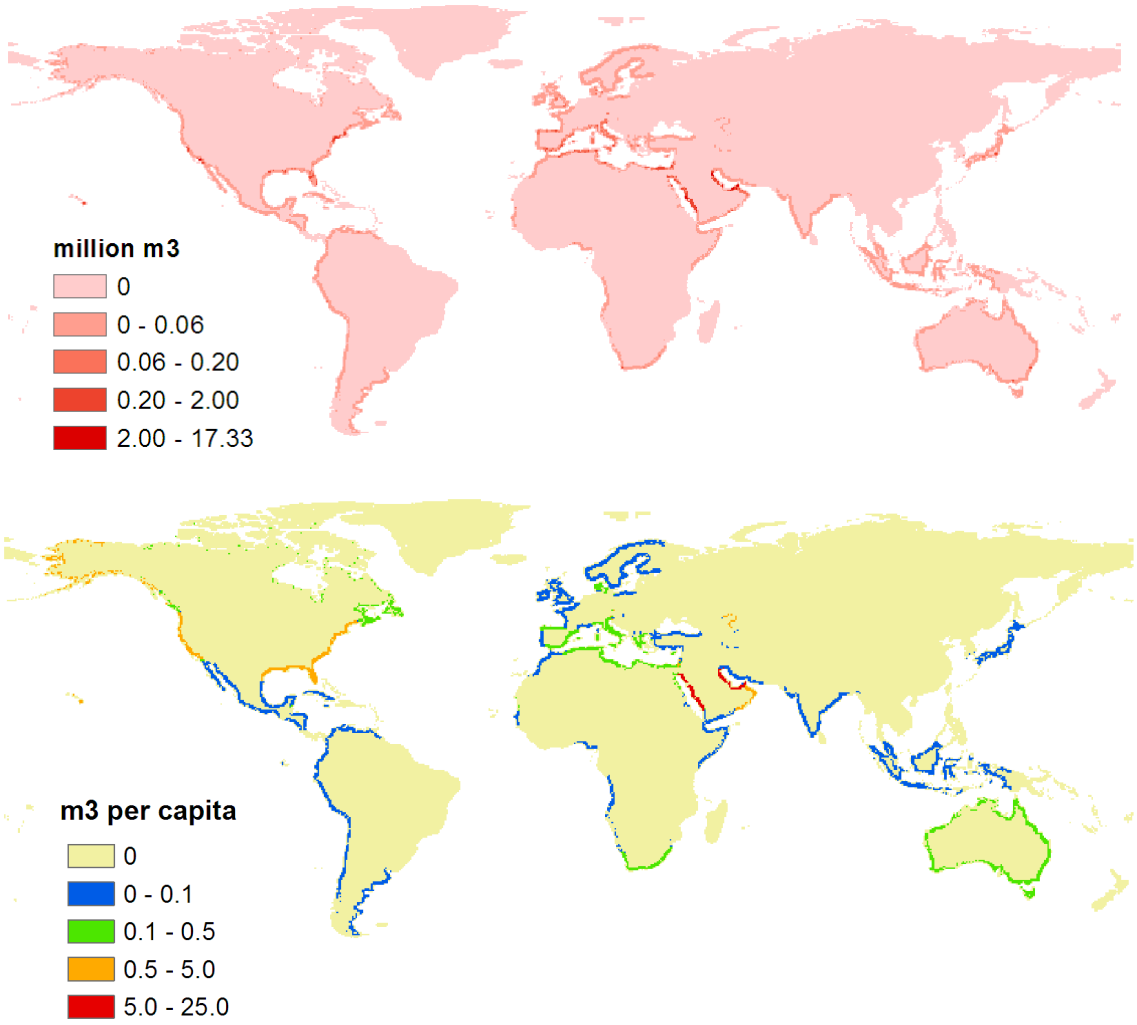

Figure 3.12: Monthly desalinated water use (million $m^3 \cdot month^{-1}$; above and $m^3 \cdot capita^{-1} \cdot month^{-1}$; below) for the year 2000.

3.8. Groundwater Abstraction

Groundwater is generally of superior quality to surface water and requires less treatment (Thyssen and EEA, 1999). The demand for groundwater exists in many regions due to the offset of scarce surface water availability. In the semi-arid regions of Mediterranean Europe, the absence of abundant rainfall and run-off increasingly encourages the use of groundwater resources, frequently leading to excessive abstraction for irrigation and over-exploitation (Thyssen and EEA, 1999). The demand for groundwater is likely to increase in the future, the main reason being increased water use globally (Kundzewicz et al., 2007).

We estimated global groundwater abstraction by using the data of IGRAC. The data on annual groundwater abstraction in m^3 per capita per country and per major groundwater regions in the year 2000 was provided by IGRAC. The original intention, therefore, was to intersect the countries with the regions, thus identifying different areas of water availability and use, and to use these areas to weigh the country-by-country statistics of water extraction internally (van Beek, 2007a). Weighing per country would have taken the following form (van Beek, 2007a):

$$C_i = \frac{A_i}{\sum_i A_i} C, \tag{3.27}$$

where C is the abstraction per capita for any country ($m^3 \cdot capita^{-1}$), i is any region present within that country and A is the abstraction expressed in m per year, to eliminate differences in region size (van Beek, 2007a).

The fractional contribution of groundwater to the total water demand was calculated using water use map of the WWDR-II. The fraction was generally around 20% on a global scale (van Beek, 2007a). Distributed groundwater use was calculated in the following way: first, the required groundwater extraction per cell was calculated using the groundwater abstraction per capita and the total population per cell (van Beek, 2007a). Population data was obtained from the WWDR-II. Then, given the total groundwater use per country, total water use multiplied by the mean fractional groundwater abstraction per country, and the required groundwater abstraction per cell, the actual groundwater abstraction was calculated (van Beek, 2007a). We estimated the annual groundwater use in millions m^3 per year at a spatial resolution of 0.5° while taking sub-grid variability of country borders into account. Figure 3.13 shows the annual

groundwater abstraction (million $m^3 \cdot year^{-1}$) and the fractional abstraction of groundwater relative to the total water use (-).

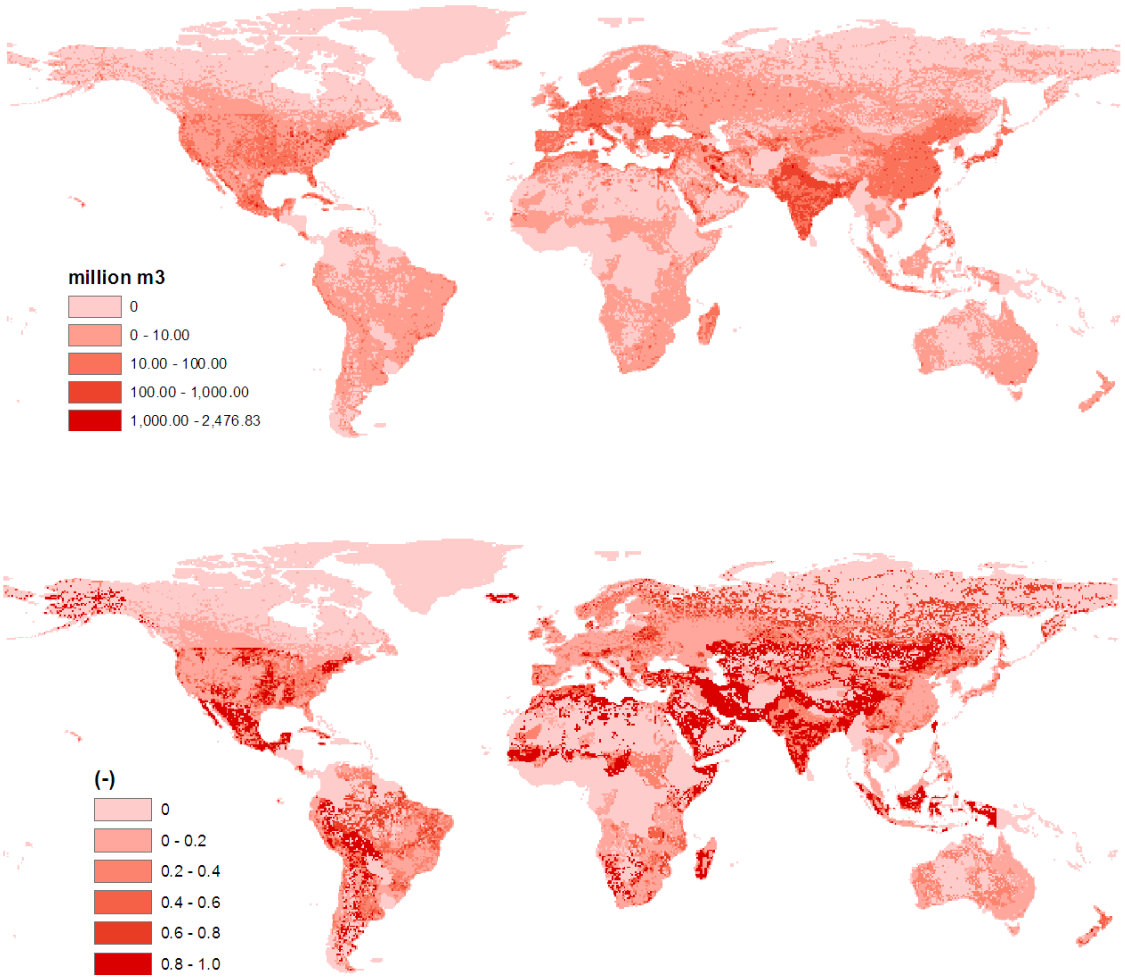

Figure 3.13: Annual groundwater abstraction (million $m^3 \cdot year^{-1}$; above) and the fractional abstraction of groundwater relative to the total water use (-; below) for the year 2000.

4. Water Stress Assessment

4.1. Introduction

Water stress is a measure of the amount of pressure put on water resources and aquatic ecosystems by the use of these resources, including agriculture, industry and households and municipalities (Flörke and Alcamo, 2004). The higher the water stress, the more vulnerable to water scarcity are those who live in a region and future water use might be significantly limited by present water use (i.e. unsustainable water use). In 1997, the United Nations estimated that approximately one-third of the world's population currently lives in countries experiencing moderate to high water stress. In addition, the United Nations forecasted that by 2025 as much as two-thirds of a much larger world population could be under stress conditions simply due to the rise in population and water use (WMO, 1997). Previous studies (Alcamo et al., 2000; Arnell, 1999a, 2004; Islam et al., 2007; Oki et al., 2001; Revenga et al., 2000; Vörösmarty et al., 2000) estimated the number of people living under high water stress ranging from 1.2 to 2.7 billion (see table 4.2). Kundzewicz et al. (2007) noted that global estimates of the number of people living in areas with high water stress differ significantly among studies (Alcamo et al., 2000; Arnell, 1999a, 2004; Islam et al., 2007; Oki et al., 2001; Vörösmarty et al., 2000).

Again, the assessment presented here mainly intends for blue water stress. There are neither assessments nor indictors for green water stress at present. This study is an initial attempt to measure the amount of pressure on green water resources by using green water availability and green water demand estimated in this study.

4.2. Water Scarcity Index

Water Scarcity Index (WSI) is commonly used to indicate the degrees of water stress on both global and regional scales. Several previous studies developed their own indicators. Alcamo et al. (1997, 2000) used “criticality ratio (CR; annual withdrawals over water availability)”. Arnell (1999a) used the simple use/resource ratio, calculated at the national scale. Alcamo et al. (2003b) and Oki et al. (2001) used the “ratio of withdrawals to availability”. This ratio is an indicator of the amount of pressure put on water resources and aquatic ecosystems by the users of these resources, including municipalities, industries, power plants and agricultural users (Alcamo, 2003b). Douglas et al. (2006) and Vörösmarty et al. (2000, 2005) used relative water stress index (RWSI) by comput-

ing the ratio of total water demand (agricultural, industrial, and domestic sectors) to river discharge (representing the renewable water supply). Smakhtin et al. (2004) assessed water stress with a similar index but they included environmental water requirement (EWR) for ecosystems. They subtracted EWR from total water availability. Their results showed that some regions have higher water stress comparing water stress assessment without EWR.

In general, the higher the ratio, the more often the water in a basin is used and the more it is degraded or depleted, therefore limiting further use of these water resources to downstream users (Alcamo et al., 2003b). A value above 0.4 commonly indicates high water stress. A value of 0.4 can be replaced by a per capita water availability of 1,000 $m^3 \cdot year^{-1}$ (based on long-term average runoff; Kundzewicz et al., 2007; see table 4.1). Table 4.1 shows two major indicators for different degrees of water stress.

Table 4.1: Two major indicators for different degrees of water stress (Falkenmark et al., 1997; Kundzewicz et al., 2007).

Degrees of water stress	Per capita water availability ($m^3 \cdot capita^{-1} \cdot year^{-1}$)	Water scarcity index: Rws (-)	Definitions of degrees of water stress
No stress	> 1,700	Rws < 0.1	No water scarcity
Low stress	-	0.1 ≦ Rws < 0.2	Potential water scarcity
Moderate stress	1,700 - 1,000	0.2 ≦ Rws < 0.4	Looming water scarcity
High stress	1,000 - 500	0.4 ≦ Rws < 0.8	Experiencing water scarcity
Very high stress	< 500	0.8 ≦ Rws	Economic development is limited by water scarcity

Although these indicators are widely used, Alcamo et al. (2000) noted that the effects of high water stress are likely to be different in different parts of the world; in developed countries and some desert areas, a value above 0.4 indicates strong competition for water, which does not necessarily trigger frequent water crises, whereas in most developing countries this value may well indicate ongoing, frequent water emergencies. Based on this idea, Alcamo et al. (2000) carried out a sensitivity analysis in which they recomputed the area of river basins in the high water stress category assuming different thresholds values for this category. They set a threshold of high water stress as variables between 0.2 and 0.6 instead of a constant value of 0.4 depending on regions. Their results showed the differences between variables and a constant value of 0.4 are insignificant. This may suggest the robustness of a threshold

value of 0.4 of WSI. Thus, we used the conventional WSI of the use/resource ratio for this water stress assessment.

4.3. Monthly Water Stress Assessment

We computed monthly water availability of river discharge, i.e. blue water, coupled with both reservoir operation scheme and exogenous runoff (i.e. α value), and soil water storage, i.e. green water, over the period between the year 1958 and 2001 (see equation 4.1). Desalinated water use and groundwater abstraction are added to total and blue water availability because they were generated from external water resources. Desalinated water use and groundwater abstraction are estimated for the year 2000. In addition, we estimated monthly water demand for agriculture (livestock and irrigation), industry, households and municipalities and rainfed agriculture. We estimated irrigation and rainfed crop water demand over the period between the year 1958 and 2001, and livestock, industrial and domestic water demand for the year 2000 (see equation 4.4). These are both at a yearly and monthly time scale. Thus, we assessed yearly and monthly water stress by comparing water availability and water demand (see equation 4.6) in terms of both blue and green water. The water scarcity index (use/resource ratio) was used to assess water stress on a global scale as described in table 4.1.

Total water availability:

$$W_{availability\_total} = R + \sum\left(\alpha D_{up} - WD_{up}\right) + (SW - SW_{wp}) + S_{desalination} + GW_{abstraction}, \quad (4.1)$$

where $W_{availability}$ is the total water availability (million $m^3 \cdot month^{-1}$), R is the local runoff (million $m^3 \cdot month^{-1}$), $\sum\left(\alpha D_{up} - WD_{up}\right)$ is the exogenous runoff (million $m^3 \cdot month^{-1}$), SW is the soil water storage (million $m^3 \cdot month^{-1}$), SW_{wp} is the soil water storage at the wilting point (million $m^3 \cdot month^{-1}$), $S_{desalination}$ is the desalinated water use (million $m^3 \cdot month^{-1}$) and $GW_{abstraction}$ is the groundwater abstraction (million $m^3 \cdot month^{-1}$).

Blue water availability:

$$W_{availability\_blue} = R + \sum\left(\alpha D_{up} - WD_{up}\right) + S_{desalination} + GW_{abstraction}, \quad (4.2)$$

where $W_{availability\_blue}$ is the blue water availability (million $m^3 \cdot month^{-1}$) and R is the local runoff (million $m^3 \cdot month^{-1}$).

Green water availability:

$$W_{availability\_green} = SW - SW_{wp}, \tag{4.3}$$

where $W_{availability\_green}$ is the green water availability (million $m^3 \cdot month^{-1}$).

Total water demand (including green water demand):

$$\begin{aligned} W_{demand\_total} &= D_{agriculture} + D_{industry} + D_{domestic} + D_{rainfed} \\ W_{demand\_total} &= \left(D_{livestock} + D_{irrigation}\right) + D_{industry} + D_{domestic} + D_{rainfed} \end{aligned}, \tag{4.4}$$

where W_{demand} is the total water demand (million $m^3 \cdot month^{-1}$), $D_{agriculture}$ is the agricultural water demand (million $m^3 \cdot month^{-1}$), $D_{livestock}$ is the livestock water demand (million $m^3 \cdot month^{-1}$), $D_{irrigation}$ is the irrigation water demand (million $m^3 \cdot month^{-1}$), $D_{industry}$ is the industry water demand (million $m^3 \cdot month^{-1}$) $D_{domestic}$ is the domestic water demand (million $m^3 \cdot month^{-1}$) and $D_{rainfed}$ is the rainfed crop water demand (million $m^3 \cdot month^{-1}$).

Blue water demand:

$$\begin{aligned} W_{demand\_blue} &= D_{agriculture\_blue} + D_{industry} + D_{domestic} \\ W_{demand\_blue} &= \left(D_{livestock} + D_{irrigation\_blue}\right) + D_{industry} + D_{domestic} \end{aligned}, \tag{4.4}$$

where W_{demand_blue} is the blue water demand (million $m^3 \cdot month^{-1}$), $D_{agriculture\_blue}$ is the agricultural water demand for blue water (million $m^3 \cdot month^{-1}$) and $D_{irrigation\_blue}$ is the net irrigation water demand (million $m^3 \cdot month^{-1}$).

Green water demand:

$$\begin{aligned} W_{demand\_green} &= D_{agriculture\_green} + D_{rainfed} \\ W_{demand\_green} &= D_{irrigation\_green} + D_{rainfed} \end{aligned}, \tag{4.5}$$

where W_{demand_green} is the green water demand (million $m^3 \cdot month^{-1}$), $D_{agriculture\_green}$ is the agricultural water demand for green water (million $m^3 \cdot month^{-1}$) and $D_{irrigation\_green}$ is the actual crop evapotranspiration, i.e. green water availability for irrigated crops (million $m^3 \cdot month^{-1}$).

In this study, water stress for blue and green water was separately assessed by comparing monthly water availability and monthly water demand. This is because green water or soil water storage is the water resource available to only crops and plants, so that green water is not available for industry and households and municipalities. Blue water or river discharge is also not the available water resources for rainfed agriculture. The results are shown in figures from 4.1 to 4.4.

Blue and green water stress:

$$R_{WS\_blue/green} = W_{demand\_blue/green} / W_{availability\_blue/green}, \quad (4.6)$$

where $R_{WS\_blue/green}$ is the water scarcity index for blue or green water (-), $W_{availability\_blue/green}$ is the water availability for blue or green water (million $m^3 \cdot month^{-1}$) and $W_{demand\_blue/green}$ is the water demand for blue or green water (million $m^3 \cdot month^{-1}$).

Table 4.2 shows population under different degrees of blue water stress in 100 millions. These estimates vary significantly depending on a spatial resolution (i.e. country-, watershed- or grid-based). The population under high water stress is much smaller (i.e. underestimated) by the country-based estimates than by the watershed- and the grid-based estimates. The country-based estimates are rather crude and hide substantial within-country variation of water availability and water demand (Arnell, 2004). The population under high water stress ranges from 1.2 to 2.7 billion based on the watershed and the grid-based estimates among previous studies. The results of this study are based on the grid-based estimates both at a yearly and at a monthly time scale. The estimated population under high water stress is 0.9 and 1.5 billion for the year 2000 based on a yearly and monthly time scale, respectively. The estimated population under moderate water stress is 0.6 and 0.8 billion for the year 2000 based on a yearly and monthly time scale, respectively. The yearly estimate of this study is close to the estimate of Islam et al. (2007). However, the population under high water stress estimated by this study is smaller than that by the study of Vörösmarty et al. (2000) and Oki et al. (2001). This is

likely caused by the difference of water availability (i.e. runoff and river discharge). Water availability computed by this study is larger than these two studies as shown in table 2.3 (see section 2.3. of chapter 2). The monthly estimate indicates larger population under high water stress than the yearly estimate. The monthly estimate considers seasonal variations of water stress over the year.

Table 4.2: Population (100 millions) under different degrees of blue water stress with different spatial resolutions.

Degrees of water stress	**No stress**	**Low stress**	**Moderate stress**	**High stress**	**Total**	**Year[20]**	**Spatial resolution**	**Temporal resolution**
Per capita water availability ($m^3 \cdot capita^{-1} \cdot year^{-1}$)	**> 1,700**	**-**	**1,700 - 1,000**	**<1,000**				
Rws	**Rws < 0.1**	**0.1≦Rws < 0.2**	**0.2≦Rws < 0.4**	**0.4≦Rws**				
Country based estimates								
WMO (1997)	17	21	14	5	57	1995	Country	Year
Arnell (1999a)	-	-	14	4	52	1990	Country	Year
Vörösmarty et al. (2000)	20	17	15	5	57	1995	Country	Year
Oki et al. (2001)	18	15	15	8	56	1995	Country	Year
Watershed based estimates								
Alcamo et al. (2000)	-	-	-	21	57	1995	Watershed	Year
Revenga et al. (2000)	31	-	7	17	57[21]	1995	Watershed	Year
Oki et al. (2001)	12	5	12	27	56	1995	Watershed[22]	Year
Arnell (2004)	-	-	8	14	57	1995	Watershed	Year
Grid based estimates								
Vörösmarty et al. (2000)	32	4	4	18	58	1995	0.5°	Year
Oki et al. (2001)	28	6	6	17	57	1995	0.5°	Year
Arnell (2004)	-	-	8	26	57	1995	0.5°	Year
Islam et al. (2007)	38	5	6	12	61	2000	0.5°	Year
This study	**40**	**6**	**6**	**9**	**61**	**2000**	**0.5°**	**Year**
This study	**30**	**8**	**8**	**15**	**61**	**2000**	**0.5°**	**Month**

[20] Year indicates the year of the population used for the estimates.
[21] About the population of 200 million people were unallocated on a global scale.
[22] α value was set as 0.0. in the watershed based estimate so that no upstream water was available to downstream reach along the river networks (see section 2.5 of chapter 2).

4.4. Seasonality

In this study, the magnitude of water stress is subject to vary over the year due to the seasonality of river discharge and soil water experiencing wet and dry seasons as well as seasonal variations of irrigation, rainfed agriculture and domestic water use. Figure 4.1 shows average blue water stress based on a monthly time scale and a yearly time scale for 44 years from the year 1958 to 2001 and subtraction from a monthly to a yearly time scale. Figure 4.2 shows average monthly blue water stress for 44 years from the year 1958 to 2001 with highlighted possible problem regions (i.e. black circles). Our blue water stress assessment identified large regions with considerable water stress that the assessment of annual and monthly water stress was mismatched.

The finer temporal resolution (i.e. month) revealed highlighted possible problem regions (i.e. high water stress or more than the water scarcity index of 0.4) which are not well represented by existing annual water stress assessments (e.g. Alcamo et al., 1997, 2000, 2003b; IWMI, 2000; Oki et al., 2001, 2006; Shiklomanov, 2000; Sullivan et al., 2003; Vörösmarty et al., 2000). These regions are Sub-Sahara, the central part of the Russian Federation, Central Asia, the eastern part of Brazil, the western part of Australia, the eastern part of the U.S.A. and India. In these possible problem regions highlighted with black circles in figure 4.2, high water stress occurs during different times of the year following the dynamics of water demand and water availability (i.e. high water demand or low rainfall).

Previous studies of global water stress assessment generally focused on only blue water availability and demand. In this study, in addition to blue water stress, we estimated green water stress at a monthly time scale as shown in figure 4.3 and 4.4. Figure 4.3 shows average green water stress based on a monthly time scale and a yearly time scale for 44 years from the year 1958 to 2001 and subtraction from a monthly to a yearly time scale. Figure 4.4 shows average monthly green water stress for 44 years from the year 1958 to 2001. Due to heavy rainfed agriculture, high water stress is occurring nearly all around the year in South Africa. High water stress appears in large regions around summer (i.e. May to August) in the Northern Hemisphere including the U.S.A., Spain, the eastern and the southern part of Europe and Central Asia. The results of assessment of green water are preliminary. As described earlier in this chapter, neither assessments nor indicators for green water stress exist at present. We simply applied the water scarcity index to green water stress.

Although there is no previous study to assess green water stress, Gerten et al. (2005) pointed out the importance of green water resources related with global water stress assessment. They also suggested a comprehensive and consistent quantification of

global green and blue water flows and of water limitations of terrestrial vegetation (both natural and agricultural vegetations), using newly developed water stress indicators and combining green water stress indicators with conventional blue water stress indicators. By using the conventional water scarcity index, however, it might be possible to point out that if green water demand is higher than or close to green water availability, crops and plants experience very high water stress so that further expansion of rainfed agriculture is not possible in these regions without a sacrifice of natural vegetation.

The assessment of this study for both blue and green water stress revealed the importance of considering the spatiotemporal variability of water stress unlike previous assessments of water stress that generally focused on the spatial variability of water stress only. The results of this study clearly showed the seasonal trends, i.e. temporal variability, of blue and green water stress on a global scale, which the conventional assessments of water stress have not yet described. The temporal variability is a decisive factor for water stress assessment especially for the region experiencing wet and dry seasons such as (sub-)tropics as shown in figure 4.2 and 4.4.

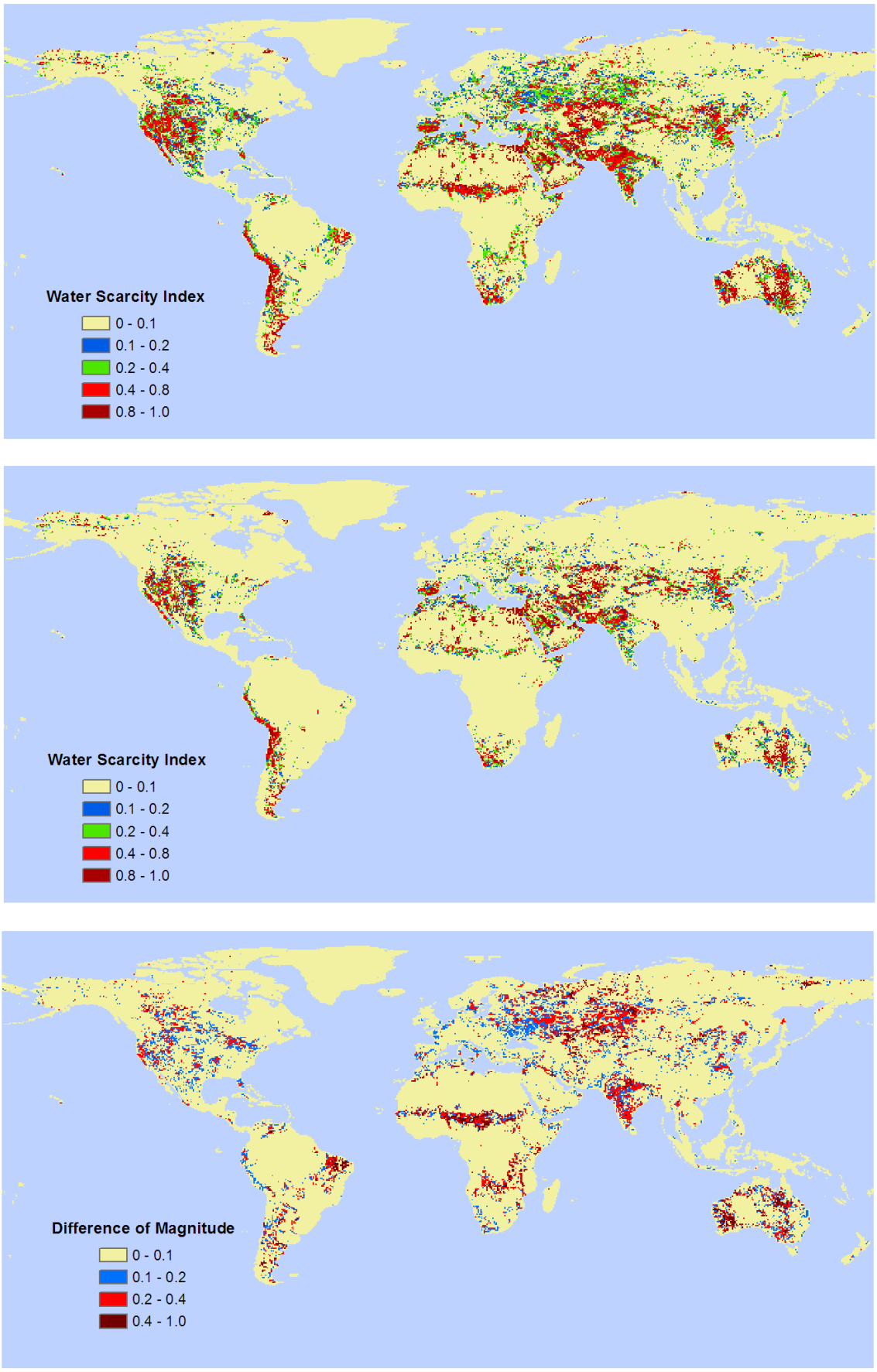

Figure 4.1: Average blue water stress based on a monthly time scale (upper) and a yearly time scale (middle) for 44 years from the year 1958 to 2001 and subtraction from a monthly to a yearly time scale (bottom).

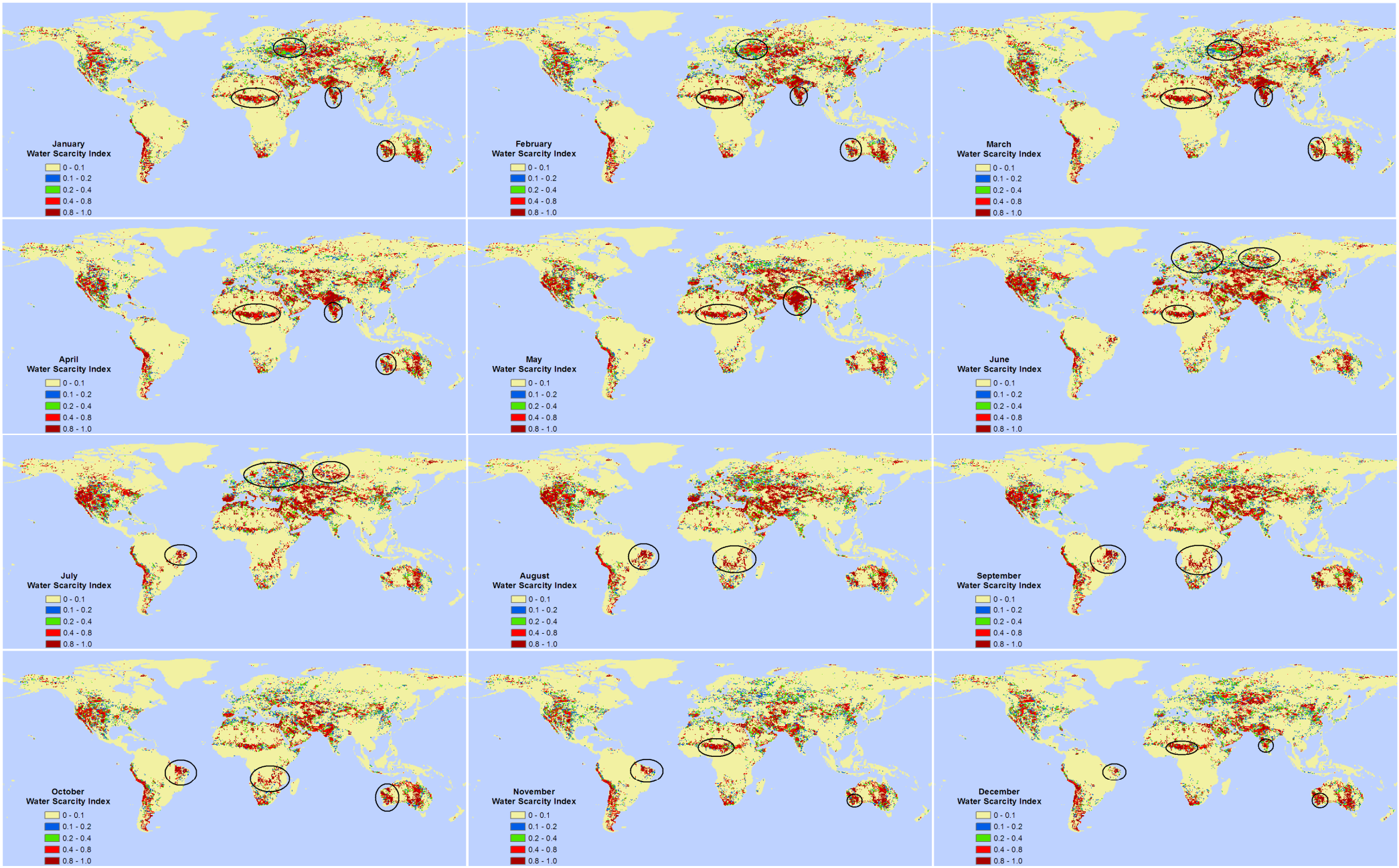

Figure 4.2: Average monthly blue water stress for 44 years from the year 1958 to 2001 with highlighted possible problem regions, see figure 4.1 for average annual blue water stress.

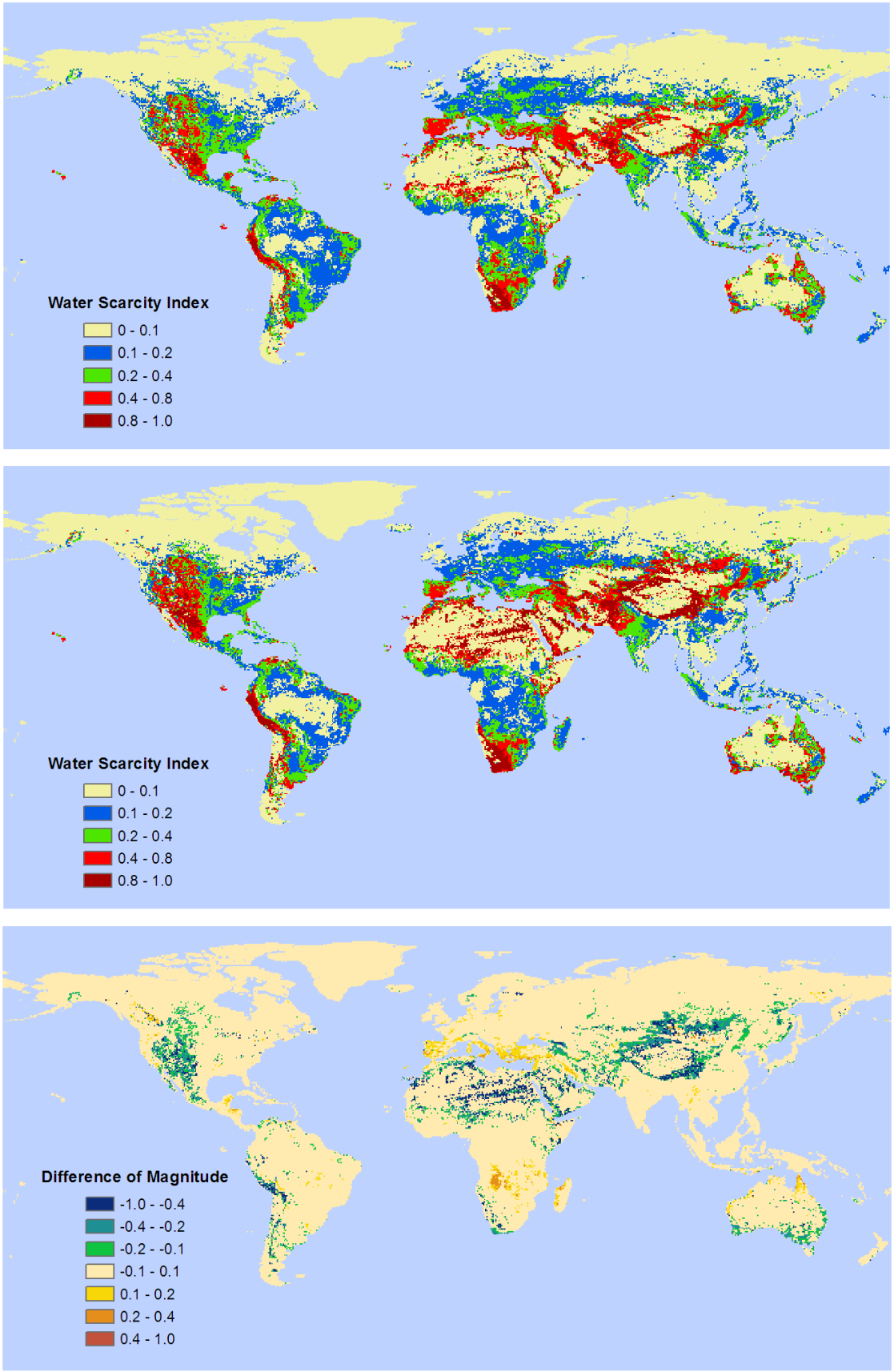

Figure 4.3: Average green water stress based on a monthly time scale (upper) and a yearly time scale (middle) for 44 years from the year 1958 to 2001 and subtraction from a monthly to a yearly time scale (bottom).

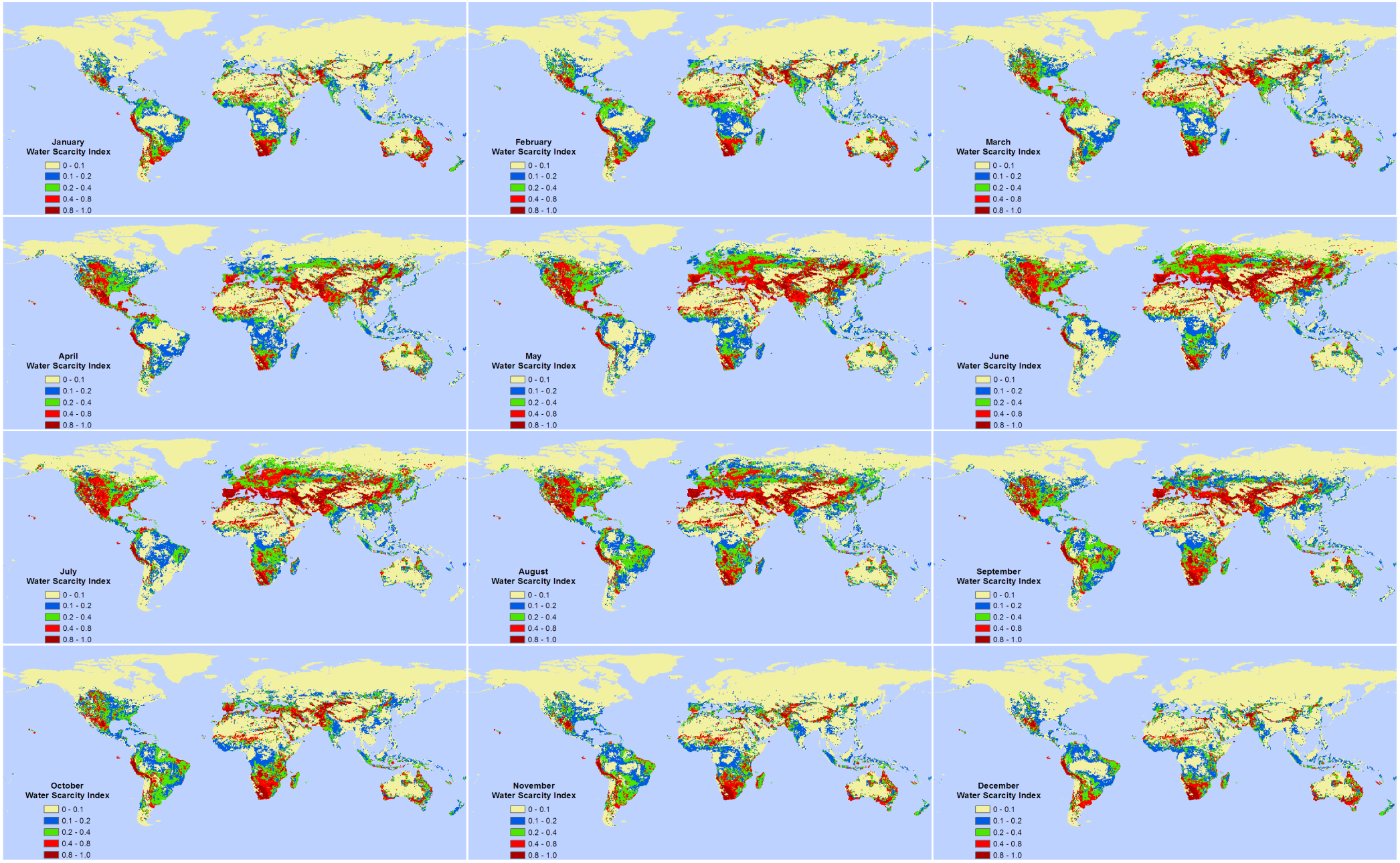

Figure 4.4: Average monthly green water stress for 44 years from the year 1958 to 2001, see figure 4.3 for average annual green water stress.

4.5. Severity

In the previous section, we highlighted possible problem regions by comparing annual and monthly water stress and pointed out a temporal variability of water stress on a global scale. In this section, we analysed the severity of water stress for different parts of the world. Since we estimated water stress for 44 years from the year 1958 to 2001, it was possible to make an analysis of the development of water stress not only within the year, but also by looking at the inter-seasonal variation over decades. This study quantified the severity of water stress during the long-term period of 44 years, i.e. 528 months. The severity of water stress was quantified by persistence, recurrence (see figure 4.5 and equation 4.7 and 4.8) and average high water stress (i.e. water stress above high water stress or the water scarcity index of 0.4). Persistence is the average length of water stress above a threshold value. The threshold value is set as high water stress or the water scarcity index of 0.4 in this study. For example, in the figure 4.5, average persistence is 5 months and high water stress continues without intermittences over these months. Recurrence is the average length between two high water stress periods (see figure 4.5). In the figure 4.5, recurrence is only 1 month in that specific year.

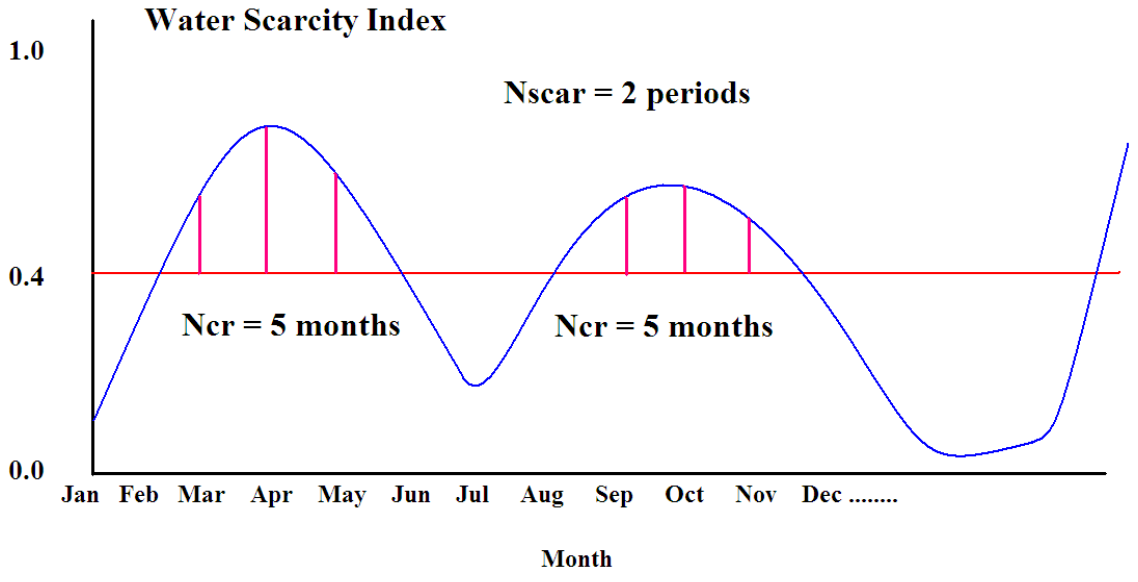

Figure 4.5: Concepts of the Ncr and Nscar with the water scarcity index of 0.4 as the threshold value.

Persistence:

$$Persistence = \frac{Ncr}{Nscar}, \tag{4.7}$$

where $Persistence$ is the average persistence of water stress with the threshold value of 0.4 (month), Ncr is the number of months with the water stress higher than 0.4 (month) and $Nscar$ is the number of periods with water stress higher than 0.4 (month).

Recurrence:

$$Recurrence = \frac{N - Ncr}{Nscar}, \tag{4.8}$$

where $Recurrence$ is the average recurrence of water stress with the threshold value of 0.4 (month), N is the total number of months (month), Ncr is the number of months with the water stress higher than 0.4 (month) and $Nscar$ is the number of periods with water stress higher than 0.4 (month).

Figure 4.6 and 4.7 show average persistence and recurrence for blue water, respectively for 44 years from 1958 to 2001. In addition to these figures, figure 4.8 shows average high water stress for blue water over 44 years. Combined, these figures reveal how long and how severe water stress is. This in turn enables us to quantify the severity of water stress. For example, in India, Australia and the northeastern part of the PRC where there is high water demand for irrigation, very high water stress occurs as shown in figure 4.8 and persistence is several months as shown in figure 4.6 and recurrence is only a couple of months as shown in figure 4.7. This indicates that high water stress occurs frequently almost without any intermittence over the year in these regions. Thus, the severity is considered as very high in India, Australia and the northeastern part of the PRC. On the other hand, in the southern part of the U.K., very high water stress occurs but persistence is one to two months and recurrence is more than several months. This indicates that although very high water stress occurs in the southern part of the U.K., it occurs only during a short period and not every year. Therefore, the severity is considered as low. The same condition holds in the northwestern part of the Russian Federation.

The severity of green water stress shows very different trends from that of blue water stress. Figure 4.9 and 4.10 show average persistence and recurrence for green

water, respectively for 44 years from 1958 to 2001. Also, figure 4.11 shows average high water stress for green water over 44 years. The severity is considered as very high in South Africa and Australia where there is high demand for rainfed agriculture. Very high water stress occurs frequently almost without any intermittence around the year in South Africa and Australia. In Western Europe except Spain, however, water stress occurs frequently but persistence is short and the magnitude of water stress is low so that the severity is considered as relatively low.

In conclusion, persistence, recurrence and average high water stress revealed the regions experiencing different degrees of severity on a global scale. Future climate change resulting lower river discharge or soil water storage may cause severe water shortage unless demand is decreased in severe water stress regions such as India, South Africa and Australia.

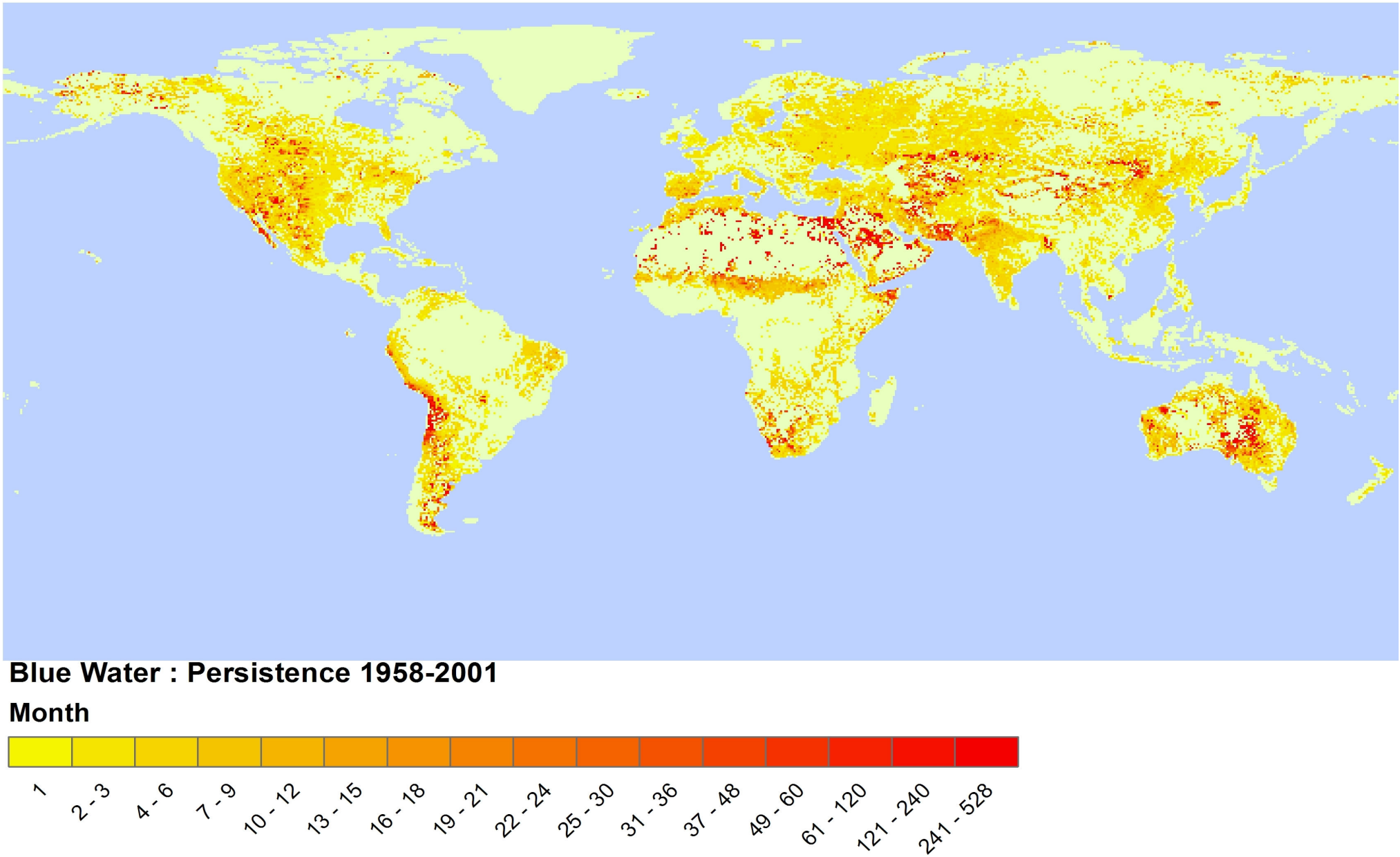

Figure 4.6: Average persistence for blue water over 44 years from the year 1958 to 2001.

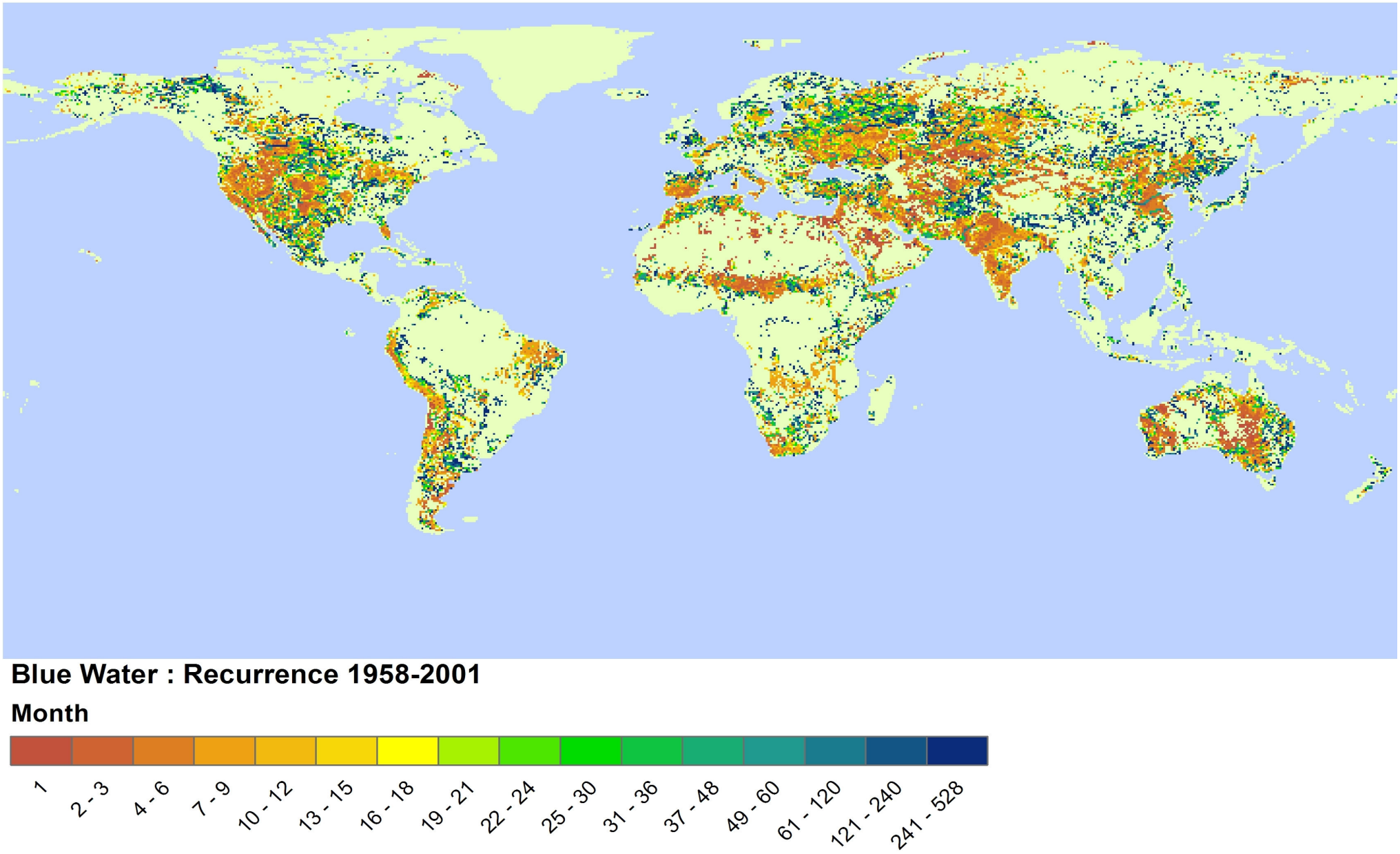

Figure 4.7: Average recurrence for blue water over 44 years from the year 1958 to 2001.

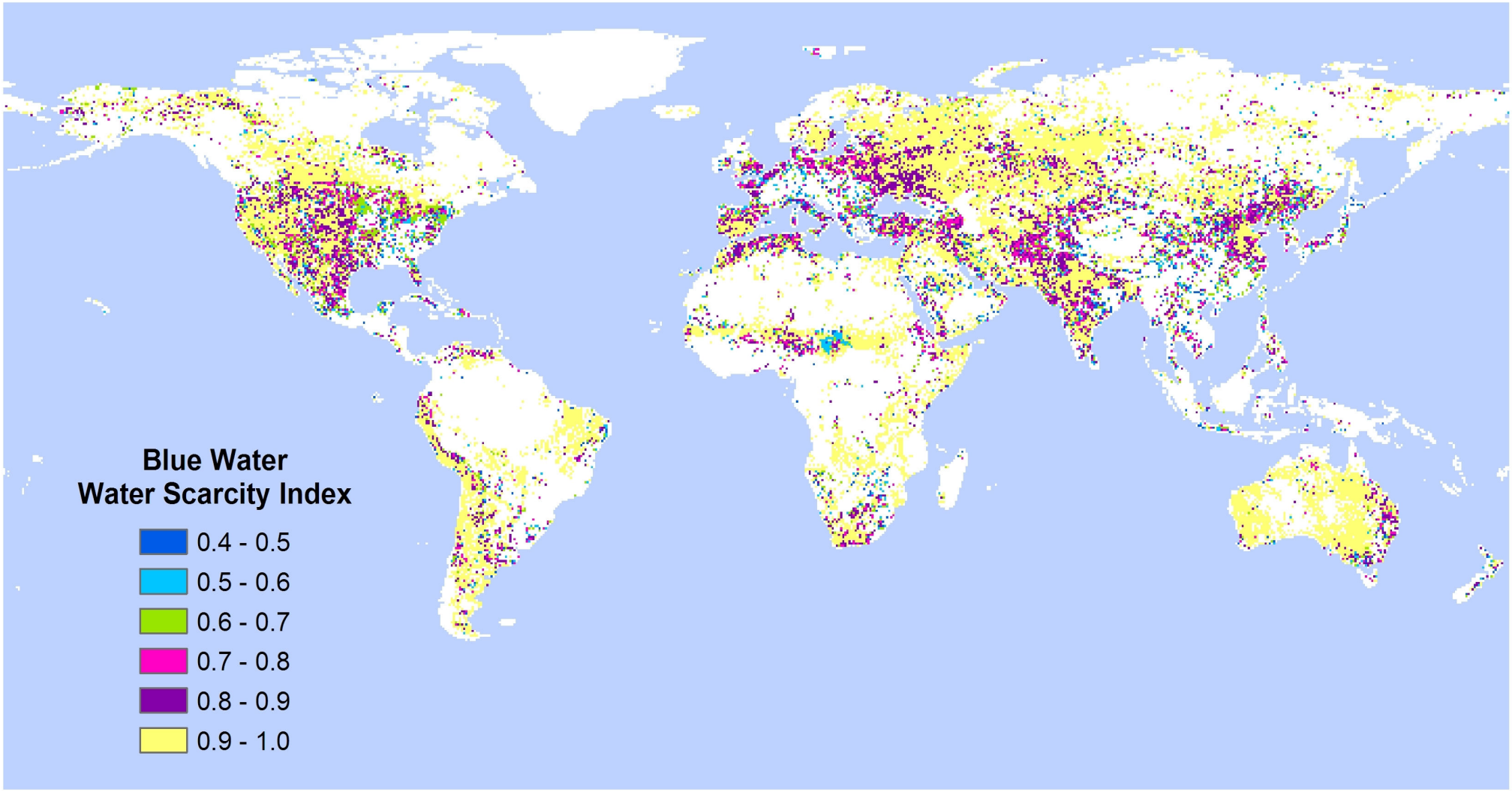

Figure 4.8: Average high water stress for blue water over 44 years from the year 1958 to 2001.

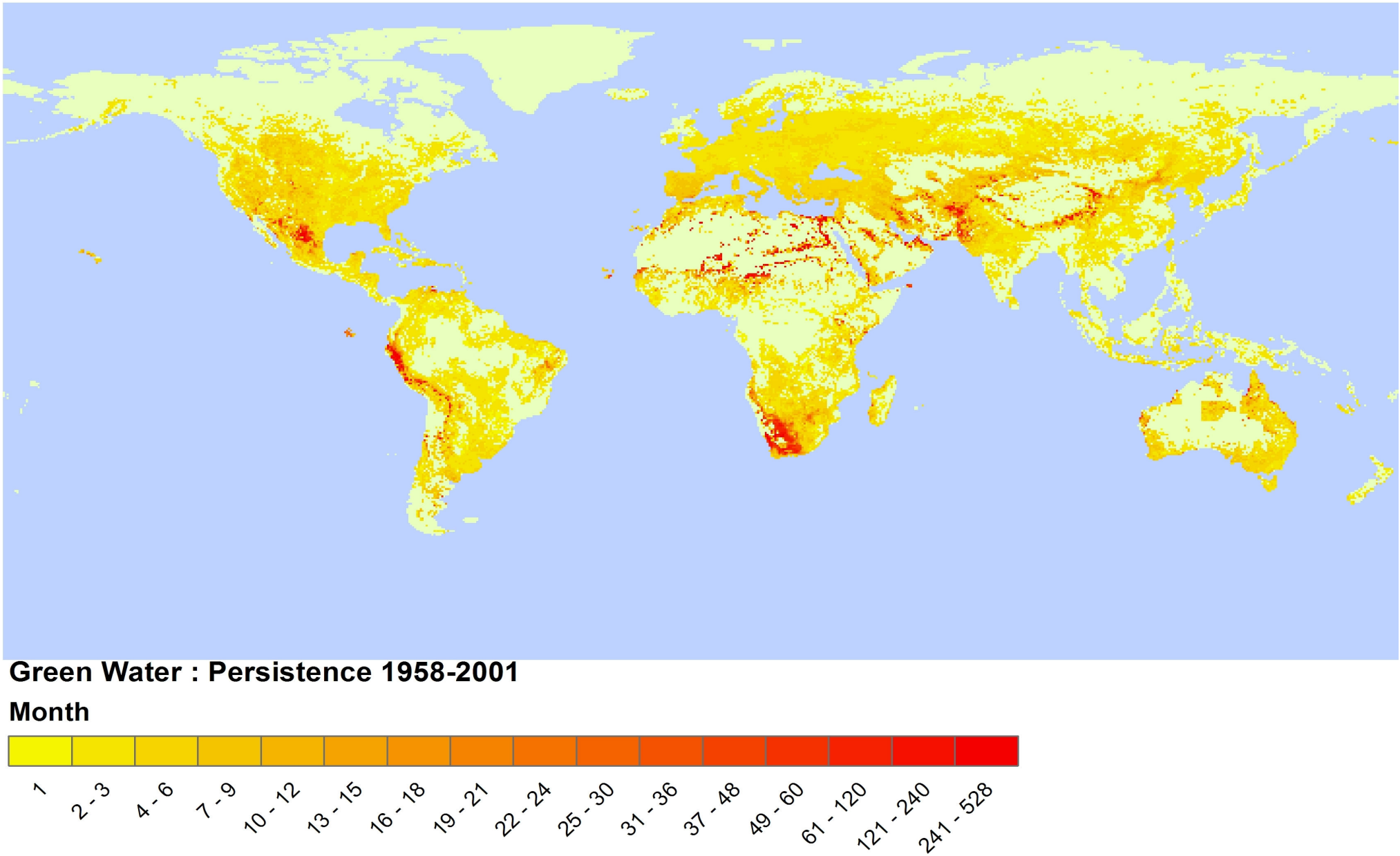

Figure 4.9: Average persistence for green water over 44 years from the year 1958 to 2001.

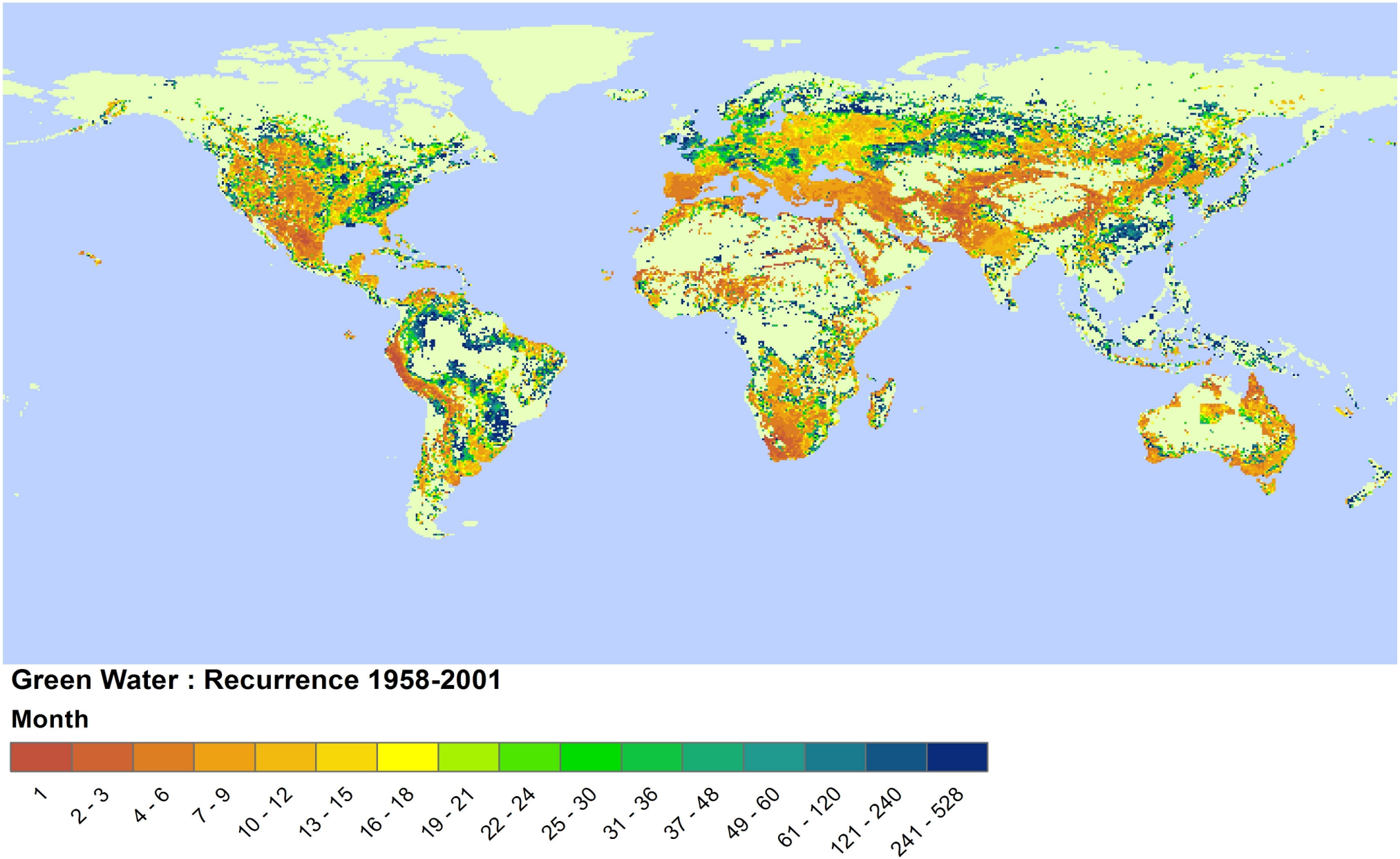

Figure 4.10: Average recurrence for green water over 44 years from the year 1958 to 2001.

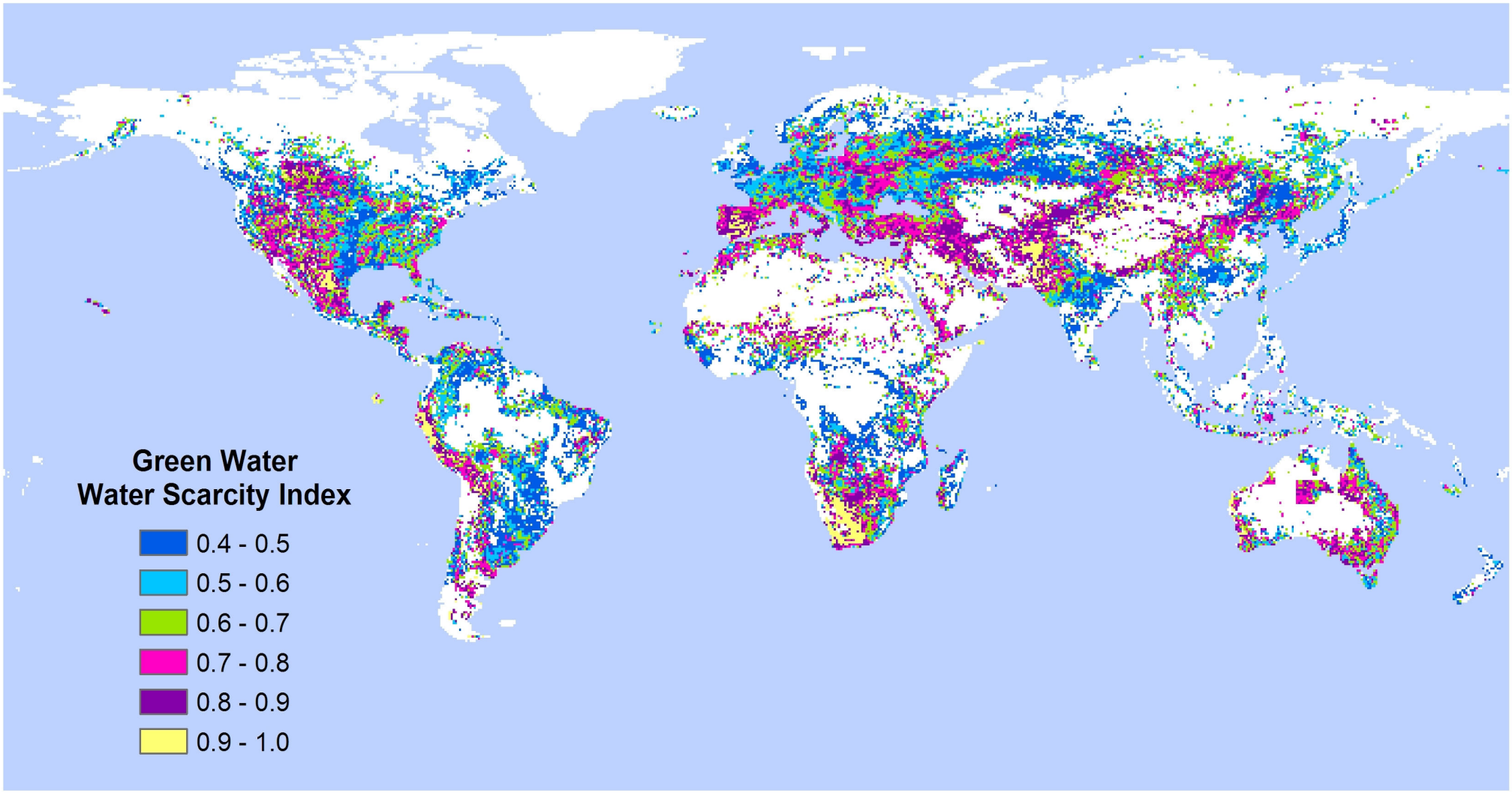

Figure 4.11: Average high water stress for green water over 44 years from the year 1958 to 2001.

4.6. Dynamic Water Stress

Apart from the water scarcity index, we also assessed water stress with dynamic water stress. The dynamic water stress was developed by Porporato et al. (2001). Unlike the water scarcity index, the dynamic water stress is a measure of total stress over a prolonged period of time taking into account the frequency and the mean length of the water stress period (Brolsma and Bierkens, 2007). The dynamic water stress enables to quantify the severity of water stress by combining the magnitude, duration and frequency of water stress. The dynamic water stress was then calculated following the method of Porporato et al. (2001):

$$WS_{dynamic} = \left(\frac{\overline{\zeta_w}\,\overline{T_{SW}}}{kT_{seas}} \right)^{1/\sqrt{n_s}}, \tag{4.9}$$

where $WS_{dynamic}$ is the dynamic water stress (-), $\overline{\zeta_w}$ is the average water stress above a threshold value (-; the threshold is set as the water scarcity index of 0.4 in this study), $\overline{T_{SW}}$ is the mean duration of a water stress period (month; comparable to persistence, see section 4.5.), k is a parameter which is a threshold where water stress occurs (-; 0.4 in this study), T_{seas} is the length of a period (month) and n_s is the frequency at which water stress occurs (-).

Figure 4.12 show dynamic water stress for blue water over 44 years from the year 1958 to 2001. Figure 4.13 shows dynamic water stress for green water over 44 years from the year 1958 to 2001. Higher values of dynamic water stress indicate severer water stress. The dynamic water stress revealed that the severity is very high in India and Australia for blue water as described in the previous section. In addition, Sub-Sahara also experiences severe water stress. For green water, on the other hand, the severity is very high in South Africa as described in the previous section. The dynamic water stress also revealed that the severity is very high in Spain as well as Mexico.

Together with the severity described in the previous section, the dynamic water stress is a useful indicator considering the temporal aspect of water stress.

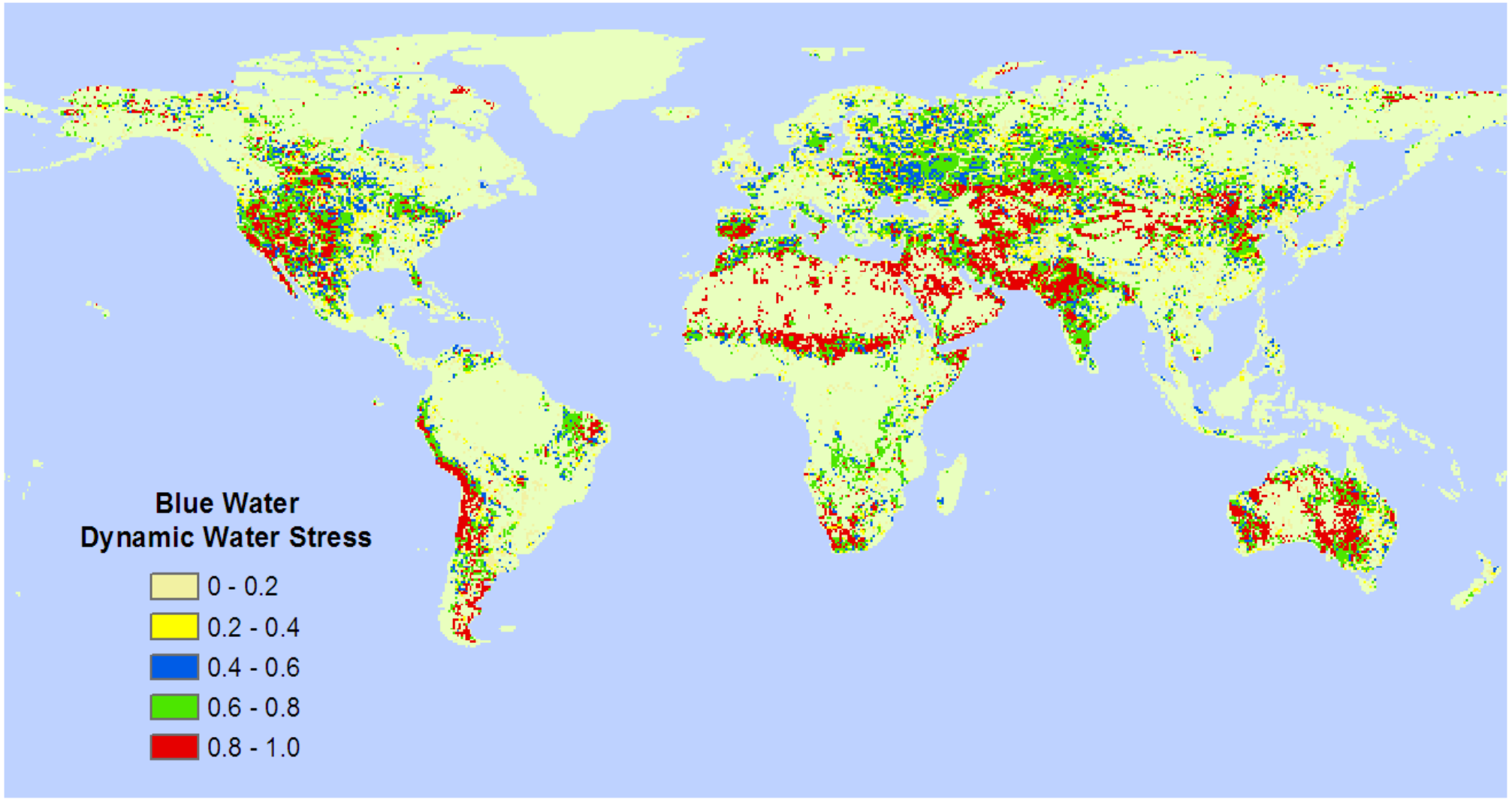

Figure 4.12: Dynamic water stress for blue water over 44 years from the year 1958 to 2001.

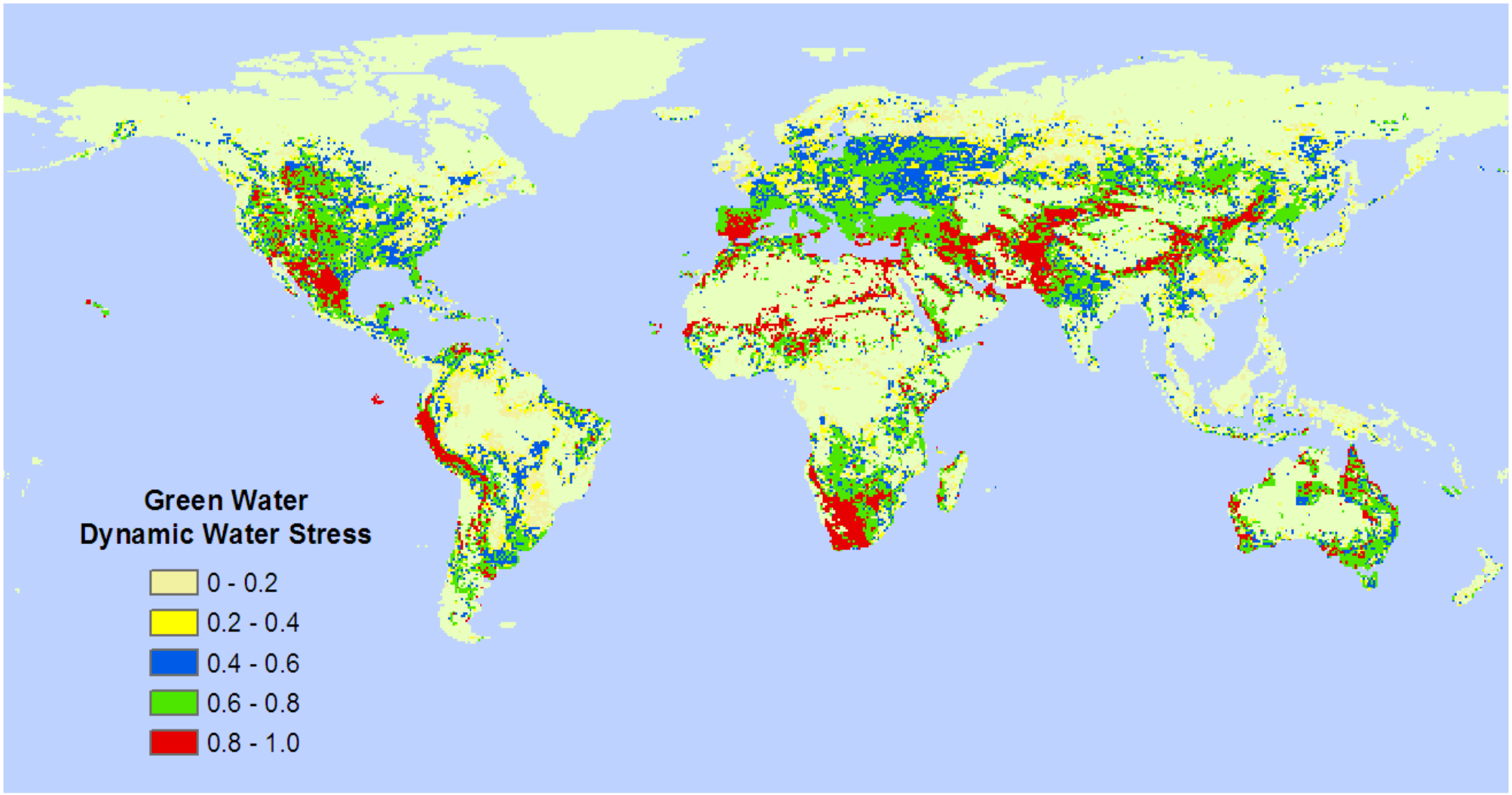

Figure 4.13: Dynamic water stress for green water over 44 years from the year 1958 to 2001.

4.7. Effect of Exogenous Runoff and α Value

In this section, we analysed the effect of exogenous runoff by using α value on blue water stress. In section 2.5 of chapter 2, we described the locally generated runoff transported to downstream from upstream through the local drainages or river networks. As described earlier, the sensitivity analysis of Oki et al. (2001) revealed that α value is a decisive factor to estimate not only water availability but also water stress. Figure 4.14 shows the effect of α on the water stress assessment by the study of Oki et al. (2001). They assessed water stress by the number of people under different degrees of water stress with different α values ranging from 0.0 to 1.0.

In this study, we compared blue water stress based on two different α values, 0.5 and 1.0, respectively. Figure 4.15 shows average blue water stress based on a monthly time scale with α = 1.0 and α = 0.5, and subtraction from α = 0.5 to α = 1.0. We estimated the total river discharge or blue water availability with α = 0.5. This resulted in higher water stress compared to the total river discharge with α = 1.0. Importantly, there is one region in Australia where lowering alpha value has a significant impact. This region is located in the northern part of Australia. This region is especially vulnerable to lower river discharge, thus sensitive to climate or meteorological conditions. However, as shown in the figure 4.15, the difference of magnitude between water stress with α = 1.0 and water stress with α = 0.5 is relatively low in many regions. This may suggest that many regions are already experiencing high water stress so that the amount of exogenous runoff does not drastically change the magnitude of water stress only by half of α = 1.0. The study of Oki et al. (2001) also showed the difference of magnitude between α = 1.0 and α = 0.5 is relatively low. Their result indicated that α plays a considerable role if α is set lower than 0.1.

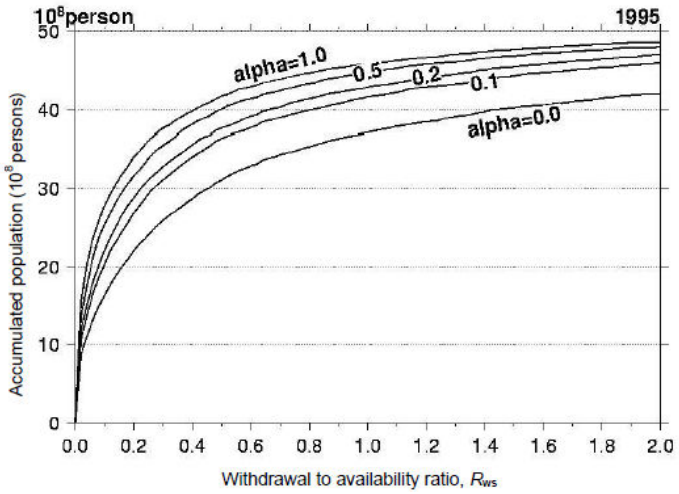

Figure 4.14: Effect of α on the grid-based water stress assessment from Oki et al. (2001).

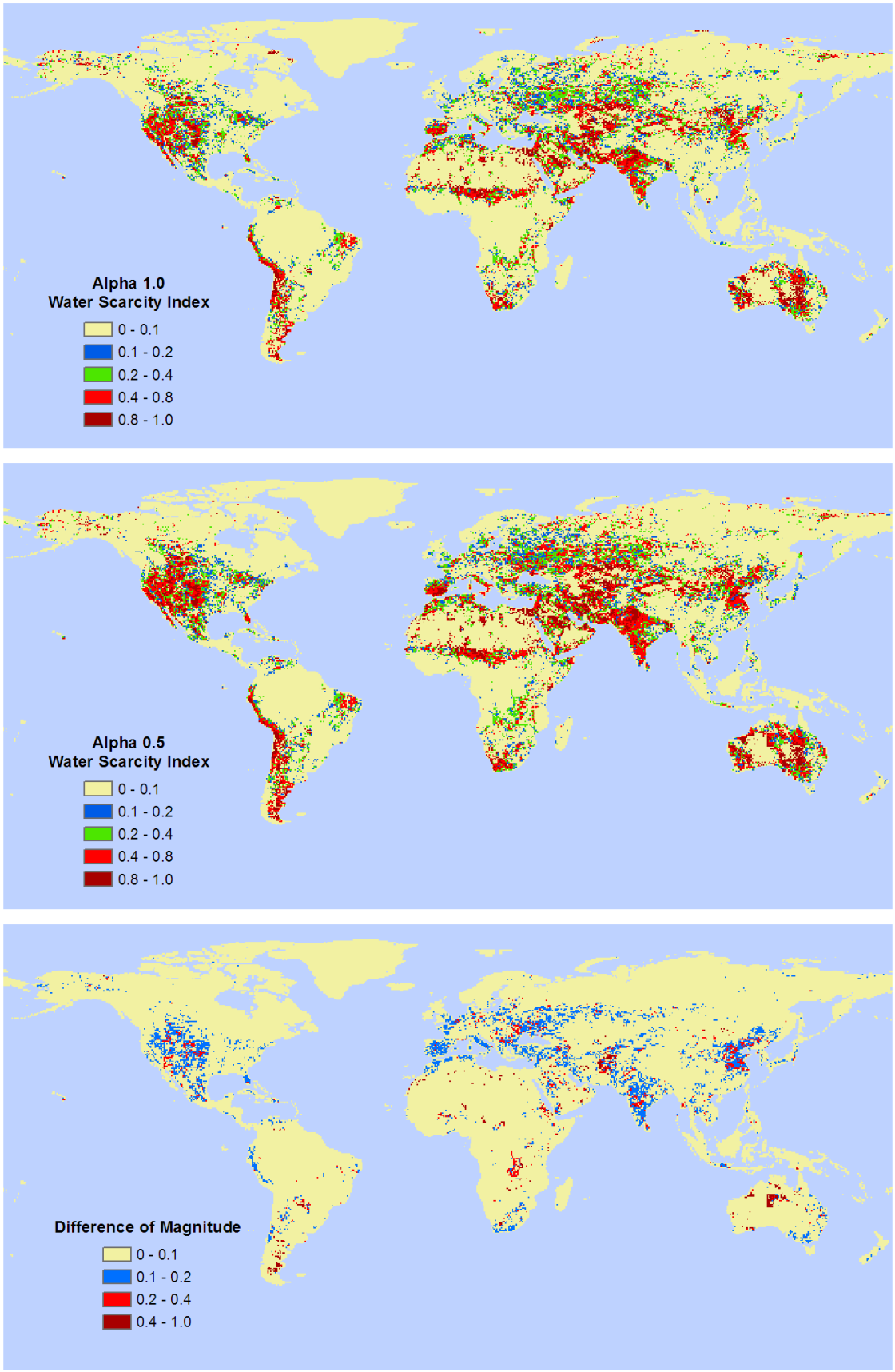

Figure 4.15: Average blue water stress based on a monthly time scale with α = 1.0 (upper) and α = 0.5 (middle) for 44 years from the year 1958 to 2001 and subtraction from α = 0.5 to α = 1.0 (bottom).

4.8. Water Stress and Climate Variability

In this study, water stress was estimated based on water demand of the year 2000 contrasted to 44 years of a long-term climate variability. In this section, we analyzed the result of blue water stress over a long-term period and compared the result to observation.

We averaged the water scarcity index within the country over grid cells to grasp the historical trend of the country. Figure 4.16 shows estimated water stress in the Netherlands. The Netherlands experienced severe water stress especially in the year 1959, 1976 and 1995 among 44 years from the year 1958 to 2001 based on the result of this study. According to the Netherlands Drought Study (http://www.droogtestudie.nl/Engels/index.html), the Netherlands experienced very dry year (once every 50 years) in the year 1959 and extremely dry year (once every 200 years) in the year 1976 (RIZA, 2003). The Netherlands suffered severer water shortage in these years than any other years between the year1958 to 2001.

Figure 4.17 shows water stress and the number of drought events in Japan. The number of droughts was calculated based on the number of events of the suspension of the water supply for agricultural, industrial and domestic sectors by the MLIT (2007). Japan experienced higher water stress in the year 1973, 1978 and 1994 than any other years based on the result of this study. The number of drought events is also higher in these years and corresponds to our result. Water shortage was extremely severe especially in the year 1978 and 1994. Water supply was suspended nearly 20 hours a day for several weeks in the city of Fukuoka and Matuyama (western part of Japan; JMA: Japanese Meteorological Agency; http://www.jma.go.jp/jma/indexe.html). However, our result does not agree well with the number of drought events in the year 1967. This is likely caused by the averaged value of the water scarcity index within the country. Due to the averaged value of many grid cells, the magnitude of water stress was lowered. If a limited region experienced severe water stress and others do not, the magnitude of water stress is significantly lowered. According to the JMA, severe water shortage occurred particularly in the southern part of Japan (i.e. Kyushu) in the year 1967.

The result of this study generally corresponds well to the observation of past water shortage (i.e. extreme events) in the Netherlands and Japan. Even though estimated water demand of the year 2000 stays constant for 44 years, water stress (thus water shortage) was well reproduced by a long-term climate variability.

In addition to these figures, there are two movie files in CD-ROM attached with this document. One movie file is water_stress_blue_1958-2001.avi and the other movie file is water_stress_green_1958-2001.avi. Transient behaviour of monthly blue (wa-

ter_stress_blue_1958-2001.avi) and green (water_stress_green_1958-2001.avi) water stress from the year 1958 to 2001 is recorded in these two movie files.

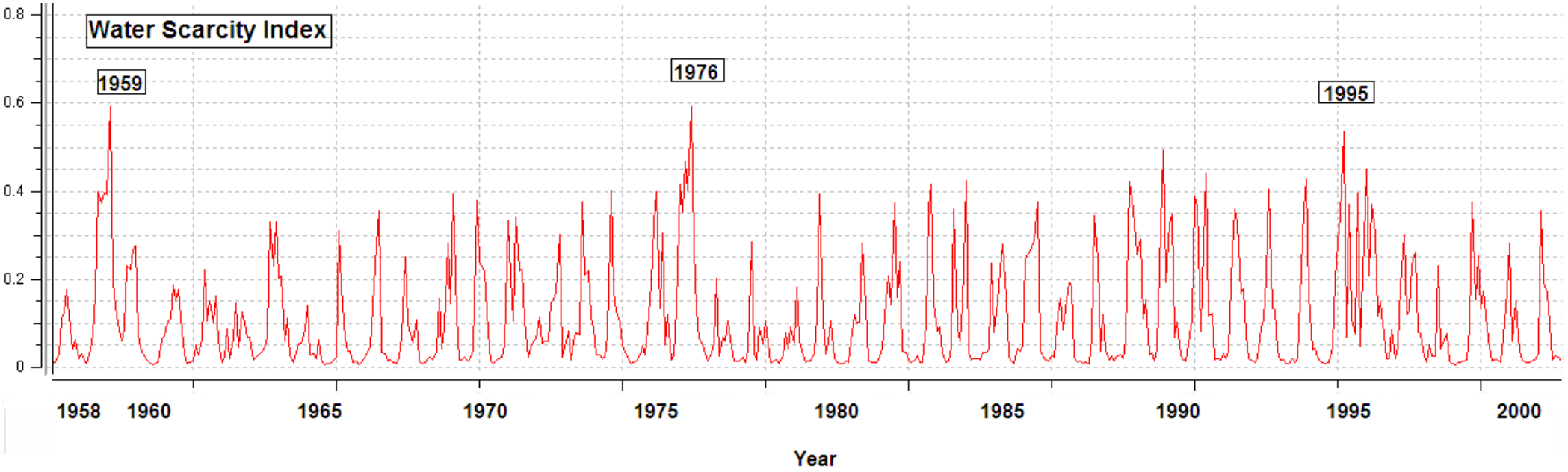

Figure 4.16: Water stress in the Netherlands from the year 1958 to 2001.

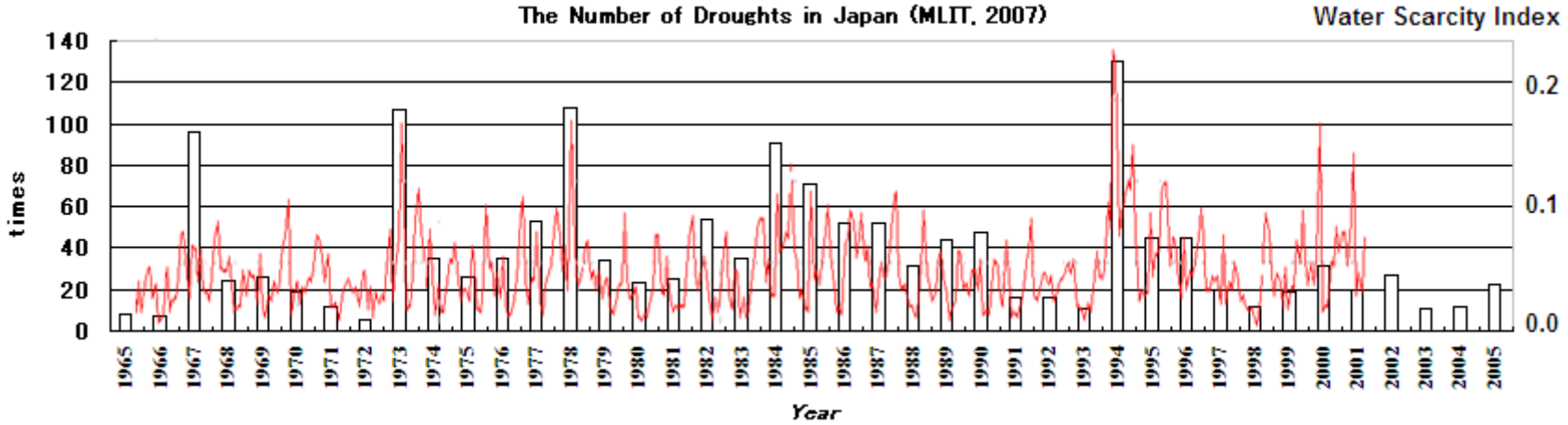

Figure 4.17: Water stress and the number of drought events in Japan.

5. Conclusions

5.1. Summary and Results

This study assessed water stress at a monthly time scale on a global scale for the first time. Water availability was computed by PCR-GLOBWB from the year 1958 to 2001. Water demand was estimated for the year 2000 as a bench mark year following the methods used in previous studies (Alcamo and Henrichs, 2002, 2003a; Flörke and Alcamo, 2004; Oki et al., 2001; Siebert and Döll, 2008; Vörösmarty et al., 2000) but with the latest available data sets (e.g. livestock, 26 irrigated crops, desalinated water use and groundwater abstraction).

The results of this study estimated that 1.5 and 2.3 billion of world's population are under moderate to high water stress but the results vary depending on a yearly and monthly time scale, respectively. This study revealed the seasonality of both blue and green water stress. In addition, our results identified the large regions where the assessment of annual and monthly water stress was mismatched. It is highly possible that water stress in those regions will be acerbated by continued population growth or impending climatic change. Importantly, the degrees of water stress were underestimated by existing annual assessments (e.g. Alcamo et al., 2003b; Alcamo and Henrichs, 2002; Arnell, 1999a, 2004; Islam et al., 2007; Oki et al., 2001; Vörösmarty et al., 2000). Although it was pointed out by Meigh et al. (1999) that water shortages often first become apparent as occasional deficits at certain times of the year, this study verified their argument on a global scale for the first time.

The severity of water stress was quantified by persistence, recurrence, average intensity as well as the dynamic water stress developed by Porporato et al. (2001). These analyses revealed the regions where the severity is particularly high such as India, Australia and Sub-Sahara, and relatively low such as the southern part of the U.K. and the northwestern part of the Russian Federation for blue water. The severity is also particularly high in South Africa, Spain and Mexico, and relatively low in Western Europe except Spain for green water. At last, the periods of past 44 years of water stress were also well reproduced by a long-term climate variability, which is good enough to capture the extreme events (i.e. severe water shortage or drought). This indicates that climate has a significant impact on water stress.

5.2. Discussion

A number of global-scale studies (Alcamo and Henrichs, 2002; Arnell, 2004, Islam et al., 2007; Oki et al., 2001; Vörösmarty et al., 2000) showed that semiarid and arid regions were the most vulnerable to water stress (Kundzewicz et al., 2007), however, they lacked for a temporal aspect. This study revealed new dimension of water stress by using a finer temporal scale (i.e. month) than previous studies. The monthly temporal scale enabled to assess the seasonality and the severity of water stress that were not well described by existing annual assessments. This study identified the regions spatiotemporally vulnerable to water stress.

However, it should be noted that there are uncertainties mainly caused by the assumptions to estimate water demand and particular water resources. Livestock and industrial water demand, desalinated water use and groundwater abstraction remains constant over the year in this study. Groundwater abstraction may have a significant impact on water stress if it varies over the year (e.g. relative to water demand). The impact will be high particularly in the mid-west of the U.S.A. and India where a large amount of groundwater is used for irrigation.

Water recycling in industry and return flow of domestic water use also cause uncertainties in this study. Water can be used more than once after it is withdrawn (Jackson et al., 2001) because water used for industry and households and municipalities is not physically consumed (although it sometimes requires further treatment; Jackson et al., 2001). The ratio interpolated by this study is preliminary due to data and time constraints. The recycling ratio is a decisive factor to determine the amount of industrial and domestic water demand. Further studies (e.g. sensitivity analysis of different recycling ratios in different countries) will be necessary to obtain more accurate ratio.

Our assessment for green water stress is preliminary because no green water stress indicators exist at present. It might be necessary to assess blue water stress combined with green water stress. This is because changes in land use affect green water flows and determine the available blue water flows further downstream (Falkenmark and Rockström, 2005).

The spatial resolution has been an important issue in water stress assessment as well. Douglas et al. (2006) noted that the degrees of water scarcity are subject to change depending on different spatial resolution. They showed that the different numbers of people were exposed to high water stress in Africa based on the 1.5 and 6 minutes spatial resolution. Their results suggest that the issue of spatial resolution needs to be studied further, even on a global scale.

5.3. Future Steps

The results of this study are preliminary. There are large potentials to improve water stress assessment further. Several important steps are described in this section.

Further estimates of monthly water demand especially in industrial and domestic sectors are necessary to improve the assessment of water stress. Accurate estimates of water demand will also feedback into simulated reservoir operations to improve river discharge and thus improve estimates of the global water balance as well. The study of green water stress indicators will be of scientific importance. This study applied the water scarcity index to green water stress although the water scarcity index focuses on human water use. It will be necessary to assess green water stress with more reasonable indicators (e.g. compare green water availability to demand for calories based on population density).

Different types of water stress are an important aspect partly studied by IWMI (2000). There is a geographical and hydroclimatic characteristic between the water-endowed regions with a temperate climate, where most of the developed countries are located, and the water-short regions where most of the developing countries tend to be located (Falkenmark and Rockström, 2005). In the former, vegetation is basically energy-constrained, while vegetation in the latter is water-constrained (Falkenmark and Rockström, 2005). The type of water stress depending on a cause will be an interesting step.

The access to water and the quality of water are playing important roles in many regions. This study partly evaluated the quality of water by using the recycling ratio. On top of that, Arnell (1999a) suggested other dimensions of water stress, related not so much to the volume of water available but rather to access to water. The access to water can be limited because of geographical reasons or water quality problems. There might be a region with abundant water resources but under extreme water stress. According to the Global Water Supply and Sanitation Assessment 2000 Report, the majority of the world's population without access to improved water supply or sanitation services lives in Africa and Asia (Meinzen-Dick and Rosegrant, 2001). In these regions, water quality plays a decisive role to control the amount of available water because people use water directly from the source without any treatments. Water pollution limits water usage of human society. This may significantly change the degree of water stress in a region.

Exogenous runoff is still not well defined as pointed out by Islam et al. (2007) although it has a huge impact on water availability downstream possibly combined with the quality of water. Water supply for various sectors of society is getting increasingly complicated as water contamination escalates, and awareness grows among water users

of the links between upstream polluters of water and downstream water users (Falkenmark and Rockström, 2005).

The reconstruction of water demand over the past 44 years and the future (e.g. up to the year 2050) will be an interesting step to reproduce an actual history and a projection of water stress. Our results indicated that the past 44 years of water stress was well reproduced solely by past climate variability. The assessments of future water stress with future climate variability or socio-economic and water demand scenarios (e.g. IPCC scenarios) will be of scientific importance. These assessments might be of use to water policy makers or the institutions which are in charge of water supply and interested in assessing when water scarcity occurs over the year to implement mitigation measures[23]. Hedelin (2007) stated the importance of the analysis and the information as one of the criteria for the assessment of sustainable water management.

[23] A temporal variability of water resources is more difficult to deal with than a spatial variability, subject as it is to higher levels of uncertainty (EEA and UNEP, 1999). Seasonal assessments of water stress can be used to look into the within-year variation that current approaches cannot provide. Seasonal assessments may be utilized for water demand management that requires an assessment of present water use (Hauschild and Döll, 2000). Model outcome together with a certain level of uncertainty is still informative to grasp trends of water stress over the year.

Acknowledgements

First of all, I would like to express my deepest gratitude to my supervisor Prof. Dr. Ir. M.F.P. (Marc) Bierkens and Dr. L.P.H. (Rens) van Beek. Prof. Dr. Ir. Marc Bierkens introduced me this research topic and enabled me to initiate the research. His clear and considerate guidance throughout my research period was invaluable. Dr. Rens van Beek was literally always there for me during the entire research period. He answered every question I asked with clear explanations and great patience. He provided me with much time for conversations about the research and comments on the writing, solving my problems and always pointing out accurate directions. This research would not be presented here without his continuous assistances.

I am also deeply indebted to Prof. Dr. Rolf Weingartner, Dr. Daniel Viviroli and Dr. Hans H. Dürr. Prof. Dr. Rolf Weingartner and Dr. Daniel Viviroli kindly accepted me to stay in their group of hydrology at the University of Bern for 3 months from January to March in the year 2008. Prof. Dr. Rolf Weingartner always gave me constructive comments and great encouragements. Dr. Daniel Viviroli always helped me in all the time of research during 3 months in Bern. I made significant progresses by his continuous support and guidance. Dr. Hans H. Dürr greatly helped me to find necessary data during my research period as these data made me possible to complete this research.

I would also like to express my appreciation to those who provided me valuable data set including the WWDR-II, FAO, WRI, IGRAC, ICOLD, GRDC, ECMWF, the CRU and the Hydrology Group of Institute of Physical Geography, Johann Wolfgang Goethe University (Frankfurt). These data gave me the possibility to complete this master's thesis.

In last, I would like to thank the Faculty of Geosciences, Utrecht University, which gave this great opportunity to me, one who has a very different study background. I learned much about Hydrology as well as Earth Science during the two years of this master's programme. I would like to express my deep appreciation to Prof. Dr. Ir. S. Majid Hassanizadeh and Prof. Dr. Ruud J. Schotting who taught me the importance of science.

"Better predictions of the future starts from making better representations of the present."

Yoshihide Wada in August, 2008 in Utrecht

References

Alcamo, J., Döll, P., Kaspar, F. and Siebert, S., 1997. Global change and global scenarios of water use and availability: An application of WaterGAP 1.0. Report A9701, Center for Environmental Systems Research, University of Kassel, Germany.

Alcamo, J., Henrichs, T. and Rösch, T., 2000. World Water in 2025-Global modeling and scenario analysis for the World Commission on Water for the 21st Century, Kassel World Water Series 2, Center for Environmental Systems Research, University of Kassel, Germany; http://www.usf.uni-kassel.de/usf/archiv/dokumente/kwws/kwws.2.pdf.

Alcamo, J. and Henrichs, T., 2002. Critical regions: A model-based estimation of world water resources sensitive to global changes. Aquatic Sciences 64: 352–362.

Alcamo, J., Döll, P., Henrichs, T., Kaspar, F., Lehner, B., Rösch, T. and Siebert, S., 2003a. Development and testing of the WaterGAP 2 global model of water use and availability. Hydrological Sciences Journal 48 (3): 317-338.

Alcamo, J., Döll, P., Henrichs, T., Kaspar, F., Lehner, B., Rösch, T. and Siebert, S., 2003b. Global estimation of water withdrawals and availability under current and "business as usual" conditions. Hydrological Science 48 (3): 339-348.

Allen, R.G., Pereira, L.S., Raes, D. and Smith, M., 1998. Crop evapotranspiration - Guidelines for computing crop water requirements, FAO Irrigation and Drainage Paper 56. FAO, Rome, Italy, p 326.

Alsdorf, D., Lettenmaier, C.,Vörösmarty, C.J. and the NASA Surface Water Working Group, 2003. The need for global, satellite-based observations of terrestrial surface waters. EOS Transactions American Geophysical Union 84(29): 275–276.

Arnell, N. W., 1999a. Climate change and global water resources. Global Environmental Change 9:31–49.

Arnell, N.W., 1999b. A simple water balance model for the simulation of streamflow over a large geographic domain. Journal of Hydrology 217: 314–335.

Arnell, N.W., 2003. Effects of IPCC SRES emissions scenarios on river runoff: a global perspective. Hydrology and Earth System Sciences 7 (5): 619-641.

Arnell, N. W., 2004. Climate change and global water resources: SRES emissions and socio-economic scenarios. Global Environmental Change 14:31–52.

Asheesh, M., 2002. Allocating the gaps of shared water resources (the scarcity index) case study Palestine Israel. Israel-Palestine Center for Research and Information; http://www.ipcri.org/watconf/papers/mohamed.pdf.

Avakyan, A. B. and Ovchinnikova, S. P., 1971. DATA ON WORLD RESERVOIRS. Power Technology and Engineering 5 (8): 773-777, DOI 10.1007/BF02403626.

Avakyan, A. B., Sharspov, V. A., Ovchinnikova, S. P. and Yakovleva, V. B., 1979. BASIC DATA ON THE WORLD'S RESERVOIRS. Power Technology and Engineering 13 (5): 504-510, DOI 10.1007/BF02309330.

Babel, M.S., Das Gupta, A. and Pradhan, P., 2007. A multivariate econometric approach for domestic water demand modeling: An application to Kathmandu, Nepal. Water Resources Management 21:573–589, DOI 10.1007/s11269-006-9030-6.

Batjes, N.H., 2005. ISRIC-WISE global data set of derived soil properties on a 0.5 by 0.5 degree grid (version 3.0), Report 2005/08. ISRIC – World Soil Information, Wageningen, The Netherlands, (with data set).

Batjes, N.H., 2006. ISRIC-WISE derived soil properties on a 5 by 5 arc-minutes global grid, Report 2006/02 (available through http://www.isric.org). ISRIC – World Soil Information, Wageningen, The Netherlands, (with data set).

Baumgartner, A. and Reichel, E., 1975. The World Water Balance Mean Annual Global, Continental and Maritime Precipitation, Evaporation and Run-off. Elsevier, Amsterdam, p 182.

Bergström, S., 1995. The HBV Model. In: Computer models of watershed hydrology. V. P. Singh. Colorado, Water Resources Publications: 443-476.

Bierkens, M.F.P. and van Beek, L.P.H., 2008. Seasonal Predictability of Stream Flow in Relation to Seasonal Weather Predictability, Hydrological Response Time and Data-assimilation. Abstract

of presentation at the Catchment-scale Hydrological Modelling and Data Assimilation International Workshop III, 9-11 January 2008, Melbourne.

Bormann, H., Diekkriiger, B. and Renschler, C., 1999. Regionalisation Concept for Hydrological Modelling on Different Scales Using a Physically Based Model: Results and Evaluation. Physics and Chemistry of the Earth (B) 24 (7): 799-804.

Bos, M.G. (ed.), 1989. Discharge measurement structures, Third revised edition. ILRI (International Institute for Land Reclamation and Improvement), the Netherlands.

Brakenridge, G.R., Nghiem, S.V., Anderson, E. and Chien, S., 2005. Space-based measurement of river runoff. EOS Transactions American Geophysical Union 86 (19): 185–188.

Brolsma, R.J. and Bierkens, M.F.P., 2007. Groundwater-soil water-vegetation dynamics in a temperate forest ecosystem along a slope. Water Resources Research 43 (1): W01414, DOI:10.1029/2005WR004696.

Bruntland, G. (ed.), 1987. Our common future: The World Commission on Environment and Development. Oxford University Press, Oxford.

Chow, V.T., Maidment, D.R. and Mays, L.W., 1988. Applied Hydrology. McGraw-Hill, New York, p 572.

Coe, M.T., 2000. Modeling terrestrial hydrological systems at the continental scale: testing the accuracy of an atmospheric GCM. Journal of Climate 13: 686–704.

CPM (Centre for Policy Modelling), 2000. Domestic Water Demand and Social Influence–an agent-based modelling approach. Manchester Metropolitan University Business School.

Dai, A. and Trenberth, K.E., 2002. Estimates of freshwater discharge from continents: latitudinal and seasonal variations. Journal of Hydrometeorology 3: 660–687.

Decharme, B. and Douville, H., 2006a. Introduction of a sub-grid hydrology in the ISBA land surface model. Climate Dynamics 26: 65–78, DOI 10.1007/s00382-005-0059-7.

Decharme, B. and Douville, H., 2006b. Uncertainties in the GSWP-2 precipitation forcing and their impacts on regional and global hydrological simulations. Climate Dynamics 27: 695–713, DOI 10.1007/s00382-006-0160-6.

Decharme, B. and Douville, H., 2007. Global validation of the ISBA sub-grid hydrology. Climate Dynamics 29: 21–37, DOI 10.1007/s00382-006-0216-7.

Dingman, S.L., 1994. Physical Hydrology. Prentice-Hall, Inc., New Jersey, p 575.

Döll, P., Kaspar, F., and Alcamo, J., 1999. Computation of global water availability and water use at the scale of large drainage basins. Mathematische Geologie 4: 111–118.

Döll, P., Lehner, B. and Kaspar, F., 2000. Global modeling of groundwater recharge and surface runoff. EcoRegio 8: 73–80.

Döll, P. and Siebert, S., 2002. Global modeling of irrigation water requirements. Water Resources Research 38(4): 8.1-8.10.

Döll, P., Kaspar, F. and Lehner, B., 2003. A global hydrological model for deriving water availability indicators: model tuning and validation. Journal of Hydrology 270:105–134.

Douglas, E. M., Githui, F., Mtafya, A., Green, P., Glidden S. and Vörösmarty, C.J., 2006. The application of water scarcity indicators at different scales in Africa. Journal of Environmental Management.

Dynesius, M. and Nilsson, C., 1994. Fragmentation and flow regulation of river systems in the northern third of the world. Science 266: 753-762.

EEA (European Environment Agency) and UNEP (United Nations Environment Programme), 1999. 1997 New Year Message: Water Stress in Europe can the challenge be met? EEA and UNEP, ISBN 92-9167-025-1.

EEA (European Environmental Agency), 2007. Climate change and water adaptation issues. EEA Technical report No 2, ISBN 978-92-9167-917-1.

Engvall, I., 2005. Global modelling of fresh water resources on a seasonal scale. Geophysical Research Abstracts 7, European Geosciences Union 2005.

Falkenmark, M., 1989. The massive water scarcity now threatening Africa-why isn't it being addressed? Ambio 18 (2): 112-118.

Falkenmark, M., 1990. Global Water Issues Confronting Humanity. Special Issue on the Challenge of Global Policy. Journal of Peace Research 27 (2): 177-190.

Falkenmark, M., Kijne, J. W., Taron, B., Murdoch, G., Sivakumar, M. V. K. and Craswell, E., 1997. Meeting Water Requirements of an Expanding World Population [and Discussion]. Philosophical Transactions: Biological Sciences 352 (1356): 929-936.

Falkenmark, M. and Rockström, J., 2004. Balancing Water for Humans and Nature. Earthscan, London.

Falkenmark, M. and Rockström, J., 2005. Rain: The Neglected Resource - Embracing Green Water Management Solutions. Swedish Water House Policy Brief Nr. 2. SIWI (Stockholm International Water Institute); http://www.siwi.org/downloads/Reports/2005_Blue_Green_Policy_Brief.pdf.

Falkenmark, M., 2007. Shift in thinking to address the 21st century hunger gap: Moving focus from blue to green water management. Water Resources Management 21:3-18, DOI 10.1007/s11269-006-9037-z.

FAO (Food and Agriculture Organization of the United Nations), 1990. FAO-UNESCO Soil Map of the World: Revised Legend. World Soil Resources Report 60. FAO, Rome, Italy [Reprinted as Technical Paper 20, International Soil Reference and Information Centre, Wageningen, The Netherlands, 1994].

FAO, 2003. Review of World Water Resources by Country, Water Reports 23. FAO, Rome, Italy, p 123, ISBN 92-5-104899-1.

FAO, 2007. Gridded livestock of the world 2007, by Wint, W. and Robinson, T., FAO, Rome, Italy, p 131; http://www.fao.org/docrep/010/a1259e/a1259e00.htm.

Fekete, B.M., Vörösmarty, C.J. and Grabs W., 1999. UNH/GRDC Composite Runoff Fields V 1.0.; http://www.grdc.sr.unh.edu/ (accessed 02.08.2008).

Fekete, B.M., Vörösmarty, C.J. and Grabs, W., 2000. Global, Composite Runoff Fields Based on Observed River Discharge and Simulated Water Balances. Technical Report 22 (Version dated 2000-02-04). Global Runoff Data Centre, Koblenz, Germany, p 115.

Fekete, B.M., Vörösmarty, C.J. and Grabs, W., 2002. High-resolution fields of global runoff combining observed river discharge and simulated water balances, Global Biogeochemical Cycles 16 (3): 1042, DOI:10.1029/1999GB001254.

Fekete, B.M., Vörösmarty, C.J., Roads, J.O. and Willmott, C.J., 2004. Uncertainties in precipitation and their impacts on runoff estimates. Journal of Climate 17: 294–304.

Flörke, M. and Alcamo, J., 2004. European Outlook on Water Use-Final Report. Center for Environmental Systems Research, University of Kassel.

Gerten, D., Schaphoff, S., Haberlandt, U., Lucht, W. and Sitch, S., 2004. Terrestrial vegetation and water balance: hydrological evaluation of a dynamic global vegetation model. Journal of Hydrology 286: 249–270.

Gerten, D., Hoff, H., Bondeau, A., Lucht, W., Smith, P. and Zaehle, S., 2005. Contemporary "green" water flows: Simulations with a dynamic global vegetation and water balance model. Physics and Chemistry of the Earth 30: 334–338.

Gleick, P.H., 1993. Water in crisis: A guide to the world's freshwater resources. Oxford University Press, New York/London, p 474.

Gleick, P.H., 1998. Water in Crisis: Paths to Sustainable Water Use. Ecological Applications 8 (3): 571-579.

Gleick, P.H., 2000. The world's water 2000-2001: the biennial report on freshwater resources. Island Press. Washington, DC., p 300.

Gleick, P.H., Cooley, H., Katz, D., Lee, E., Morrison, J., Palaniappan, M., Samulon, A. and Wolff, G.H. (eds.), 2006. The World's Water 2006-2007: The Biennial Report on Freshwater Resources. Island Press. Washington, DC., p 392.

Graham, L. P., Hagemann, S., Jaun, S. and Beniston, M., 2007. On interpreting hydrological change from regional climate models. Climatic Change 81:97–122, DOI 10.1007/s10584-006-9217-0.

GRDC (Global Runoff Data Centre), 2004. Long Term Mean Annual Freshwater Surface Water Fluxes into the World Oceans, Comparisons of GRDC freshwater flux estimate with literature; http://grdc.bafg.de/servlet/is/7083/ [accessed 15.02. 2008].

GRDC (Global Runoff Data Centre), 2007. All river discharge data stations categorised by time series' end (Status: 11.10.2007); http://grdc.bafg.de/servlet/is/1660/ [accessed 15.02.2008].

Guo, S., Wang, J., Xiong, L., Ying, A. and Li, D., 2002. A macro-scale and semi-distributed monthly water balance model to predict climate change impacts in China. Journal of Hydrology 268, pp. 1-15.

Gusev, E. M., Nasonova, O. N. and Kovalev, E. E., 2006. Modeling the Components of Heat and Water Balance for the Land Surface of the Globe. Water Resources 33 (6): 616–627, DOI: 10.1134/S0097807806060030.

Haddeland, I., Letternmaier, D.P. and Skaugen, T., 2006. Effects of irrigation on the water and energy balances of the Colorado and Mekong river basins. Journal of Hydrology 324: 210-223.

Hagemann, S., Botzet, M., Dümenil, L. and Machenhauer, B., 1999. Derivation of global GCM boundary conditions from 1 km land use satellite data, MPI Report No. 289. Max Planck Institute for Meteorology, Hamburg, Germany; http://www.mpimet.mpg.de/fileadmin/publikationen/Reports/max_scirep_289.pdf.

Hagemann, S. and Gates, L.D., 2003. Improving a subgrid runoff parameterization scheme for climate models by the use of high resolution data derived from satellite observations. Climate Dynamics 21: 349–359.

Hanasaki, N., Kanae, S. and Oki, T. 2006. A reservoir operation scheme for global river routing models. Journal of Hydrology 327: 22– 41.

Hanasaki, N., Kanae, S., Oki, T., Masuda, K., Motoya, K., Shen, Y. and Tanaka. K., 2007a. An integrated model for the assessment of global water resources-Part 1: Input meteorological forcing and natural hydrological cycle modules. Hydrology and Earth System Sciences Discussions 4: 3535-3582.

Hanasaki, N., Kanae, S., Oki, T. and Shirakawa, N., 2007b. An integrated model for the assessment of global water resources-Part 2: Anthropogenic activities modules and assessments. Hydrology and Earth System Sciences Discussions 4: 3583-3626.

Hauschild, M. and Döll, P., 2000. Water Management Modeling in Ceará and Piauí (Northeast of Brazil). German-Brazilian Workshop on Neotropical Ecosystems-Achievements and Prospects of Cooperative Research, Session 3: Water Quality, Water Dynamics, Water Management, Hamburg, September 3-8, 2000; http://www.biologie.uni-hamburg.de/bzf/oknu/proceedingsneotropecosys/p0523_hauschild.pdf.

Hedelin, B., 2007. Criteria for the Assessment of Sustainable Water Management. Environmental Management 39: 151–163, DOI 10.1007/s00267-004-0387-0.

Heindl, L.A., 1979. International Cooperation in Water Resources. GeoJournal 3.5: 481-487.

ICOLD (International Commission on Large Dams), 1998. World Register of Dams. International Commission on Large Dams, Paris.

ICOLD (International Commission on Large Dams), 2003. World Register of Dams. International Commission on Large Dams, Paris.

Islam, S., Aramaki, T. and Hanaki, K., 2005. Development and Application of an Integrated Water Balance Model to Study the Sensitivity of the Tokyo Metropolitan Area Water Availability Scenario to Climatic Changes. Water Resources Management 19: 423–445, DOI: 10.1007/s11269-005-3277-1.

Islam, S., Oki, T., Kanae, S., Hanasaki, N., Agata, Y. and Yoshimura, K., 2007. A grid-based assessment of global water scarcity including virtual water trading. Water Resources Management 21:19–33, DOI 10.1007/s11269-006-9038.

IWMI (International Water Management Institute), 2000. World water supply and demand in 2025. In World Water Scenarios Analyses. Rijsberman, F.R. (ed.), Earthscan Publications, London.

Jackson, R.B., Carpenter, S.R., Dahm, C.N., McKnight, D.M., Naiman, R.J., Postel, S.L. and Running, S.W., 2001. Water in a Changing World. Ecological Applications 11 (4): 1027-1045.

Kållberg, P., Berrisford, P., Hoskins, B., Simmons, A., Uppala,S., Lamy-Thepaut, S. and Hine, R., 2005. ERA-40 Project Report Series 19: ERA-40 Atlas. European Centre for Medium Range Weather Forecasts (ECMWF), Shinfield Park, Reading, England; http://www.ecmwf.int/publications/library/ecpublications/_pdf/era40/ERA40_PRS19_rev.pdf.

Klepper, O. and van Drecht, G., 1998. WARibaS, Water Assessment on a River Basin Scale; A computer program for calculating water demand and satisfaction on a catchment basin level for global scale analysis of water stress. Report 402001009. RIVM, The Netherlands.

Korzun, V.I., Sokolow, A.A., Budyko, M.I., Voskresensky, K.P., Kalininin, G.P., Konoplyanstev, A.A., Korotkevich, E.S., Kuzin, P.S. and Lvovich, M.I. (Eds.), 1978. World Water Balance and Water Resources of the Earth. Studies and Reports in Hydrology 25. UNESCO, Paris, p 663.

Kulshreshtha, S. N., 1998. A Global Outlook for Water Resources to the Year 2025. Water Resources Management 12: 167–184.

Kulshreshtha, S. N., 1993. World Water Resources and Regional Vulnerability: Impact of future Changes. IIASA Research Report RR-93-010.

Kundzewicz, Z.W., Mata, L.J., Arnell, N.W., Döll, P., Kabat, P., Jiménez, B., Miller, K.A., Oki, T., Sen, Z. and Shiklomanov, I.A., 2007. Freshwater resources and their management. Climate Change 2008: Impacts, Adaptation and Vulnerability. Contribution of Working Group II to the Fourth Assessment Report of the Intergovernmental Panel on Climate Change. Parry, M.L., Canziani, O.F., Palutikof, J.P., van der Linden, P.J. and Hanson, C.E., (eds.), Cambridge University Press, Cambridge, UK, pp. 173-210.

Ledger, D. C., 1972. The Warwickshire Avon: A Case Study of Water Demands and Water Availability in an Intensively Used River System. Transactions of the Institute of British Geographers 55: 83-110.

Legates, D.R. and Mather, J.R., 1992. An Evaluation of the Average Annual Global Water Balance. Geographical Review 82 (3): 253-267.

Leff, B., Ramankutty, N. and Foley, J., 2004. Geographic distribution of major crops across the world, Global Biogeochemical Cycles 18: GB1009, p 27, DOI:10.1029/2003GB002108.

Lens, P., Pol, L.H., Wilderer, P. and Asano, T. (eds.), 2002. Water Recycling and Resource Recovery in Industry: Analysis, technologies and implementation. Integrated Environmental Technology Series. IWA Publishing, London, UK.

Loh, M. and Coghlan, P., 2003. Domestic Water Use Study In Perth,Western Australia 1998-2001. Water Corporation of Western Australia, Australia.

L'vovich, M.I., 1979. World Water Resources and Their Future. AGU (American Geophysical Union), Washington, D.C., p 415 (original Russian script was published in Moscow in 1974).

Mahvi, A.H. and Norouzi, H.A., 2005. Domestic Water Consumption in Rural Areas: A Case Study. Pakistan Journal of Biological Sciences 8 (8): 1170-1172.

Marengo, J.A., 2005. Characteristics and spatio-temporal variability of the Amazon River Basin Water Budget. Climate Dynamics 24: 11–22, DOI 10.1007/s00382-004-0461-6.

Martinez-ESPIÑEIRA, R., 2002. Residential Water Demand in the Northwest of Spain. Environmental and Resource Economics 21: 161–187.

Meigh, J.R., McKenzie, A.A. and Sene, K.J., 1999. A grid-based approach to water scarcity estimates for Eastern and Southern Africa. Water Resources Management 13 (2): 85–115.

Meinzen-Dick, R.S. and Rosegrant, M.W. (eds.), 2001. A 2020 Vision for Food, Agriculture and the Environment-Focus 9: Overcoming water scarcity and quality constraints. International Food Policy Research Institute, Washington, D.C., p 29.

Mitchell, T.D. and Jones, P.D., 2005. An improved method of constructing a database of monthly climate observations and associated high-resolution grids. International Journal of Climatology 25 (6): 693–712, DOI:10.1002/joc.1181.

MLIT (Ministry of Land, Infrastructure, and Transport in Japan), 2007. Water Resources in Japan. MLIT, Tokyo.

Monfreda, C., Ramankutty, N. and Foley, J.A., 2008. Farming the planet: 2. Geographic distribution of crop areas, yields, physiological types, and net primary production in the year 2000. Global Biogeochemical Cycles 22: GB1022, p 19, DOI:10.1029/2007GB002947.

Moore, R.J., 1985. The probability-distributed principle and runoff production at point and basin scales. Hydrological Science Journal 30: 273-297.

MWR (Ministry of Water Resources) of the People's Republic of China (PRC), 2007; http://www.mwr.gov.cn/english1/20070226/82438.asp [accessed 20.01. 2008].

New, M., Hulme, M. and Jones, P.D., 1999. Representing twentieth century space-time climate variability. Part I: development of a 1961-90 mean monthly terrestrial climatology. Journal of Climate 12, 829-856.

New, M., Hulme, M. and Jones, P.D., 2000. Representing twentieth century space-time climate variability. Part II: development of 1901-96 monthly grids of terrestrial surface climate. Journal of Climate 13, 2217-2238.

New, M., Lister, D., Hulme, M. and Makin, I., 2002. A high-resolution data set of surface climate over global land areas. Climate Research 21: 1-25.

Nijssen, B., Schnur, R.. and Lettenmaier, D.P., 2001a. Global retrospective estimation of soil moisture using the variable infiltration capacity land surface model, 1980–93. Journal of Climate 14: 1790–1808.

Nijssen, B., O'Donnell, G.M., Lettenmaier, D.P., Lohmann, D. and Wood, E.F., 2001b. Predicting the discharge of global rivers. Journal of Climate 14: 3307–3323.

Nilsson, C., Reidy, C.A., Dynesius, M. and Revenga, C., 2005. Fragmentation and flow regulation of the world's large river systems. Science 308: 405–408.

Nyong, A.O. and Kanaroglou, P.S., 1999. Domestic Water Use in Rural Semiarid Africa: A Case Study of Katarko Village in Northeastern Nigeria. Human Ecology 27 (4): 537-555.

Oki, T., Musiake, K., Matsuyama, H. and Masuda, K., 1995: Global atmospheric water balance and runoff from large river basins. Hydrological Processes 9: 655–678.

Oki, T., Nishimura, T. and Dirmeyer, P., 1999. Assessment of annual runoff from land surface models using Total Runoff Integrating Pathways (TRIP). Journal of the Meteorological Society of Japan 77: 235–255.

Oki, T., Agata, Y., Kanae, S., Saruhashi, T., Yang, D. and Musiake, K., 2001. Global assessment of current water resources using total runoff integrating pathways. Hydrological Science Journal 46(6): 983–996.

Oki, T., Valeo, C. and Heal, K. (Eds.), 2005. Hydrology 2020: An Integrating Science to Meet World Water Challenges. IAHS, Wallingford, UK.

Oki, T. and Kanae, S., 2006. Global Hydrological Cycles and World Water Resources. Science 313: 1068-1072, DOI: 10.1126/science.1128845.

Oki, T., Tang, Q., Kanae, S. and Hu, H., 2006. The influence of precipitation variability and partial irrigation within grid cells on a hydrological simulation; http://hydro.iis.u-tokyo.ac.jp/DBHdownload/Ref/subgrid_ams.pdf.

Ormsbee L.E. and Khan, A.Q., 1989. A parametric model for steeply sloping forested watersheds. Water Resources Research 20: 1815–1822.

PCRaster Research and Development Team, 2005. PCRaster Version 2 Manual. Department of Physical Geography, Utrecht University; http://pcraster.geo.uu.nl/download/doc/PCRaster Manual18Feb2005.pdf.

Portmann, F., Siebert, S., Bauer, C. & Döll, P., 2008. Global data set of monthly growing areas of 26 irrigated crops. Frankfurt Hydrology Paper 06, Institute of Physical Geography, University of Frankfurt, Frankfurt am Main, Germany, p 400.

Porporato, A.; Laio, F., Ridolfi, L. and Rodriguez-Iturbe, I., 2001. Plants in water-controlled ecosystems : active role in hydrologic processes and response to water stress: III. Vegetation water stress. Advances in Water Resources 24 (7): 725-744.

Postel, S. L., Daily, G. C. and Ehrlich, P. R., 1996. Human Appropriation of Renewable Fresh Water. Science 271: 785-788.

Ramankutty, N., Evan, A.T., Monfreda, C. and Foley, J.A., 2008. Farming the planet: 1. Geographic distribution of global agricultural lands in the year 2000. Global Biogeochemical Cycles 22: GB1003, p 19, DOI:10.1029/2007GB002952.

Raskin, P., Gleick, P., Kirshen, P., Pontius, G. and Strzepek, K., 1997. Water futures: Assessment of long-range patterns and problems. Background paper Comprehensive Assessment of the Freshwater Resources of the World, Stockholm Environment Institute, Stockholm, Sweden, p 78.

Revenga, C., Brunner, J., Henninger, N., Kassem, K. and Payne, N., 2000. Pilot Analysis of Global Ecosystems: Freshwater Ecosystems. World Resources Institute, Washington, DC., the U.S.A.; http://www.wri.org/wr2000.

RIZA (Institute for Inland Water Management and Waste Water Treatment), 2003. Netherlands Drought Study: Final report phase 1. RIZA, Lelystad, the Netherlands.

Shiklomanov, I. A., 1993. World fresh water resources. Gleick, P. H. (ed.), Water in crisis. Oxford University Press, New York, New York, the U.S.A., pp. 13-24.

Shiklomanov, I.A. (Ed.), 1997. Assessment of water resources and water availability in the world. Comprehensive assessment of the freshwater resources of the world. WMO (World Meteorological Organization) and SEI (Stockholm Environmental Institute), p 88.

Shiklomanov, I.A., 1998. World Water Resources. UNESCO, Paris.

Shiklomanov, I.A., 2000. World water resources and water use: Present assessment and outlook for 2025. In World Water Scenarios Analyses, Rijsberman, F.R. (ed.), Earthscan Publications, London.

Shiklomanov, I.A., 2000. Appraisal and assessment of world water resources. Water International 25-1, 11-32.

Shiklomanov, I.A., Lammers, R.B. and Vörösmarty, C.J., 2002. Widespread decline in hydrological monitoring threatens Pan-Arctic research. EOS Transactions American Geophysical Union 83(2): 16–17.

Siebert, S., Hoogeveen, J. and Frenken, K., 2006. Irrigation in Africa, Europe and Latin America. Update of the Digital Global Map of Irrigation Areas to Version 4. Frankfurt Hydrology Paper 05. Institute of Physical Geography, Frankfurt University, Frankfurt am Main, Germany, p 134.

Siebert, S. and Döll, P., 2007. Irrigation water use - A global perspective. In: Lozán, J.L., Graßl, H., Hupfer, P., Menzel, L. and Schönwiese, C.D. (eds.). Global Change: Enough Water for all? University of Hamburg, Hamburg, 104-107.

Siebert, S. and Döll, P., 2008. The Global Crop Water Model (GCWM): Documentation and first results for irrigated crops. Frankfurt Hydrology Paper 07, Institute of Physical Geography, University of Frankfurt, Frankfurt am Main, Germany, p 42.

Sloan, P.G. and Moore, I.D., 1984. Modeling subsurface stormflow on steeply sloping forested watersheds. Water Resources Research 20: 1815–1822.

Smakhtin, V., Revenga, C. and Döll, P., 2004. Taking into Account Environmental Water Requirements in Global-scale Water Resources Assessments. Comprehensive Assessment Research Report 2, Colombo, Sri Lanka, The Comprehensive Assessment Secretariat.

Smith, M., 1992. CROPWAT – a computer program for irrigation planning and management.

Sophocleous, M., 2004. Global and Regional Water Availability and Demand: Prospects for the Future. Natural Resources Research13 (2): 61-75.

Sullivan, C.A., Meigh, J.R., Giacomello, A.M., Fediw, T., Lawrence, P., Samad, M., Mlote, S., Hutton, C., Allan, J.A., Schulze, R.E., Dlamini, D.J.M., Cosgrove, W., Delli Priscoli, J., Gleick, P., Smout, I., Cobbing, J., Calow, R., Hunt, C., Hussain, A., Acreman, M.C., King, J., Malomo, S., Tate, E.L., O'Regan, D., Milner, S. and Steyl, I., 2003. The Water Poverty Index: Development and application at the community scale. Natural Resources Forum 27: 189–199.

Sullivan, C.A., Meigh, J.R. and Lawrence, P., 2006. Application of the Water Poverty Index at different scales: a cautionary tale. Water International, Special Issue.

Takahashi, K., Matsuoka, Y. and Harasawa, H., 1998. Impacts of climate change on water resources, crop production and natural ecosystem in the Asia and Pacific region. Journal of Global Environmental Engineering 4: 91-103.

Takahashi, K., Matsuoka, Y., Shimada, Y. And Shimamura, R., 2000, Development of the model to assess water resource problems under climate change. A Report of 8th Earth Environment Symposium: 175-180; http://www.nies.go.jp/social/kojin/takahasi/file/takahasi200001.pdf (in Japanese).

Tanaka, K., Yorozu, K., Hamabe, R. and Ikebuchi, S., 2005. Validation of the GSWP2 baseline simulation. 19th Conference on Hydrology, The 85th American Meteorological Society Annual Meeting, San Diego; http://ams.confex.com/ams/pdfpapers/87730.pdf.

The Intergovernmental Panel on Climate Change (IPCC), 1997. IPCC Special Report on the Regional Impacts of Climate Change: An Assessment of Vulnerability.

The Intergovernmental Panel on Climate Change (IPCC), 2000. IPCC Special Report on Emissions Scenarios; http://www.grida.no/climate/ipcc/emission/.

The Intergovernmental Panel on Climate Change (IPCC), 2001. IPCC Third Assessment Report: Climate Change 2001.

The WHO (World Health Organization) and UNICEF (United Nations Children's Fund) Joint Monitoring Programme for Water Supply and Sanitation (JMP), 2000. Global Water Supply and Sanitation Assessment 2000 Report. WHO and UNICEF, New York, the U.S.A., p 87; ISBN 92-4-156202-1; http://www.who.int/water_sanitation_health/monitoring/jmp2000.pdf.

The World Bank, 2000-2004. World Development Indicators 2000-2004. The World Bank, Washington, D.C.; http://web.worldbank.org/data/publications/archives/.

The World Bank, 2006a. World Development Indicators (WDI) 2006. The World Bank; http://devdata.worldbank.org/wdi2006/contents/index2.htm [accessed 20.02.2008].

The World Bank, 2006b. Country Classification; http://web.worldbank.org/data/ [accessed 20.01.2008].

The World Bank, 2007. World Development Indicators (WDI) 2007. The World Bank, Washington, D.C., ISBN 0-8213-6959-8.

Thenkabail, P.S., Biradar, C.M., Turral, H., Noojipady, P., Li, Y.J., Vithanage, J., Dheeravath, V., Velpuri, M., Schull, M., Cai, X.L., Dutta, R. and Sadir, M., 2006. An irrigated area map of the world (1999) derived from remote sensing. Research Report 105. Colombo, Sri Lanka: International Water Management Institute.

Thyssen, N. and EEA, 1999. Sustainable water use in Europe Part 1: Sectoral use of water, Environmental assessment report No 1. EEA, Copenhagen.

Todini, E., 1996. The ARNO rainfall-runoff model. Journal of Hydrology 175: 339-382.

Troccoli, A. and Kållberg, P., 2004., ERA-40 Project Report Series 13: Precipitation Correction in the ERA-40 Reanalysis. European Centre for Medium Range Weather Forecasts (ECMWF), Shinfield Park, Reading, England; http://www.ecmwf.int/publications/library/ecpublications/_pdf/era40/ERA40_PRS19_rev.pdf.

UNEP (United Nations Environment Programme), 2007. The GEO Data Portal. UNEP/DEWA/GRID-Europe and ESRI (Environmental Systems Research Institute) ArcAtlas: Our Earth Dams (1996); http://geodata.grid.unep.ch.

UNESCO (United Nations Educational, Scientific and Cultural Organization), 1966. International Hydrological Decade: Final Report of the First Session, Co-ordinating Council, Working Group on the World Water Balance, UNESCO, Paris.

UNESCO, 1971. A contribution to the International Hydrological Decade: Scientific framework of world water balance, Technical papers in hydrology 7. UNESCO, Paris.

UNESCO, 2000. Water Use in the World: Present Situation/Future Needs. UNESCO, Paris.

UNESCO, 2006. Water: a shared responsibility, The United Nations World Water Development Report 2. UNESCO and Berghahn Books, Paris and New York.

van Beek, L.P.H. and Bierkens, M.F.P., 2005. Influence of the quality of climate input on the performance of a MHM for several large catchments. In Geophysical Research Abstracts 7, EUGU05-A-05173. Vienna, Austria: European Geosciences Union.

van Beek, L.P.H. and Bierkens, M.F.P., 2006. Base flow calibration in a global hydrological model. Abstract of presentation at the AGU Fall Meeting 2006, San Francisco, H23B-06.

van Beek, L.P.H., 2007a. Obtaining global water use. A report of global water use. Utrecht University (18th, May).

van Beek, L.P.H., 2007b. The macro-scale hydrological model PCR-GLOBWB, Department of Physical Geography, Utrecht University (confidential).

van Beek, L.P.H., 2007c. PCR-GLOBWB model description. In: Integration of GFS Data with PCR-GLOBWB using FEWS. (WL Delft Hydraulics, Delft).

van Beek, L.P.H. and Bierkens, M.F.P., 2008. Another Global Hydrological Model: Conceptualization, Parameterization and Verification. Department of Physical Geography, Utrecht University, Utrecht, the Netherlands.

Vörösmarty, C.J., Moore III, B., Grace, A.L., Gildea, M.P., Melillo, J.M., Peterson, B.J., Rastetter, E.D. and Steudler, P.A., 1989. Continental-scale models of water balance and fluvial transport: An application to South America, Global Biogeochemical Cycles 3(3): 241–265.

Vörösmarty, C.J., Sharma, K.P., Fekete, B.M., Copeland, A.H., Holden, J., Marble, J. and Lough, J.A., 1997. The storage and aging of continental runoff in large reservoir systems of the world. Ambio 26 (4):210–219.

Vörösmarty, C.J., Federer, C.A. and Schloss, A.L., 1998. Potential evaporation functions compared on US watersheds: possible implications for global-scale water balance and terrestrial ecosystem modeling. Journal of Hydrology 207: 147–169.

Vörösmarty, C.J., Green, P., Salisbury, J. and Lammers, R. B., 2000. Global water resources: Vulnerability from climate change and population growth. Science 289: 284-288.

Vörösmarty, C.J, 2002. Global water assessment and potential contributions from Earth systems science. Aquatic Sciences 64: 328–351.

Vörösmarty, C.J., Lettenmaier, D., Leveque, C., Meybeck, M., Pahl-Wostl, C., Alcamo, J., Cosgrove, W., Grassl, H., Hoff, H., Kabat, P., Lansigan, F., Lawford, R. and Naiman, R., 2004. Humans transforming the global water system. EOS Transactions American Geophysical Union 85 (48): 509-520.

Vörösmarty, C.J., Douglas, E.M., Green, P.A. and Revenga, C., 2005a. Geospatial indicators of emerging water stress: An application to Africa. Ambio 34 (3): 230-236.

Vörösmarty, C.J., Leveque, C. and Revenga, C., 2005b. Chapter 7: Freshwater. In: Millennium Ecosystem Assessment Volume 1: Conditions and Trends, Working Group Report, Island Press.

Wesseling, C.G., Karssenberg, D., van Deursen, W.P.A. and Burrough, P.A., 1996. Integrating dynamic environmental models in GIS: the development of a Dynamic Modelling language. Transactions in GIS 1: 40-48.

Widén-Nilsson, E., Halldin, S. and Xu, C., 2007. Global water-balance modelling with WASMOD-M: Parameter estimation and regionalization. Journal of Hydrology 340: 105-118.

WMO (World Meteorological Organisation), 1997. Comprehensive Assessment of the Freshwater Resources of the World. WMO, Geneva, p 34.

World Water Council, 2006. Final Report of the 4th World Water Forum: Local Actions for a Global Challenge. World Water Council, Mexico, ISBN 968-817-782-2.

WRI (World Resources Institute), 1998. 1998–99 World Resources. Report of UNEP, UNDP & World Bank, Oxford University Press, Oxford, UK.

Yates, D.N., 1997. Approaches to continental scale runoff for integrated assessment models. Journal of Hydrology 291: 289–310.

Zhao, R.J., 1977. Flood forecasting method for humid regions of China, East China College of Hydraulic Engineering, Nanjing.

Appendix A - Data

A.1. Data Table[i] [ii]

	Hydrology						Climate						Geomorphology/Land use								Water use						Society			Spatiotemporal scale		
	Precipitation	(Potential) Evapo(transpi)ration	Runoff	River discharge	Groundwater use/availability	Soil moisture/Climate moisture indices	Air/Water temperature	Wind speed	Cloud cover/Height	Vapour pressure/Humidity	Radiation (short/long)/Albedo	Ice/Permafrost/Snow cover	River network/Basin	Sediment transport	Dam/Reservoir	Lake density/volume	Wetland/Floodplain	Irrigated/Crop/Arable land	Soil Property	Elevation/Water height	Land use/Vegetation/Topology	Irrigated water use	Domestic water use	Industrial water use	Desalinated/Waste water (re-)use	Water quality	Crop Area/Type of crop	Population (density)	GDP/Economics	Global/Regional Map	Spatial scale	Temporal scale	Period
1.Global-RIMS[iii]	X	X	X	X			X											X	X	X	X	X	X	X			X	X			Globe Region[iv]	Year	1950-2050[v]
2.LBA-hydronet	X						X		X	X																					South America	Month Day	1905-1995
3.R-hydronet	X			X			X																								Mid-south America	Year Month Year	1967-2002
4.ArcticCHAPM	X						X	X																							Arctic	Month Day	1973-2000
5.ArcticRIMS	X	X	X			X	X			X	X	X					X		X		X										Arctic	Year Month Day	1930-2006
6.AQUASTAT[vi]	X				X									X	X			X			X	X	X	X	X	X	X	X			Globe	Year	1960-2010
7.SoilFAO						X													X												Globe	Year	1960-2006
8.EORC	X						X		X		X									X	X										Globe Country	Month Day	1997-2007

	Hydrology						Climate						Geomorphology/Land use								Water use						Society			Spatiotemporal scale		
	Precipitation	(Potential) Evapo(transpi)ration	Runoff	River discharge	Groundwater use/availability	Soil moisture/Climate moisture indices	Air/Water temperature	Wind speed	Cloud cover/Height	Vapour pressure/Humidity	Radiation (short/long)/Albedo	Ice/Permafrost/Snow cover	River network/Basin	Sediment transport	Dam/Reservoir	Lake density/volume	Wetland/Floodplain	Irrigated/Crop/Arable land	Soil Property	Elevation/Water height	Land use/Vegetation/Topology	Irrigated water use	Domestic water use	Industrial water use	Desalinated/Waste water (re-)use	Water quality	Crop Area/Type of crop	Population (density)	GDP/Economics	Global/Regional Map	Spatial scale	Temporal scale	Period
9.EROS																				X	X									X	Globe Country	Month Day	1972-2007
10.EarthTrendsWRI				X	X		X											X			X	X	X	X		X	X	X	X		Globe Continent Country	Year	2004-2006
11. ERGO																					X										Globe	Year	2000, 2005
12.FAOSTAT																					X						X	X			Country	Year	1961-2006
13. GEMStat				X			X																			X					Globe Region Country	Year Month	1979-2007
14. CRSSA	X						X		X		X		X						X		X							X	X		Globe Continent Country	Year Month	1930-1988
15. GRID/DEWA	X	X	X	X		X	X	X	X	X	X						X		X	X	X					X		X		X		Globe Region Country	Year Month Day	1930-1997
16.WORLD-SOTER																			X		X										Globe	Year	1960-2006

	Hydrology						Climate						Geomorphology/Land use									Water use					Society			Spatiotemporal scale		
	Precipitation	(Potential) Evapo(transpi)ration	Runoff	River discharge	Groundwater use/availability	Soil moisture/Climate moisture indices	Air/Water temperature	Wind speed	Cloud cover/Height	Vapour pressure/Humidity	Radiation (short/long)/Albedo	Ice/Permafrost/Snow cover	River network/Basin	Sediment transport	Dam/Reservoir	Lake density/volume	Wetland/Floodplain	Irrigated/Crop/Arable land	Soil Property	Elevation/Water height	Land use/Vegetation/Topology	Irrigated water use	Domestic water use	Industrial water use	Desalinated/Waste water (re-)use	Water quality	Crop Area/Type of crop	Population (density)	GDP/Economics	Global/Regional Map	Spatial scale	Temporal scale	Period
17.Oki Laboratory																												X		X	Region Globe	Year	1990-2002
18. GOSIC	X	X		X			X	X	X	X	X	X				X			X		X					X					Globe Region	Year Month Day	1980-2007
19.GPWv3-GRUMP																												X		X	Globe	Year	1990-2015
20.IAHS	X		X										X					X													Globe	Year Month	1967-2002
21.ICOLD-WCD															X																Globe	Year	1988, 1998
22.IGRAC					X																										Globe	Year	1998-2002
23.ISLSCP	X	X	X	X			X		X	X	X	X									X							X	X	X	Globe	Month Hour	1986-1995
24. ISRIC																			X												Globe Region Country	Year	1960-2000
25.R-Arcticnet				X																										X	Arctic	Year Month	1912-1993

	Hydrology						Climate						Geomorphology/Land use									Water use						Society			Spatiotemporal scale		
	Precipitation	(Potential) Evapo(transpi)ration	Runoff	River discharge	Groundwater use/availability	Soil moisture/Climate moisture indices	Air/Water temperature	Wind speed	Cloud cover/Height	Vapour pressure/Humidity	Radiation (short/long)/Albedo	Ice/Permafrost/Snow cover	River network/Basin	Sediment transport	Dam/Reservoir	Lake density/volume	Wetland/Floodplain	Irrigated/Crop/Arable land	Soil Property	Elevation/Water height	Land use/Vegetation/Topology	Irrigated water use	Domestic water use	Industrial water use	Desalinated/Waste water (re-)use	Water quality	Crop Area/Type of crop	Population (density)	GDP/Economics	Global/Regional Map	Spatial scale	Temporal scale	Period
26.STN													X								X										Globe	Year	1950-2000
27.SPOT																				X	X								X	Globe Country	Month Day	2004-2007
28.TERRASTAT																		X	X		X									Globe Region	Year	2002
29. BADC	X						X	X	X	X																				Globe Region Country	Year Month	1901-2100
30.CIESIN																					X						X			Globe Region	Year	1990-2015
31. SAGE	X	X	X	X	X	X	X			X	X	X	X			X	X	X		X	X					X	X	X		Globe Continent Region	Year Month Day	1700-1998
32. WWF													X		X	X	X			X	X									Globe Continent	Year	1988-2007
33.DSS	X	X	X	X									X					X			X	X	X	X		X		X		X	Globe Africa	Year Month	1950-2000

	Hydrology						Climate						Geomorphology/Land use									Water use						Society			Spatiotemporal scale		
	Precipitation	(Potential) Evapo(transpi)ration	Runoff	River discharge	Groundwater use/availability	Soil moisture/Climate moisture indices	Air/Water temperature	Wind speed	Cloud cover/Height	Vapour pressure/Humidity	Radiation (short/long)/Albedo	Ice/Permafrost/Snow cover	River network/Basin	Sediment transport	Dam/Reservoir	Lake density/volume	Wetland/Floodplain	Irrigated/Crop/Arable land	Soil Property	Elevation/Water height	Land use/Vegetation/Topology	Irrigated water use	Domestic water use	Industrial water use	Desalinated/Waste water (re-)use	Water quality	Crop Area/Type of crop	Population (density)	GDP/Economics	Global/Regional Map	Spatial scale	Temporal scale	Period
34. DCW													X								X							X		X	Globe Continent Country	Year	1960-1990
35.ERA-40 (15)	X	X	X				X	X	X	X	X	X																			Globe	Year Month Day	1957-2002
36.Locclim	X	X					X	X		X	X																				Globe	Month	2002
37.GAEZ																		X			X						X				Globe	Year	2000
38.GEWEX	X	X	X	X			X	X	X	X	X	X	X			X				X	X							X	X	X	Globe	Year	1950-2000
39.GRDD				X																											Continent Country	Year	1969-1998
40.GEO-UNEP	X	X			X	X	X			X					X	X	X	X	X	X	X	X	X	X	X	X	X	X	X	X	Globe Region Country	Year Month Day	1961-2007
41. GHRC	X						X	X	X	X																					Globe Region Country	Year Month Day	1979-2000

	Hydrology					Climate						Geomorphology/Land use									Water use					Society			Spatiotemporal scale		
	Precipitation	(Potential) Evapo(transpi)ration	Runoff	River discharge	Groundwater use/availability	Soil moisture/Climate moisture indices	Air/Water temperature	Wind speed	Cloud cover/Height	Vapour pressure/Humidity	Radiation (short/long)/Albedo	Ice/Permafrost/Snow cover	River network/Basin	Sediment transport	Dam/Reservoir	Lake density/volume	Wetland/Floodplain	Irrigated/Crop/Arable land	Soil Property	Elevation/Water height	Land use/Vegetation/Topology	Irrigated water use	Domestic water use	Industrial water use	Desalinated/Waste water (re-)use	Water quality	Crop Area/Type of crop	Population (density)	GDP/Economics	Global/Regional Map	Spatial scale	Temporal scale	Period
42.GRDC			X	X									X																		Globe Continent	Year Month	1950-2006
43.GSWP-2	X					X		X			X								X	X	X										Globe Continent	Month Day	1986-1995
44. GSMDB						X												X													Globe Country	Month Day	1952-2002
45.GT-NET	X			X		X				X		X	X	X																	Globe	Month Day	1951-2007
46. GUONet																										X		X			Country	Year	1990-2020
47.IDA-UNIDO																													X		Country	Year	1990-2007
48.IWMI																		X			X									X	Globe	Year	2006
49.JMP																										X		X			Globe Region Country	Year	1995-2005
50.NOAA	X						X	X	X	X	X	X									X									X	Globe Continent Country	Day Hour Minute	1946-2007

	Hydrology						Climate						Geomorphology/Land use									Water use					Society			Spatiotemporal scale		
	Precipitation	(Potential) Evapo(transpi)ration	Runoff	River discharge	Groundwater use/availability	Soil moisture/Climate moisture indices	Air/Water temperature	Wind speed	Cloud cover/Height	Vapour pressure/Humidity	Radiation (short/long)/Albedo	Ice/Permafrost/Snow cover	River network/Basin	Sediment transport	Dam/Reservoir	Lake density/volume	Wetland/Floodplain	Irrigated/Crop/Arable land	Soil Property	Elevation/Water height	Land use/Vegetation/Topology	Irrigated water use	Domestic water use	Industrial water use	Desalinated/Waste water (re-)use	Water quality	Crop Area/Type of crop	Population (density)	GDP/Economics	Global/Regional Map	Spatial scale	Temporal scale	Period
51.TRMM	X																														Tropic	Year Month	2001-2003
52.Tyndall-CRU	X						X	X	X	X																					Globe Region Country	Year Month	1901-2100
53.WB																												X	X	X	Globe Region Country	Year	2005-2006
54.WCRP	X						X				X																				Globe Region	Month	1979-2007
55.WHYCOS	X						X						X								X										Region Country	Year Month	1997-2007
56.WWDR-II	X	X	X	X		X							X	X	X	X	X	X				X	X	X		X		X			Globe Africa	Year	1950-2000
57.WHYMAP					X																										Globe Continent Region	Year	2000-2006

	Hydrology						Climate					Geomorphology/Land use								Water use						Society			Spatiotemporal scale		
	Precipitation	(Potential) Evapo(transpi)ration	Runoff	River discharge	Groundwater use/availability	Soil moisture/Climate moisture indices	Air/Water temperature	Wind speed	Cloud cover/Height	Vapour pressure/Humidity	Radiation (short/long)/Albedo	Ice/Permafrost/Snow cover	River network/Basin	Sediment transport	Dam/Reservoir	Lake density/volume	Wetland/Floodplain	Irrigated/Crop/Arable land	Soil Property	Elevation/Water height	Land use/Vegetation/Topology	Irrigated water use	Domestic water use	Industrial water use	Desalinated/Waste water (re-)use	Water quality	Crop Area/Type of crop	Population (density)	GDP/Economics	Global/Regional Map	Spatial scale	Temporal scale	Period
58.UCAR									X		X										X										Globe Continent	Year Month	1980-2099
59.UNEP-RBIS	X	X	X																	X	X	X	X	X				X			Africa	Year	2003
60.UNPIN																												X			Globe Region Country	Year	1950-2050
61.CEPIS																										X		X			Americas	Year	2000
62.WasterwaterFAO																		X				X	X	X	X	X	X	X			Continent Country	Year	2002

[i] Most of these available data are based on observation and some of data are derived by model simulation.
[ii] Sources of some of these data are based on same observation. There are some overlaps of data.
[iii] Prefix number corresponds to the detail reference of available data in appendix.
[iv] Spatial scale includes both global and regional data although its data does not sometimes cover the whole globe.
[v] Period includes the future projection. The length of period depends on a type of variable.
[vi] AQUASTAT database provides water sources (surface/groundwater) for water uses (irrigation/domestic/industry).

A.2. Detailed Data References

1. A Global Rapid Integrated Monitoring System (Global-RIMS); http://rbis.sr.unh.edu/ for soil property, runoff, water demand and population.

2. A Regional, Electronic Hydrometeorological Data Network; http://www.lba-hydronet.sr.unh.edu/ for precipitation and discharge.

3. A Regional Hydrometeorological Data Network; http://www.r-hydronet.sr.unh.edu/english/ for hydrometeorologtical data in South America, Central America and Caribbean.

4. Arctic CHAMP (Community-wide Hydrologic Analysis and Monitoring Program); http://arcticchamp.sr.unh.edu/featuredproject/index.shtml for daily meteorological data of precipitation, temperature and wind speed in the Arctic regions.

5. ArcticRIMS Project; http://rims.unh.edu/data.shtml, http://wale.unh.edu/data.shtml for daily and monthly meteorological data of precipitation, radiation, temperature and wind speed in the Arctic regions.

6. AQUASTAT, Food and Agriculture Organization (FAO); http://www.fao.org/nr/water/aquastat/main/index.stm for water resources, lnd use and population, irrigation and water use by sector and by source.

7. Digital soil map of the world, FAO; http://www.fao.org/ag/AGL/agll/dsmw.htm for soil property.

8. Earth Observation Research Center (EORC), the Japan Aerospace Exploration Agency (JAXA); http://www.eorc.jaxa.jp/en/imgdata/index.html for meteorological and topographic data.

9. Earth Resources Observation and Science (EROS) and the Landsat Project, The United Sates Geological Survey (USGS); http://eros.usgs.gov/index.html for high-resolution topographic data.

10. EarthTrends, The Environmental Information Portal, The World Resources Institute (WRI); http://earthtrends.wri.org/select_action.php?tool=1 for water resources, water withdrawals, and population, etc.

11. Environmental Research Group Oxford (ERGO), Oxford University, FAO GeoNetwork; http://ergodd.zoo.ox.ac.uk/websites.htm, http://www.fao.org/ag/AGAinfo/resources/en/glw/GLW_dens.html for global gridded data of livestock densities.

12. FAOSTAT, FAO; http://faostat.fao.org/ for land use, irrigation and population.

13. GEMStat, Global Environment Monitoring System (GEMS), The United Nations Environment Programme (UNEP); http://www.gemstat.org/default.aspx for global water quality data and statistics.

14. Global Dataset Project, Center for Remote Sensing and Spatial Analysis (CRSSA), Cook College, Rutgers University, the U.S. Army Corps of Engineers and the International Institute for Applied System Analyses (IIASA); http://www.crssa.rutgers.edu/projects/global/ for global climate, hydrology, land use and economic data.

15. Global Resource Information Database (GRID), The Division of Early Warning and Assessment (DEWA), UNEP, The International Institute for Applied System Analyses (IIASA); http://www.grid.unep.ch/data/index.php for climate, hydrology, land use and socio-economic data.

16. Global Soil and Terrain Database (WORLD-SOTER), FAO; http://www.fao.org/ag/agl/agll/soter.stm for land use and soil property.

17. Global Water Resources Data Archive, Oki and Kanae Laboratory, The University of Tokyo; http://hydro.iis.u-tokyo.ac.jp/GW/ for base map and population.

18. Global Terrestrial Observing System-Terrestrial Ecosystem Monitoring Sites (GTOS-TEMS), The Global Climate Observing System (GCOS), Global Observing Systems Information Center (GOSIC); http://www.fao.org/gtos/index.html, http://www.fao.org/gtos/tems/, http://www.wmo.ch/pages/prog/gcos/index.php?name=networks, http://www.gosic.org/default.htm for global climatic and terrestrial data.

19. Gridded Population of the World, version 3 (GPWv3) and the Global Rural-Urban Mapping Project (GRUMP); http://sedac.ciesin.columbia.edu/gpw/global.jsp for gridded global population.

20. International Association of Hydrological Sciences (IAHS): Global Water Database, Meta-data System; http://www.wsag.unh.edu/cgi-bin/displaymd for runoff, irrigated areas and reservoirs, etc.

21. International Commission on Large Dams (ICOLD), The World Commission on Dams (WCD); http://www.icold-cigb.org/, http://www.icold-cigb.net/, http://www.dams.org/ for dams and reservoirs.

22. International Groundwater Resources Assessment Centre (IGRAC); http://www.igrac.nl/ for annual groundwater abstraction.

23. International Satellite Land-Surface Climatology Project (ISLSCP); http://islscp2.sesda.com/ISLSCP2_1/html_pages/islscp2_home.html for hydro-climate, socio-economic and vegetation.

24. International Soil Reference and Information Centre (ISRIC); http://www.isric.org/UK/About+Soils/Soil+data/ for soil property data.

25. Pan-Arctic Drainage System; http://www.r-arcticnet.sr.unh.edu/ for pan-Arctic river discharge.

26. Simulated Topological Networks; http://www.wsag.unh.edu/Stn-30/stn-30.html for 30-minute topological data.

27. SPOT Image; http://www.spot.com/web/SICORP/402-sicorp-products-and-services.php for a resolution of 2.5 metres topographical and vegetation data.

28. TERRASTAT, FAO; http://www.fao.org/ag/agl/agll/terrastat/ for arable land, deserts and dry areas, etc.

29. The British Atmospheric Data Centre (BADC), the Natural Environment Research Council's (NERC) Designated Data Centre for the Atmospheric Sciences; http://badc.nerc.ac.uk/data/ for atmospheric and meteorological data.

30. The Center for International Earth Science Information Network (CIESIN); http://www.ciesin.columbia.edu/download_data.html for gridded population of the world (GIS Format).

31. The Center for Sustainability and the Global Environment (SAGE), Nelson Institute, The University of Wisconsin-Madison; http://www.sage.wisc.edu/pages/datamodels.html for global hydrometeorologcial, land use and socio-economic data (from various different data sources).

32. The Conservation Science Program, World Wildlife Fund (WWF); http://www.wwfus.org/science/data.cfm for global lakes and wetlands, and global hydrological database.

33. The Data Synthesis System for World Water Resources (DSS); http://www.wwap-dss.sr.unh.edu/download.html, http://www.wwap-dss.sr.unh.edu/africa/Metadata-WWAP.htm for basin and country data in Africa.

34. The Digital Chart of the World (DCW), Penn State University Library, Environmental Systems Research Institute (ESRI), the U.S. Defense Mapping Agency's (DMA) Operational Navigation Chart (ONC); http://www.esri.com/data/index.html, http://www.maproom.psu.edu/dcw/, http://www.lib.ncsu.edu/gis/dcw.html for country boundaries, population and geomorphological data.

35. The ECMWF 40 Years Re-analysis (ERA-40), The ECMWF 15 Years Re-analysis (ERA-15), The European Centre for Medium-Range Weather Forecasts (ECMWF), The Development of a European Multimodel Ensemble system for seasonal to inTERannual prediction (DEMETER), Distributed European Infrastructure for Supercomputing Applications (DEISA), Data grids for process and product development using numerical simulation and knowledge discovery (SIMDAT); http://data.ecmwf.int/data/, http://www.ecmwf.int/research/demeter/, http://www.deisa.org/, http://www.scai.fraunhofer.de/simdat.html for global 40 and 15 years climate data sets.

36. The FAO Local Climate Estimator; http://www.fao.org/sd/locclim/srv/en/locclim.home for temperature, precipitation, potential evapotranspiration and water vapour pressure.

37. The FAO Global Agro-ecological Zones; http://www.iiasa.ac.at/Research/LUC/GAEZ/index.htm for agricultural and arable lands.

38. The Global Energy and Water Cycle Experiment (GEWEX), the Global Precipitation Climatology Project (GPCP); http://www.gewex.org/datasets.html, http://www.gewex.org/gpcpdata.htm for the hydrological cycle and energy fluxes in the atmosphere, at land surface and in the upper oceans.

39. The Global Environment Outlook (GEO) Data Portal, UNEP; http://geodata.grid.unep.ch/ for global, regional and national climate, hydrology, soico-economic data (more than 450 different variables from various different data sources).

40. The Global Hydrology Resource Center (GHRC), The Convection and Moisture Experiment (CAMEX),The Passive Microwave Earth Science Information Partner (PM-ESIP), The Global Hydrology and Climate Center, The National Aeronautics and Space Administration (NASA); http://ghrc.msfc.nasa.gov/ghrc.html, http://datapool.nsstc.nasa.gov/ for global climate and hydrology data.

41. The Global River Discharge Database; http://www.rivdis.sr.unh.edu/ for global river discharge.

42. The Global Runoff Data Centre (GRDC); http://grdc.bafg.de/servlet/is/987/, http://www.grdc.sr.unh.edu/index.html for time series river discharge.

43. The Global Soil Moisture Data Bank (GSMDB), The State University of New Jersey-Rutgers; http://climate.envsci.rutgers.edu/soil_moisture/ for soil moisture and land use data.

44. The Global Soil Wetness Project (GSWP-2); http://www.iges.org/gswp/ for 1° grids of land surface parameters and meteorological forcing data.

45. The Global Terrestrial Network for Hydrology (GTN-H), Global Terrestrial Network for River Discharge (GTN-R), The Global Precipitation Climatology Centre (GPCC), The Global Terrestrial Observing Network (GT-NET), The World Meteorological Organization (WMO); http://gtn-h.unh.edu/PHP/index.php, http://gtn-r.bafg.de/, http://www.dwd.de/en/FundE/Klima/KLIS/int/GPCC/, http://www.fao.org/gtos/GT-NET.html for global hydrological data.

46. The Global Urban Observatory Network (GUONet), The United Nations Human Settlements Programme (UN-HABITAT); http://ww2.unhabitat.org/programmes/guo/ for urban and rural population, and the number of people who have accesses to water.

47. The Industrial Development Abstracts (IDA), The Industrial Statistics, The United Nations Industrial Development Organization (UNIDO); http://www.unido.org/doc/3533, http://www.unido.org/en/doc/3474/ for Economic data.

48. The International Water Management Institute (IWMI); http://www.iwmigiam.org/info/main/index.asp for global irrigated area maps.

49. The Joint Monitoring Programme (JMP), The World Health Organization (WHO), The United Nations Children's Fund (UNICEF); http://www.wssinfo.org/en/welcome.html, http://www.who.int/water_sanitation_health/en/, http://www.childinfo.org/eddb/water.htm for water supply and quality data.

50. The National Geophysical Data Center (NGDC), National Environmental Satellite, Data and Information Service (NESDIS), National Oceanic and Atmospheric Administration (NOAA); http://www.ngdc.noaa.gov/ngdcinfo/onlineaccess.html, http://www.nesdis.noaa.gov/datainfo.html, http://www.noaa.gov/index.html, for global and regional climatic and meteorological data.

51. The Tropical Rainfall Measuring Mission (TRMM); http://trmm.gsfc.nasa.gov/data_dir/data.html for precipitation in tropical regions.

52. The Tyndall Centre-Climate Research Unit, The University of East Anglia (UEA); http://www.cru.uea.ac.uk/~timm/data/index.html, http://www.cru.uea.ac.uk/cru/data/, http://www.cru.uea.ac.uk/cru/data/hrg.htm for high-resolution climate data.

53. The World Bank; http://web.worldbank.org/WBSITE/EXTERNAL/DATASTATISTICS/0,,contentMDK:20535285~menuPK:1192694~pagePK:64133150~piPK:64133175~theSitePK:239419,00.html for GDP, economic development and population.

54. The World Climate Research Programme (WCRP); http://www.wmo.ch/pages/prog/wcrp/ResearchProducts_index.html for climatic data.

55. The World Hydrological Cycle Observing System (WHYCOS), The Hydrology and Water Resources Programme (HWRP); http://www.whycos.org/, http://www.wmo.ch/ for global hydrological data.

56. The World Water Assessment Programme (WWDR-II): World Water Development Report II, Indicators for World Water Assessment Programme, Global Data Sets; http://wwdrii.sr.unh.edu/download.html for water balance, reservoirs, population and water use, etc.

57. The World-wide Hydrogeological Mapping and Assessment Programme (WHYMAP); http://www.whymap.org/cln_006/whymap/EN/Home/whymap__node.html?__nnn=true for global groundwater related data.

58. UCAR/NCAR/UOP; http://www.ucar.edu/tools/data.jsp for atmospheric and meteorological data.

59. UNEP Global River Basin Information System (UNEP-RBIS); http://rbis-unep.sr.unh.edu/index.html for precipitation, population and water demand.

60. United Nations Population Information Network; http://www.un.org/popin/data.html for global population data.

61. Virtual library on health and the environment, World Health Organization (WHO), Pan-American Health Organization (PAHO), Pan-American Centre for Sanitary Engineering and Environmental Sciences (CEPIS); http://www.cepis.ops-oms.org/sde/ops-sde/bvsdeeng.shtml, http://www.cepis.ops-oms.org/enwww/eva2000/infopais.html for drinking water and population.

62. Wastewater database, FAO; http://www.fao.org/landandwater/aglw/waterquality/dboverview.stm for wastewater re-use volume.

Appendix B - Additional Figures of Water Stress

B.1. Blue Water Stress

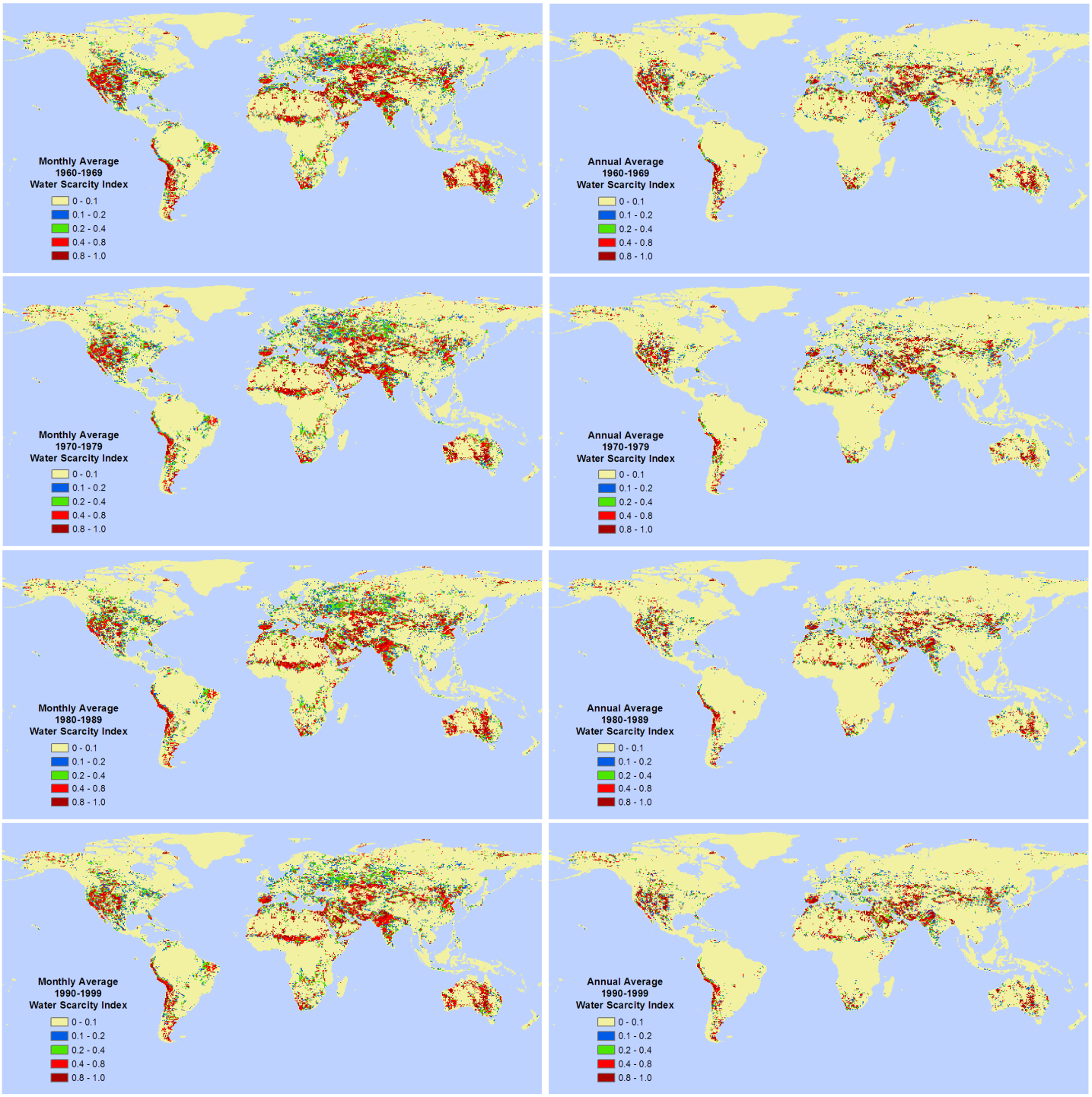

Figure B.1 Average blue water stress based on a monthly time scale (left) and a yearly time scale (right) for four decades of 1960s, 1970s, 1980s and 1990s.

B.2. Green Water Stress

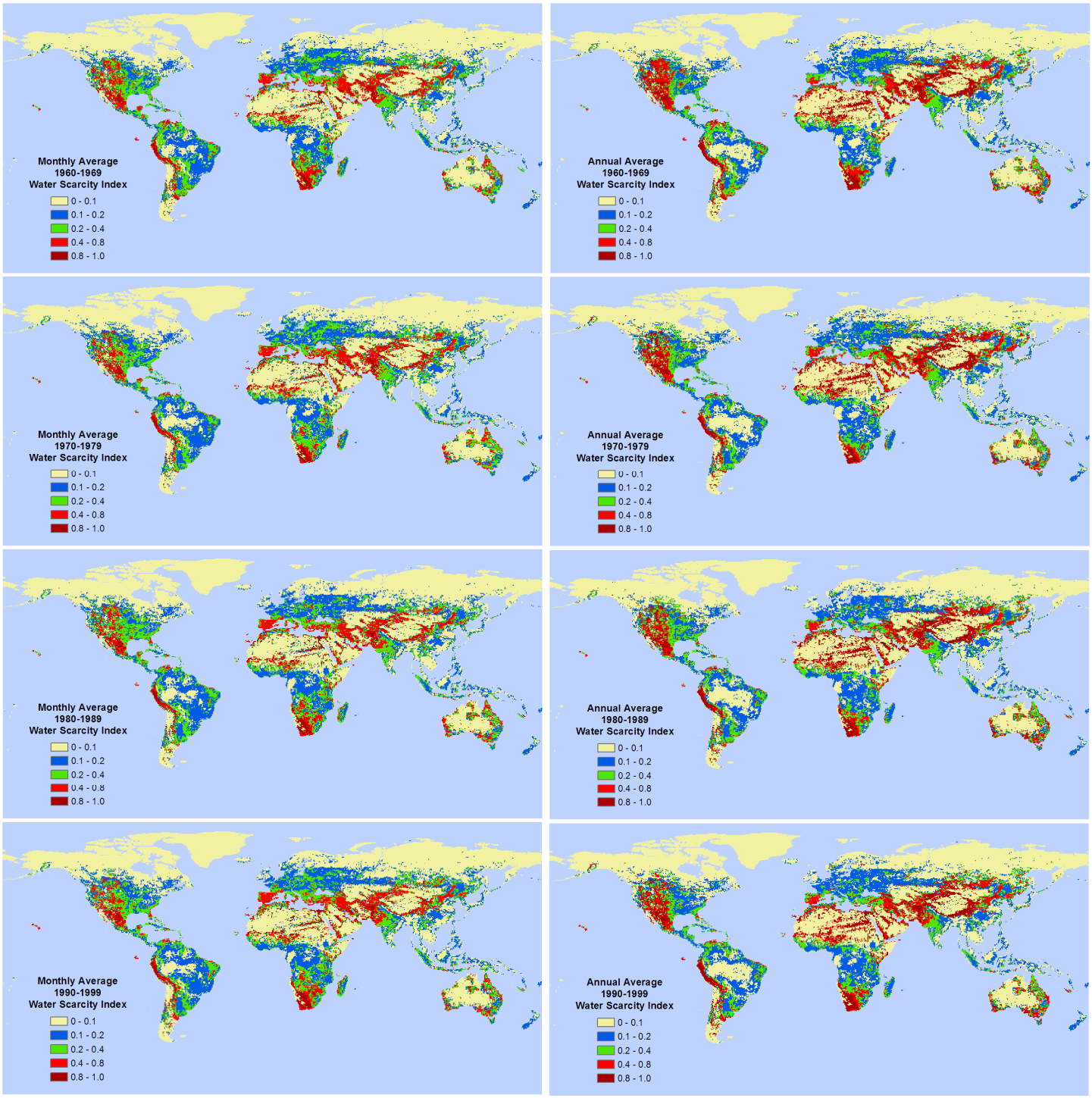

Figure B.2 Average green water stress based on a monthly time scale (left) and a yearly time scale (right) for four decades of 1960s, 1970s, 1980s and 1990s.